

WESTINGHOUSE CLASS 3  
CUSTOMER DESIGNATED DISTRIBUTION

WCAP-11763

BACKGROUND AND TECHNICAL BASIS FOR THE  
HANDBOOK ON FLAW EVALUATION FOR THE  
JOSEPH M. FARLEY NUCLEAR PLANT  
UNITS 1 & 2 REACTOR VESSEL  
BELTLINE & NOZZLE-TO-SHELL WELDS

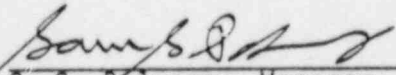
April 1988

W. H. Bamford  
K. R. Balkey  
Y. S. Lee

Verified by:

  
L. Cranford

Approved by:

  
S. S. Palusamy, Manager  
Structural Materials Engineering

Although information contained in this report is nonproprietary, no distribution shall be made outside Westinghouse or its licensees without the customer's approval.

WESTINGHOUSE ELECTRIC CORPORATION  
Nuclear Energy Systems  
P.O. Box 355  
Pittsburgh, Pennsylvania 15230

## TABLE OF CONTENTS

Section	Title	Page
1	INTRODUCTION	1-1
	1.1 CODE ACCEPTANCE CRITERIA	1-2
	1.1.1 Criteria Based on Flaw Size	1-3
	1.1.2 Criteria Based on Stress Intensity Factor	1-3
	1.1.3 Primary Stress Limits	1-5
	1.2 GEOMETRY	1-5
	1.3 SCOPE OF THIS WORK	1-5
2	LOAD CONDITIONS, FRACTURE ANALYSIS METHODS, AND MATERIAL PROPERTIES	2-1
	2.1 TRANSIENTS FOR THE REACTOR VESSEL	2-1
	2.2 STRESS INTENSITY FACTOR CALCULATIONS	2-1
	2.3 FRACTURE TOUGHNESS	2-3
	2.4 IRRADIATION EFFECTS	2-4
	2.5 CRITICAL FLAW SIZE DETERMINATION	2-6
3	FATIGUE CRACK GROWTH	3-1
	3.1 ANALYSIS METHODOLOGY	3-1
	3.2 STRESS INTENSITY FACTOR EXPRESSIONS	3-2
	3.3 CRACK GROWTH RATE REFERENCE CURVES	3-3
	3.4 FATIGUE CRACK GROWTH RESULTS	3-4
4	DETERMINATION OF LIMITING TRANSIENTS	4-1
	4.1 INTRODUCTION	4-1

TABLE OF CONTENTS (Cont'd.)

Section	Title	Page
4.2	SELECTION OF GOVERNING EMERGENCY AND FAULTED TRANSIENTS	4-1
4.2.1	Background and History	4-1
4.2.2	PTS Risk for a Typical Westinghouse PWR	4-3
4.2.3	Treatment of Transient Severity	4-4
4.2.4	Emergency and Faulted Conditions - Beltline Region	4-7
4.2.5	Faulted Conditions Evaluation for Other Regions	4-8
5	SURFACE FLAW EVALUATION	5-1
5.1	CODE CRITERIA	5-1
5.2	LONGITUDINAL FLAWS VS. CIRCUMFERENTIAL FLAWS	5-2
5.3	BASIC DATA	5-2
5.3.1	Fatigue Crack Growth	5-2
5.3.2	Minimum Critical Flaw Size $a_c$ and $a_i$	5-3
5.4	TYPICAL SURFACE FLAW EVALUATION CHART	5-4
5.5	PROCEDURE FOR THE CONSTRUCTION OF SURFACE FLAW EVALUATION CHART	5-5
6	EMBEDDED FLAW EVALUATION	6-1
6.1	EMBEDDED VS. SURFACE FLAWS	6-1
6.2	CODE CRITERIA	6-2
6.3	BASIC DATA	6-3
6.4	FATIGUE CRACK GROWTH FOR EMBEDDED FLAWS	6-4
6.5	TYPICAL EMBEDDED FLAW EVALUATION CHART	6-6

TABLE OF CONTENTS (Cont'd.)

Section	Title	Page
6.6	PROCEDURES FOR THE CONSTRUCTION OF EMBEDDED FLAW EVALUATION CHARTS	6-9
6.7	COMPARISON OF EMBEDDED FLAW CHARTS WITH ACCEPTANCE STANDARDS OF IWB-3500	6-11
7	REFERENCES	7-1
APPENDIX-A FLAW EVALUATION		
A-1	INTRODUCTION TO EVALUATION PROCEDURE	A-1
A-2	BELTLINE (INCLUDING MIDDLE-TO-UPPER SHELL CIRCUMFERENTIAL WELD, LOWER-TO-MIDDLE SHELL CIRCUMFERENTIAL WELD AND LONGITUDINAL SEAM WELDS)	A-11
	A-2.1 SURFACE FLAWS	A-11
	A-2.2 EMBEDDED FLAWS	A-12
A-3	INLET NOZZLE TO SHELL WELD (PENETRATION)	A-19
	A-3.1 SURFACE FLAWS	A-19
	A-3.2 EMBEDDED FLAWS	A-20
A-4	OUTLET NOZZLE TO SHELL WELD	A-26
	A-4.1 SURFACE FLAWS	A-26
	A-4.2 EMBEDDED FLAWS	A-27
A-5	LOWER HEAD RING TO LOWER SHELL WELD	A-33
	A-15.1 SURFACE FLAWS	A-33
	A-15.2 EMBEDDED FLAWS	A-34
APPENDIX B-CRITICAL FLAW SIZE RESULTS		E-1
APPENDIX C-FATIGUE CRACK GROWTH RESULTS		C-1

## SECTION 1 INTRODUCTION

This flaw\* evaluation handbook, has been designed for the evaluation of indications which may be discovered during inservice inspection of the Joseph Farley Unit 1 and Unit 2 reactor vessels. The tables and charts provided herein allow the evaluation of any indication discovered in the regions listed below without further fracture mechanics calculations. The fracture analysis work has been done in advance, and is documented in this report. Use of the handbook will allow the acceptability of much larger indications than would be allowable by only using the standards tables of the ASME Code, Section XI [1]. This report provides the background and technical basis for the handbook, as well as the handbook charts themselves.

The handbook has been developed for the following locations in the Joseph Farley Units 1 and 2 reactor vessels:

- o Beltline (core region) (Fig. 1-1)
- o Inlet nozzle to shell weld (Fig. 1-3)
- o Outlet nozzle to shell weld (Fig. 1-4)
- o Lower head ring to lower shell weld (Fig. 1-2)

The geometry of each of these regions is shown in figures 1-1 through 1-4.

The highlight of the handbook is the design of a series of flaw evaluation charts for both surface flaws and the embedded flaws. Since the characteristics of the two types of flaws are different, the evaluation charts designed for each are distinctively different in style. One section of this technical basis document deals with surface flaws at various locations, and another section concentrates on the evaluation of embedded flaws.

\* The use of the term "flaw" in this document should be taken to be synonymous with the term "indication" as used in Section XI of the ASME Code.

The flaw evaluation charts were designed based on the Section XI code criteria of acceptance for continued service without repair. Through use of the charts, a flaw can be evaluated instantaneously, and no follow-up hand calculation is required. Most important of all, no fracture mechanics knowledge is needed by the user of the handbook charts.

It is important to note that indications which are large enough that they exceed the standards limits, and must be evaluated by fracture mechanics, will also require additional inservice inspection in the future, as discussed in Section XI, paragraph IWB-2420.

### 1.1 CODE ACCEPTANCE CRITERIA

There are two alternative sets of flaw acceptance criteria for continued service without repair in paragraph IWB-3600 of ASME Code Section XI [1]. Either of the criteria below may be used, at the convenience of the user.

1. Acceptance Criteria Based on Flaw Size (IWB-3611)
2. Acceptance Criteria Based on Stress Intensity Factor (IWB-3612)

Both criteria are comparable in accuracy for thick sections, and the acceptance criteria (2) have been assessed by past experience to be less restrictive for thin sections, and for outside surface flaws in many cases. In all cases, the most beneficial criteria have been used and only one calculation has been made. The criteria actually used for each region are listed in Table 1-1.

Since the fracture mechanics results for surface flaws have been presented in terms of critical flaw size, it is more straight forward to construct the surface flaw evaluation charts by using criteria (1) in this handbook. This has been done for inside surface flaws in all cases except the safe end region, where criteria (2) are more beneficial because of the small section thickness. All of the embedded flaw and most outside surface flaw evaluation charts in this handbook were constructed using acceptance criteria (2), for ease of use, as well as to obtain the maximum benefit, since these criteria will generally be less restrictive for embedded flaws.

### 1.1.1 CRITERIA BASED ON FLAW SIZE

The code acceptance criteria stated in IWB-3611 of Section XI are:

$$a_f \leq .1 a_c \quad \begin{array}{l} \text{For Normal Conditions} \\ \text{(Upset \& Test Conditions Inclusive)} \end{array}$$

and

$$a_f \leq .5 a_i \quad \begin{array}{l} \text{For Faulted Conditions} \\ \text{(Emergency Condition Inclusive)} \end{array}$$

where

$a_f$  = The maximum size to which the detected flaw is calculated to grow at the end of a specified period, or until the next inspection time.

$a_c$  = The minimum critical flaw size under normal operating conditions (upset and test conditions inclusive)

$a_i$  = The minimum critical flaw size for initiation of nonarresting growth under postulated faulted conditions. (emergency conditions inclusive)

To determine whether a surface flaw is acceptable for continued service without repair, both criteria must be met simultaneously. However, both criteria have been considered in advance before the charts were constructed. Only the most restrictive results were used in these charts.

### 1.1.2 CRITERIA BASED ON STRESS INTENSITY FACTOR

As mentioned in the preceding paragraphs, the criteria used for the evaluation of embedded flaws, including most outside surface flaws and those in the nozzle safe-end regions are from IWB-3612 of Section XI.

The term stress intensity factor ( $K_I$ ) is defined as the driving force on a crack. It is a function of the size of the crack and the applied stresses, as well as the overall geometry of the structure. In contrast, the fracture toughness ( $K_{Ia}$ ,  $K_{Ic}$ ) is a measure of the resistance of the material to propagation of a crack. It is a material property, and a function of temperature.

The criteria are:

$$K_I \leq \frac{K_{Ia}}{\sqrt{10}} \text{ For normal conditions (upset \& test conditions inclusive)}$$

$$K_I \leq \frac{K_{Ic}}{\sqrt{2}} \text{ For faulted conditions (emergency conditions inclusive)}$$

where

$K_I$  = The maximum applied stress intensity factor for the flaw size  $a_f$  to which a detected flaw will grow, during the conditions under consideration, for a specified period, or to the next inspection.

$K_{Ia}$  = Fracture toughness based on crack arrest for the corresponding crack tip temperature.

$K_{Ic}$  = Fracture toughness based on fracture initiation for the corresponding crack tip temperature.

To determine whether a surface flaw is acceptable for continued service without repair, both criteria must be met simultaneously. However, both criteria have been considered in advance before the charts were constructed. Only the most restrictive results were used in the charts.

### 1.1.3 PRIMARY STRESS LIMITS

In addition to satisfying the fracture criteria, it is required that the primary stress limits of the ASME Code Section III, paragraph NB-3000 be satisfied. A local area reduction of the pressure retaining membrane must be used, equal to the area of the indication, and the stresses increased to reflect the smaller cross section. All the flaw acceptance tables provided in this handbook have included this consideration, as demonstrated herein. The allowable flaw depths determined using this criterion have been summarized in Table 1-2 for each of the locations for which handbook charts have been constructed.

### 1.2 GEOMETRY

The geometry of the reactor vessel is shown in Figures 1-1 through 1-4. The cladding on the inside of the vessel has been neglected in the stress analysis. It has been accounted for in the thermal analysis by adjusting the film coefficient for the conditions analyzed. The outside surfaces have been assumed to be insulated. The notation used for both surface and embedded flaws in this work is illustrated in Figure 1-5.

### 1.3 SCOPE OF THIS WORK

The fracture and fatigue crack growth evaluations carried out to develop the handbook charts have employed the recommended procedures and material properties for low alloy steels, as contained in Section XI, Appendix A. Therefore, the charts apply strictly to those materials.

TABLE 1-1

SUMMARY OF CRITERIA USED IN PREPARATION OF HANDBOOK CHARTS

REGION	INSIDE SURFACE FLAW CHARTS	OUTSIDE SURFACE FLAW CHARTS	EMBEDDED FLAWS
Beltline	1	2	2
Inlet Nozzle to Shell Weld	1	2	2
Outlet Nozzle to Shell Weld	1	2	2
Lower Head Ring to Shell Weld	1	2	2

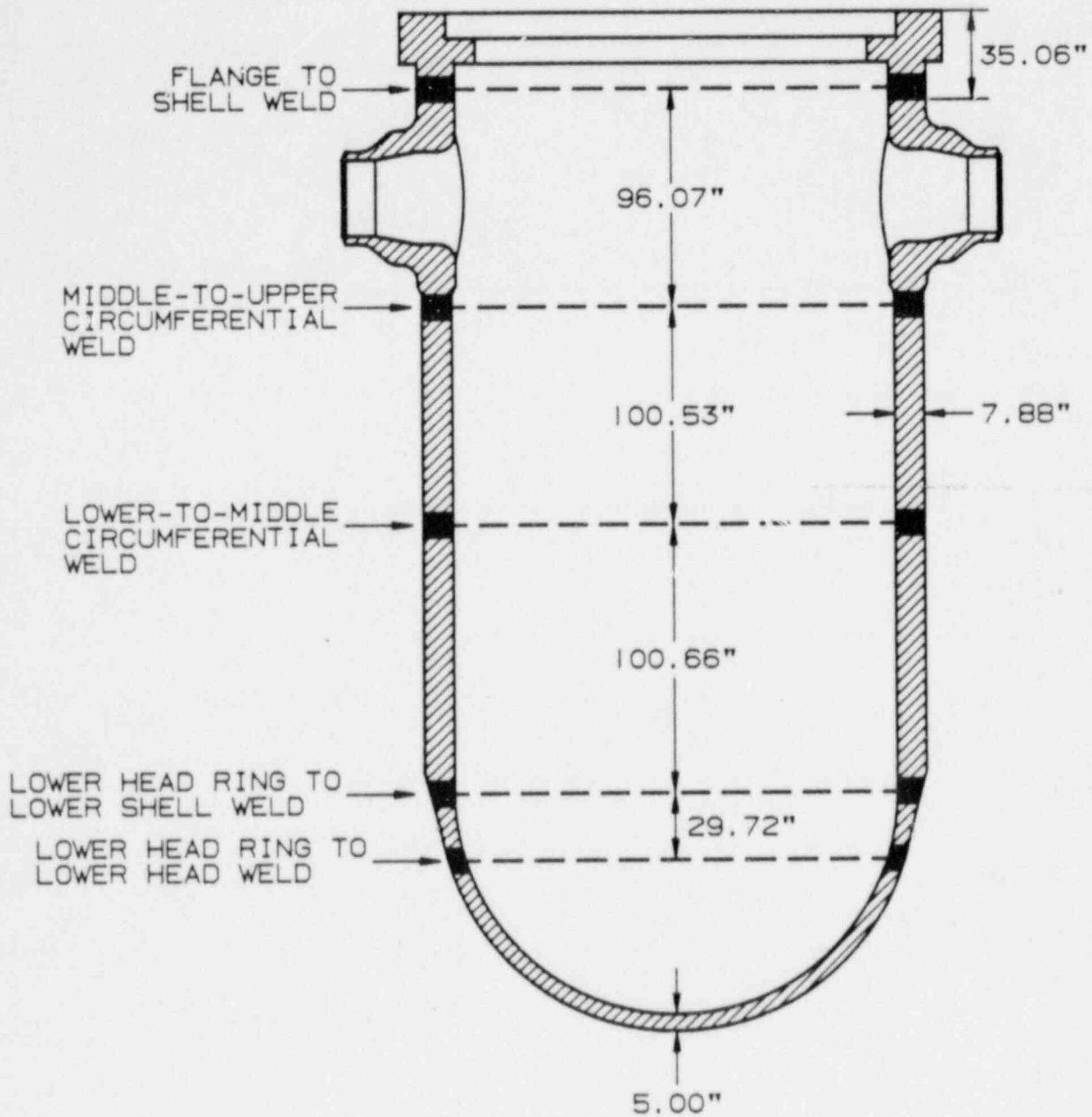
KEY: 1 Criteria on Flaw Size (IWB-3611)  
 2 Criteria on  $K_I$  (IWB-3612)

TABLE 1-2

SUMMARY OF ALLOWABLE FLAW DEPTHS  
BASED ON PRIMARY STRESS LIMIT CRITERIA

REGION	ALLOWABLE DEPTH OF FLAW, a/t (longitudinal)	ALLOWABLE DEPTH OF FLAW, a/t (circumferential)
Beltline	0.49	0.54
Inlet Nozzle to Shell Weld	0.51	0.63
Outlet Nozzle to Shell Weld	0.58	0.65
Lower Head Ring to Shell Weld	0.41	0.96

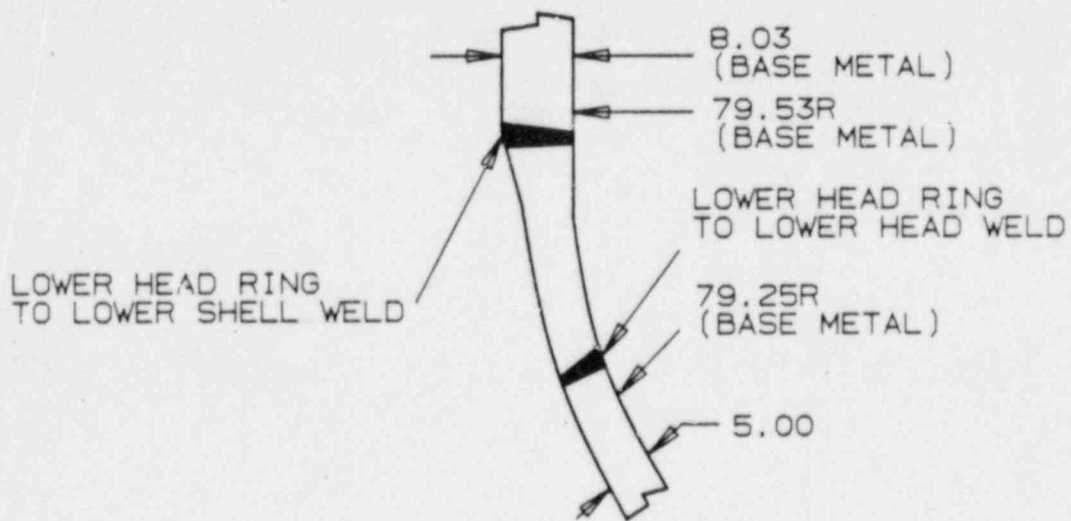
NOTE: Allowable depths indicated are relative to the inside surface.



NOTE: THICKNESSES DO NOT INCLUDE INSIDE CLADDING

044-A-25004-1A

Figure 1-1. Reactor Vessel Welds



BELTLINE AND LOWER HEAD REGIONS

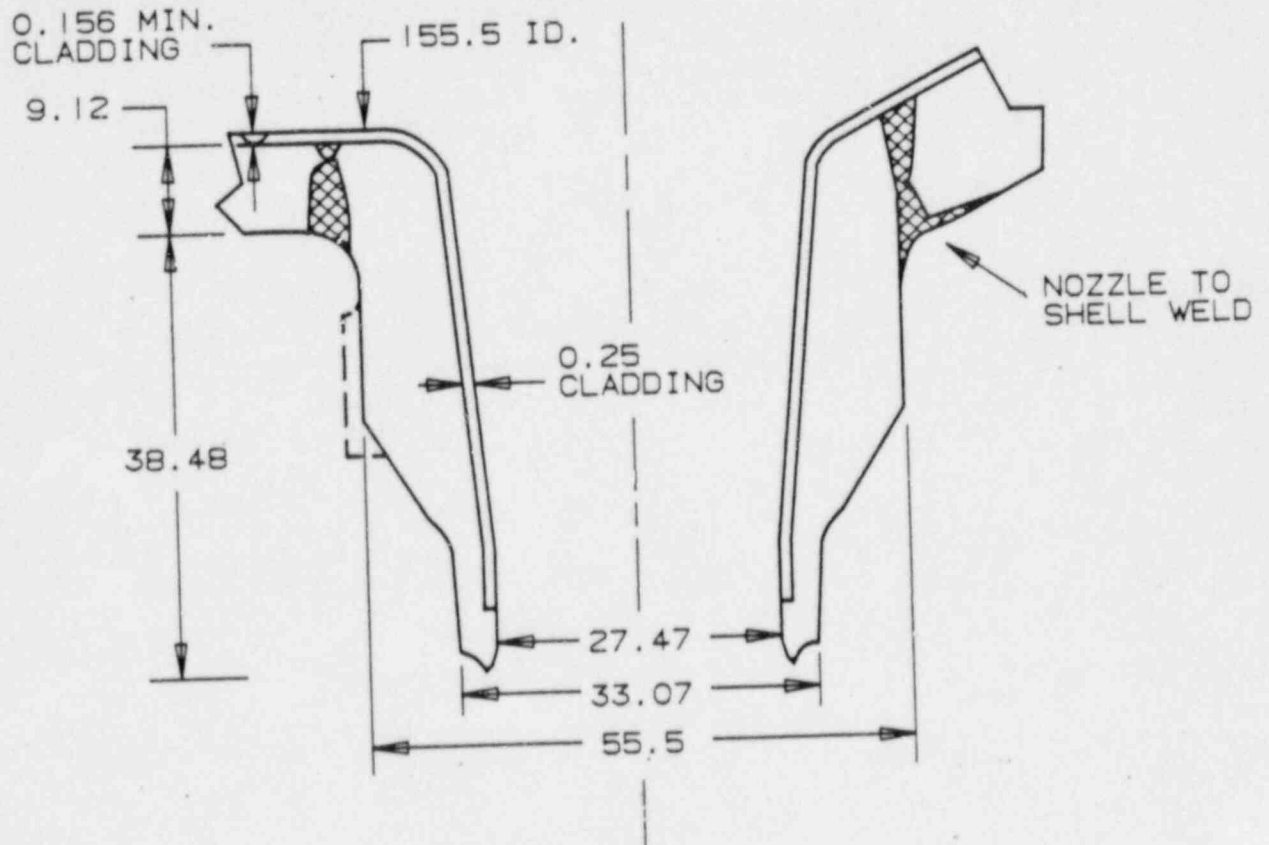
- NOTES: 1. DIMENSIONS DO NOT INCLUDE CLADDING  
 2. ALL DIMENSIONS ARE IN INCHES

044-A-25004-3

Figure 1-2. Beltline and Lower Head Region (dimensions in inches)

SIDE VIEW

TOP VIEW

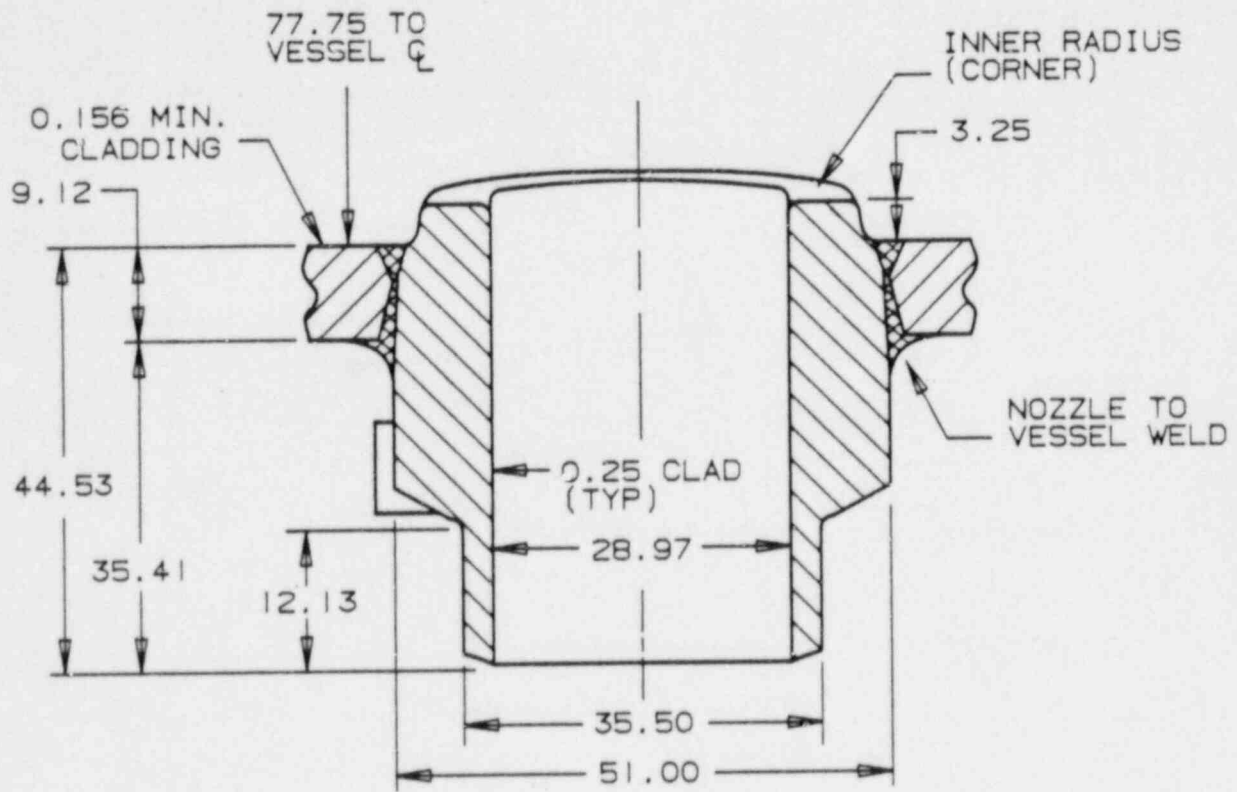


NOTES:

1. DIMENSIONS DO NOT INCLUDE CLAD
2. ALL DIMENSIONS ARE IN INCHES

044-A-25004-4

Figure 1-3. Reactor Vessel Inlet Nozzle



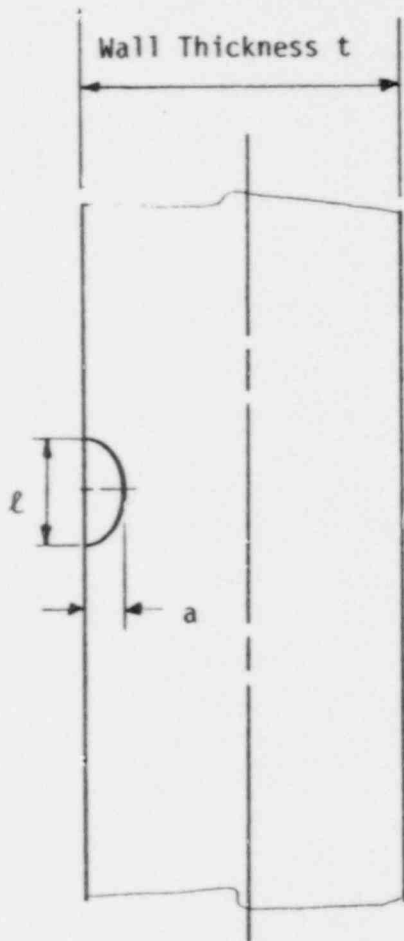
NOTES:

1. DIMENSIONS DO NOT INCLUDE CLAD
2. ALL DIMENSIONS ARE IN INCHES

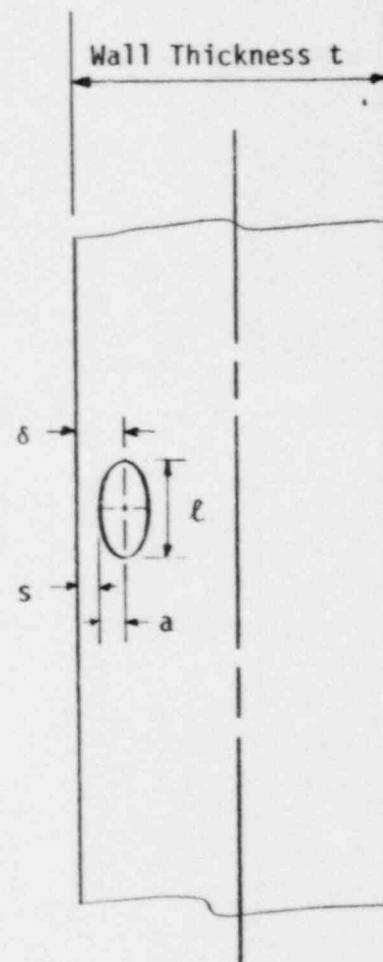
044-A-25004-2A

Figure 1-4. Longitudinal Cross Section of Outlet Nozzle to Vessel  
Juncture Region (Side View Only)

Figure 1-5. Typical Notation for Surface and Embedded Flaw Indications



TYPICAL SURFACE FLAW INDICATION



TYPICAL EMBEDDED FLAW INDICATION

1-12

## SECTION 2

### LOAD CONDITIONS, FRACTURE ANALYSIS METHODS AND MATERIAL PROPERTIES

#### 2.1 TRANSIENTS FOR THE REACTOR VESSEL

The design transients for the Joseph Farley Units 1 and 2 reactor vessels are listed in Table 2-1. Both the minimum critical flaw sizes, such as  $a_c$  under normal operating conditions, or  $a_f$  under faulted conditions for criteria (1) of IWB-3611, and the stress intensity factors,  $K_I$ , for criteria (2) of IWB-3612 are a function of the stresses at the cross-section where the flaw of interest is located, along with the material properties. Therefore, the first step for the evaluation of a flaw indication is to determine the appropriate limiting load conditions for the location of interest.

The selection of the most limiting transient for normal/upset/test conditions was straightforward. The transient with the highest surface stress in the area where the flaw was postulated was chosen as the worst case. Note that this can result in a different limiting transient for an inside flaw as opposed to an outside flaw, as may be seen in the detailed treatments of the individual locations. The governing transient for each region is listed in the tables of Appendix B where the critical flaw depths are provided. The transients listed in these tables are the governing ones for the region involved, regardless of the criterion used to construct the flaw evaluation charts, [either the criteria on flaw size (Section 1.1.1) or on applied  $K_I$  (Section 1.1.2)]. The selection of the most limiting emergency and faulted condition transient is discussed in Section 4.

#### 2.2 STRESS INTENSITY FACTOR CALCULATIONS

One of the key elements of the critical flaw size calculations is the determination of the driving force or stress intensity factor ( $K_I$ ). This was done for each of the regions using expressions available from the literature. In all cases the stress intensity factor for the critical flaw size calculations utilized a representation of the actual stress profile rather than a linearization. This was necessary to provide the most accurate determination possible of the critical flaw size, and is particularly

important for consideration of emergency and faulted conditions, where the stress profile is generally nonlinear and often very steep. The stress profile was represented by a cubic polynomial:

$$\sigma(x) = A_0 + A_1 \frac{x}{t} + A_2 \left(\frac{x}{t}\right)^2 + A_3 \left(\frac{x}{t}\right)^3 \quad (2-1)$$

where  $x$  is the coordinate distance into the wall

$t$  = wall thickness

$\sigma$  = stress perpendicular to the plane of the crack

$A_i$  = coefficients of the cubic fit

For the surface flaw with length six times its depth, the stress intensity factor expression of McGowan and Raymund [2] was used. The stress intensity factor  $K_I(\phi)$  can be calculated anywhere along the crack front. The point of maximum crack depth is represented by  $\phi = 0$ . The following expression is used for calculating  $K_I(\phi)$ , where  $\phi$  is the angular location around the crack.

$$K_I(\phi) = \left[\frac{\pi a}{Q}\right]^{0.5} \left(\cos^2 \phi + \frac{a^2}{c^2} \sin^2 \phi\right)^{1/4} \left(A_0 H_0 + \frac{2}{\pi} \frac{a}{t} A_1 H_1 + \frac{1}{2} \frac{a^2}{t^2} A_2 H_2 + \frac{4}{3\pi} \frac{a^3}{t^3} A_3 H_3\right) \quad (2-2)$$

The magnification factors  $H_0(\phi)$ ,  $H_1(\phi)$ ,  $H_2(\phi)$  and  $H_3(\phi)$  are obtained by the procedure outlined in Reference [2].

The stress intensity factor calculation for a semi-circular surface flaw, (aspect ratio 2:1) was carried out using the expressions developed by Raju and Newman [3]. Their expression utilizes the same cubic representation of the stress profile and gives precisely the same result as the expression of McGowan and Raymund for the 6:1 aspect ratio flaw, and the form of the equation is similar to that of McGowan and Raymund above.

The stress intensity factor expression used for a continuous surface flaw was that developed by Buchalet and Bamford [4]. Again the stress profile is represented as a cubic polynomial, as shown above, and these coefficients as well as the magnification factors are combined in the expression for  $K_I$

$$K_I = \sqrt{\pi a} \left[ A_0 F_1 + \frac{2a}{\pi} A_1 F_2 + \frac{a^2}{2} A_2 F_3 + \frac{4}{3\pi} a^3 A_3 F_4 \right] \quad (2-3)$$

where  $F_1, F_2, F_3, F_4$  are magnification factors, available in [6].

The stress intensity factor calculation for an embedded flaw was taken from work by Shah and Kobayashi [5] which is applicable to an embedded flaw in an infinite medium, subjected to an arbitrary stress profile. This expression has been shown to be applicable to embedded flaws in a thick-walled pressure vessel in a paper by Lee and Bamford [6].

### 2.3 FRACTURE TOUGHNESS

The other key element in the determination of critical flaw sizes is the fracture toughness of the material. The fracture toughness has been taken directly from the reference curves of appendix A, section XI. In the transition temperature region, these curves can be represented by the following equations:

$$K_{Ic} = 33.2 + 2.806 \exp. [0.02 (T - RT_{NDT} + 100^\circ F)] \quad (2-4)$$

$$K_{Ia} = 26.8 + 1.233 \exp. [0.0145 (T - RT_{NDT} + 160^\circ F)] \quad (2-5)$$

where  $K_{Ic}$  and  $K_{Ia}$  are in  $\text{ksi}\sqrt{\text{in}}$ .

The upper shelf temperature regime requires utilization of a shelf toughness which is not specified in the ASME Code. A value of  $200 \text{ ksi}\sqrt{\text{in}}$  has been used here in all the regions. This value is consistent with general practice in such evaluations, as shown for example in reference [7], which provides the background and technical basis of Appendix A of Section XI.

The other key element in the determination of the fracture toughness is the value of  $RT_{NDT}$ , which is a parameter determined from Charpy V-notch and drop-weight tests. The material chemistry and initial  $RT_{NDT}$  values for all the welds, plates and forgings in the Joseph Farley Units 1 and 2 reactor vessels are provided in Tables 2-2 and 2-3. The core region materials are identified in Figures 2-1 and 2-2 for Units 1 and 2 respectively. This information was determined from the vendors material certification reports, surveillance capsule tests, and weld chemistry studies by Westinghouse, EPRI, and others. When no information on the chemistry or  $RT_{NDT}$  was available, conservative assumptions were made, and these cases are clearly marked in the tables. The limiting material properties from both the Unit 1 and Unit 2 vessels were used in the analyses here, taken from references 8 and 9. This has very little impact on the results, however, as the properties are similar in both units, and differences in allowable flaw size are not significant.

## 2.4 IRRADIATION EFFECTS

Neutron irradiation has been shown to produce embrittlement which reduces the toughness properties of reactor vessel steels. The decrease in the toughness properties can be assessed by determining the shift to higher temperatures of the reference nil-ductility transition temperature,  $RT_{NDT}$ . Because the chemistry (especially copper and nickel content) of reactor vessel steel has been identified as a major contributor to radiation embrittlement, trend curves have been developed to relate the magnitude of the shift to  $RT_{NDT}$  to the amount of neutron fluence. The reference fracture toughness curve, indexed to  $RT_{NDT}$ , will shift along the temperature scale with a value equal to the increase in the  $RT_{NDT}$  for given levels of irradiation.

Based on the initial  $RT_{NDT}$  value and the material chemistry of the limiting core region materials, the post irradiation  $RT_{NDT}$  values are determined from the trend curves. These final  $RT_{NDT}$  values are subsequently used to calculate  $K_{Ic}$  and  $K_{Ia}$  as a function of the fractional depth through the wall. Irradiation effects were accounted for in all regions analyzed, but only had a significant impact on the properties in the beltline region.

The extent of the shift in  $RT_{NDT}$  is enhanced by certain chemical elements (such as copper, nickel and phosphorus) present in reactor vessel steels. Westinghouse, other NSSS vendors, the U.S. Nuclear Regulatory Commission and others have developed trend curves for predicting adjustment of  $RT_{NDT}$  as a function of fluence and copper, nickel and/or phosphorus content. The Nuclear Regulatory Commission (NRC) trend curve is published in Regulatory Guide 1.99. Regulatory Guide 1.99 was originally published in July 1975 with a Revision 1 being issued in April 1977. Currently, a Revision 2 [10] to Regulatory Guide 1.99 has been finalized by the NRC and is in the final stages of printing. The chemistry factor, "CF" ( $^{\circ}F$ ), a function of copper and nickel content identified in Regulatory Guide 1.99, Revision 2 is given in Table 2-4 for welds and Table 2-5 for base metal (plates and forgings). Interpolation is permitted. The value, "f", is the calculated value of the neutron fluence at the location of interest in the vessel at the location of the postulated defect,  $n/cm^2$  ( $E > 1$  MeV) divided by  $10^{19}$ . The fluence factor is determined from Figure 2-3.

The Adjusted Reference Temperature (ART) based on the methods of Reg. Guide 1.99 Revision 2 (Draft) can be compactly described by the sequence of equations listed below:

$$ART = \text{Initial } RT_{NDT} + \Delta RT_{NDT} + \text{Margin} \quad (2-6)$$

$$\Delta RT_{NDT} = [\Delta RT_{NDT \text{ SURFACE}}][\text{EXP}(-0.067X)] \quad (2-7)$$

$$X = \text{Depth into vessel wall from inner (wetted) surface} \\ (1/4T \text{ and } 3/4T) \quad (2-8)$$

$$\Delta RT_{NDT \text{ SURFACE}} = [CF]_F (0.28 - 0.10 \text{ LOG } F) \quad (2-9)$$

$$F = \text{Neutron fluence divided by } 10^{19} \quad (2-10)$$

$$CF = \text{Chemistry factor from tables* (if no data use 0.35\% Cu} \\ \text{and 1.0\% Ni)} \quad (2-11)$$

\*See tables 2-4 and 2-5.

$$\text{MARGIN} = 2 [\sigma_I^2 + \sigma_\Delta^2]^{0.5} \quad (2-12)$$

$\sigma_I$  = Mean value of initial  $RT_{NDT}$ ; if initial  $RT_{NDT}$  measured,  
 $\sigma_I = 0$ , otherwise  $\sigma_I$  obtained from set of data to get  
 initial  $RT_{NDT}$  (2-13)

$\sigma_\Delta$  = Standard deviation of initial  $RT_{NDT}$  (2-14)  
 28°F for welds  
 17°F for base metal

[ $\sigma_\Delta$  need not exceed 1/2 times  $RT_{NDT}$  surface]

## 2.5 CRITICAL FLAW SIZE DETERMINATION

The applied stress intensity factor ( $K_I$ ) and the material fracture toughness values ( $K_{Ia}$  and  $K_{Ic}$ ) can be used to determine the critical flaw size values used to construct the handbook charts. For normal, upset and test conditions, the critical flaw size  $a_c$  is determined as the depth at which the applied stress intensity factor  $K_I$  exceeds the arrest fracture toughness  $K_{Ia}$ .

For emergency and faulted conditions the minimum flaw size for crack initiation is obtained from the first intersection of the applied stress intensity factor ( $K_I$ ) curve with the static fracture toughness ( $K_{Ic}$ ) curve. Intersection of the  $K_I$  curve with the crack arrest toughness ( $K_{Ia}$ ) curve determines the crack arrest size. The critical flaw depth for emergency and faulted conditions ( $a_i$ ) as defined earlier, is the minimum flaw depth for initiation of non-arresting growth. Non-arresting growth is defined as growth which arrests at a depth greater than 75 percent of the wall depth. An example of this type of calculation is shown in Figure 2-4. The critical flaw depth is determined at point A in this figure.

TABLE 2-1 SUMMARY OF REACTOR VESSEL TRANSIENTS

NUMBER	TRANSIENT IDENTIFICATION	NUMBER OF OCCURRENCES	
		SPECIFIED	USED IN THE ANALYSIS
<u>Normal Conditions</u>			
1	Heatup and Cooldown at 100°F/hr (pressurizer cooldown 200°F/hr)	200	200
2	Load Follow Cycles (Unit loading and unloading at 5% of full power/min)	18300*	18300
3	Step load increase and decrease of 10% of full power	2000	2000
4	Large step load decrease, with steam dump	200	200
5	Steady state fluctuations	Infinite	10 <sup>6</sup>
<u>Upset Conditions</u>			
6	Loss of load, without immediate turbine or reactor trip	80	80
7	Loss of power (blackout with natural circulation in the Reactor Coolant System)	40	40
8	Loss of flow (partial loss of flow, one pump only)	80	80
9	Reactor trip from full power	400	400
10	Inadvertent Auxiliary Spray	10	10
<u>Faulted Conditions</u>			
11	Large Loss of Coolant Accident (LOCA)	1	1
12	Large Steam Line Break (LSB) (other transients described in section 4)	1	1
13	Safe Shutdown Earthquake	1	1

\* This number is 29,000 for Farley Unit 1, and 18,300 for Farley Unit 2. 18,300 cycles were used in the analysis.

TABLE 2-1 SUMMARY OF REACTOR VESSEL TRANSIENTS (cont.)

NUMBER	TRANSIENT IDENTIFICATION	NUMBER OF OCCURRENCES	
		SPECIFIED	USED IN THE ANALYSIS
	<u>Test Conditions</u>		
14	Turbine roll test	10	10
15	Primary Side Hydrostatic test conditions	50	50
16	Cold Hydrostatic test @ 3105 psig	5	5

TABLE 2-2  
 CHEMISTRY AND PROPERTIES OF JOSEPH FARLEY UNIT 1 REACTOR VESSEL MATERIALS

Component	Code No.	Material Type	Cu (%)	P (%)	Ni (%)	T <sub>NDT</sub> (°F)	RT <sub>NDT</sub> (°F)	Upper Shelf Energy NMWD <sup>(d)</sup>	Energy MKD <sup>(c)</sup>
Closure head dome	B6901	A533,B,C1.1	0.16	0.009	0.50	-30	-20[a]	-	140
Closure head segment	B6902-1	A533,B,C1.1	0.17	0.007	0.52	-20	-20[a]	-	138
Closure head flange	B6915-1	A508, C1.2	0.10	0.012	0.64	60[a]	60[a]	-	75[a]
Vessel flange	B6913-1	A508, C1.2	0.17	0.011	0.69	60[a]	60[a]	-	106[a]
Inlet nozzle	B6917-1	A508, C1.2	-	0.010	0.83	60[a]	60[a]	110	-
Inlet nozzle	B6917-2	A508, C1.2	-	0.008	0.80	60[a]	60[a]	80	-
Inlet nozzle	B6917-3	A508, C1.2	-	0.008	0.87	60[a]	60[a]	98	-
Outlet nozzle	B6916-1	A508, C1.2	-	0.007	0.77	60[a]	60[a]	96.5	-
Outlet nozzle	B6916-2	A508, C1.2	-	0.011	0.78	60[a]	60[a]	97.5	-
Outlet nozzle	B6916-3	A508, C1.2	-	0.009	0.78	60[a]	60[a]	100	-
Upper shell	B6914-1	A508, C1.2	-	0.010	0.68	30	30[a]	-	148
Inter. shell	B6903-2	A533,B,C1.1	0.13	0.011	0.60	0	0	97	151.5
Inter. shell	B6903-3	A533,B,C1.1	0.12	0.014	0.56	10	10	100	134.5
Lower shell	B6919-1	A533,B,C1.1	0.14	0.015	0.55	-20	15	90.5	133
Lower shell	B6919-2	A533,B,C1.1	0.14	0.015	0.56	-10	5	97	134
Bottom head ring	B6912-1	A508, C1.2	-	0.010	0.72	10	10[a]	-	163.5
Bottom head segment	B6906-1	A533,B,C1.1	0.15	0.011	0.52	-30	-30[a]	-	147
Bottom head dome	B6907-1	A533,B,C1.1	0.17	0.014	0.60	-30	-30[a]	-	143.5
Inter. shell long. weld seam	M1.33	Sub Arc Weld	0.25	0.017	0.21	0[a]	0[a]	-	-
Inter. to lower shell weld seams	G1.18	Sub Arc Weld	0.22	0.011	<0.20[b]	0[a]	0[a]	-	-
Lower shell long. weld seams	G1.18	Sub Arc Weld	0.17	0.022	<0.20[b]	0[a]	0[a]	-	-

[a] Estimate per NUREG-0800 "USNRC Standard Review Plan" Branch Technical Position MTEB 5-2. [11]

[b] Estimated (low nickel weld wire used in fabricating vessel weld seams).

[c] Major working direction.

[d] Normal to major working direction.

TABLE 2-3  
 CHEMISTRY AND PROPERTIES OF JOSEPH FARLEY UNIT 2 REACTOR VESSEL MATERIALS

Component	Code No.	Grade	Cu (%)	P (%)	Ni (%)	T <sub>NDT</sub> (°F)	RT <sub>NDT</sub> (°F)	Average Upper Shelf Energy	
								Normal to Principal Working Direction (ft-lb)	Principal Working Direction (ft-lb)
CL. HD. Dome	B7215-1	A533,B,CL.1	0.17	0.010	0.49	-30	16(a)	83(a)	128
CL. HD. Flange	B7207-1	A508,CL.2	0.14	0.011	0.65	60(a)	60(a)	>56(a)	>86(c)
Vessel Flange	B7206-1	A508,CL.2	0.10	0.012	0.67	60(a)	60(a)	>71(a)	>109
Inlet Noz.	B7218-2	A508,CL.2	-	0.010	0.68	50(a)	50(a)	103(a)	158
Inlet Noz.	B7218-1	A508,CL.2	-	0.010	0.71	32(a)	32(a)	112(a)	172
Inlet Noz.	B7218-3	A508,CL.2	-	0.010	0.72	60(a)	60(a)	96(a)	150
Outlet Noz.	B7217-1	A508,CL.2	-	0.010	0.73	60(a)	60(a)	100(a)	154
Outlet Noz.	B7217-2	A508,CL.2	-	0.010	0.72	6(a)	6(a)	108(a)	167
Outlet Noz.	B7217-3	A508,CL.2	-	0.010	0.72	48(a)	48(a)	103(a)	158
Upper Shell	B7216-1	A508,CL.2	-	0.010	0.73	30	30(a)	97(a)	149
Inter Shell	B7203-1	A533,B,CL.1	0.14	0.010	0.60	-40	15	99	140
Inter Shell	B7212-1	A533,B,CL.1	0.20	0.018	0.60	-30	-10	99	134
Lower Shell	B7210-1	A533,B,CL.1	0.13	0.010	0.56	-40	18	103	128
Lower Shell	B7210-2	A533,B,CL.1	0.14	0.015	0.57	-30	0	99	145
Bottom Head Ring	B7208-1	A508,CL.2	-	0.010	0.73	40	40(a)	89(a)	137
Bottom Head Dome	B7214-1	A533,B,CL.1	0.11	0.007	0.48	-30	-2(a)	87(a)	134
Inter. Shell	A1.46	SMAW	0.02	0.009	0.96	0(a)	0(a)	>131	-
Long Seams	A1.40	SMAW	0.02	0.010	0.93	-50	-60	>106	-
Inter Shell to Lower Shell	G1.50	SAW	0.13	0.016	<.20 <sup>(b)</sup>	-40	-40	>102	-
Lower Shell Long Seams	G1.39	SAW	0.05	0.006	<.20 <sup>(b)</sup>	-70	-70	>126	-

(a) Estimate per NUREG 0800 "USNRC Standard Review Plan" Branch Technical Position MTEB 5-2. [11]

(b) Estimated.

(c) Upper shelf not available, value represents minimum energy at the highest test temperature.

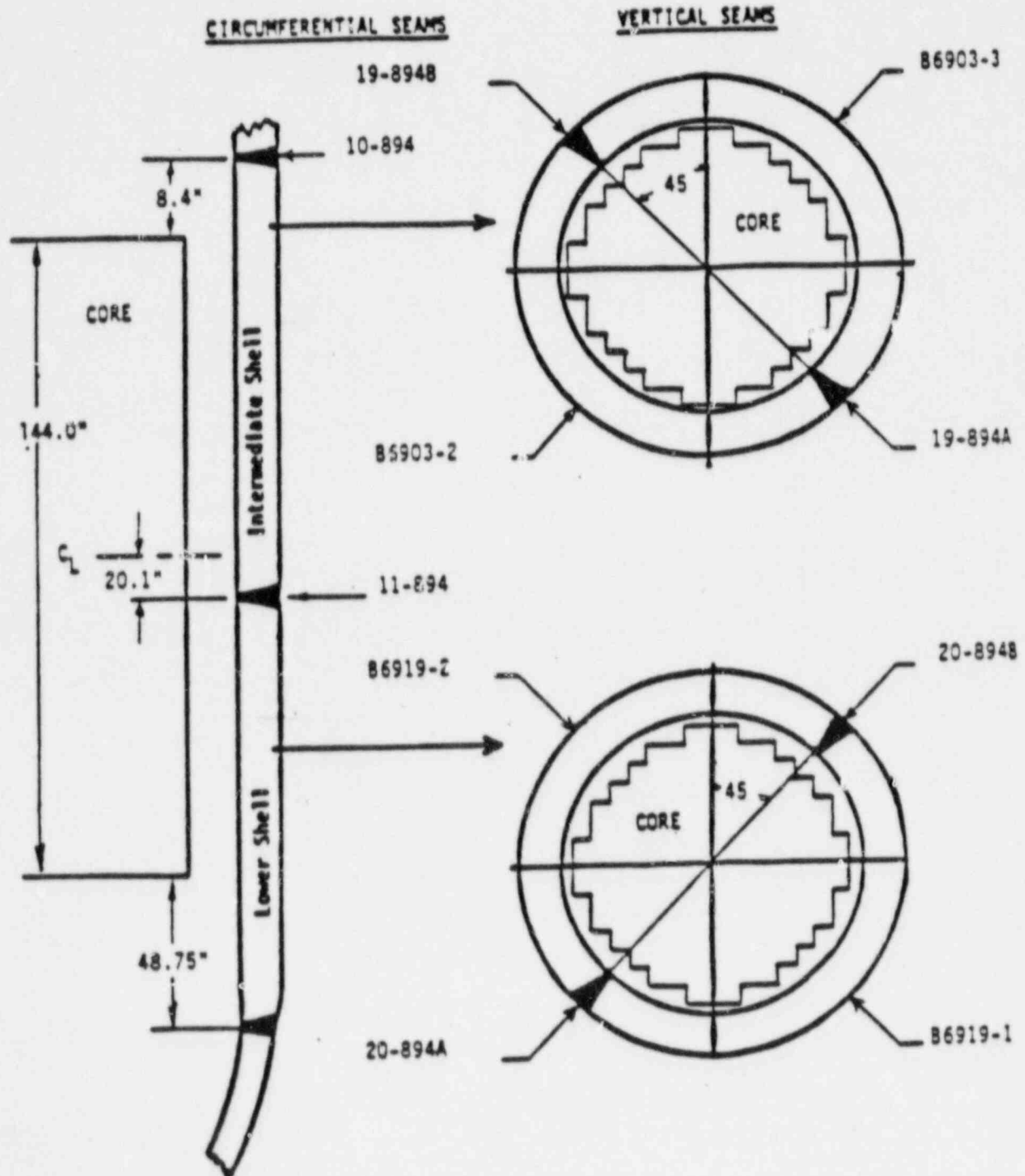
TABLE 2-4  
CHEMISTRY FACTOR FOR WELDS, °F

Copper, Wt-%	Nickel, Wt-%						
	0	0.20	0.40	0.60	0.80	1.00	1.20
0	20	20	20	20	20	20	20
0.01	20	20	20	20	20	20	20
0.02	21	26	27	27	27	27	27
0.03	22	35	41	41	41	41	41
0.04	24	43	54	55	54	54	54
0.05	26	49	67	68	68	68	68
0.06	29	52	77	82	82	82	82
0.07	32	55	85	95	95	95	95
0.08	36	58	90	106	108	108	108
0.09	40	61	94	115	122	122	122
0.10	44	65	97	122	133	135	135
0.11	49	68	101	130	144	148	148
0.12	52	72	103	135	153	161	161
0.13	58	76	106	139	162	172	176
0.14	61	79	109	142	168	182	188
0.15	66	84	112	146	175	191	200
0.16	70	88	115	149	178	199	211
0.17	75	92	119	151	184	207	221
0.18	79	95	122	154	187	214	230
0.19	83	100	126	157	191	220	238
0.20	88	104	129	160	194	223	245
0.21	92	108	133	164	197	229	252
0.22	97	112	137	167	200	232	257
0.23	101	117	140	169	203	236	263
0.24	105	121	144	173	206	236	268
0.25	110	126	148	176	209	243	272
0.26	113	130	151	180	212	246	276
0.27	119	134	155	184	216	249	280
0.28	122	138	160	187	218	251	284
0.29	128	142	164	191	222	254	287
0.30	131	146	167	194	225	257	290
0.31	136	151	172	198	228	260	293
0.32	140	155	175	202	231	263	296
0.33	144	160	180	205	231	266	299
0.34	149	164	184	209	238	269	302
0.35	153	168	187	212	241	272	305
0.36	158	172	191	216	245	275	308
0.37	162	177	196	220	248	278	311
0.38	166	182	200	223	250	281	314
0.39	171	185	203	227	254	285	317
0.40	175	189	207	231	257	288	320

TABLE 2-5  
CHEMISTRY FACTOR FOR BASE METAL, °F

Copper, Wt-%	Nickel, Wt-%						
	0	0.20	0.40	0.60	0.80	1.00	1.20
0	20	20	20	20	20	20	20
0.01	20	20	20	20	20	20	20
0.02	20	20	20	20	20	20	20
0.03	20	20	20	20	20	20	20
0.04	22	26	26	26	26	26	26
0.05	25	31	31	31	31	31	31
0.06	28	37	37	37	37	37	37
0.07	31	43	44	44	44	44	44
0.08	34	48	51	51	51	51	51
0.09	37	53	58	58	58	58	58
0.10	41	58	65	65	67	67	67
0.11	45	62	72	74	77	77	77
0.12	49	67	79	83	86	86	86
0.13	53	71	85	91	96	96	96
0.14	57	75	91	100	105	106	106
0.15	61	80	99	110	115	117	117
0.16	65	84	104	118	123	125	125
0.17	69	88	110	127	132	135	135
0.18	73	92	115	134	141	144	144
0.19	78	97	120	142	150	154	154
0.20	82	102	125	149	159	164	165
0.21	86	107	129	155	167	172	174
0.22	91	112	134	161	176	181	184
0.23	95	117	138	167	184	190	194
0.24	100	121	143	172	191	199	204
0.25	104	126	148	176	199	208	214
0.26	109	130	151	180	205	216	221
0.27	114	134	155	184	211	225	230
0.28	119	138	160	187	218	233	239
0.29	124	142	164	191	221	241	248
0.30	129	146	167	194	225	249	257
0.31	134	151	172	198	228	255	266
0.32	139	155	175	202	231	260	274
0.33	144	160	180	205	234	264	282
0.34	149	164	184	209	238	268	290
0.35	153	168	187	212	241	272	298
0.36	158	173	191	216	245	275	303
0.37	162	177	196	220	248	278	308
0.38	166	182	200	223	250	281	313
0.39	171	185	203	227	254	285	317
0.40	175	189	207	231	257	288	320

Figure 2-1. Identification and Location of Beltline Region Material for the Joseph Farley Unit No. 1 Reactor Vessel



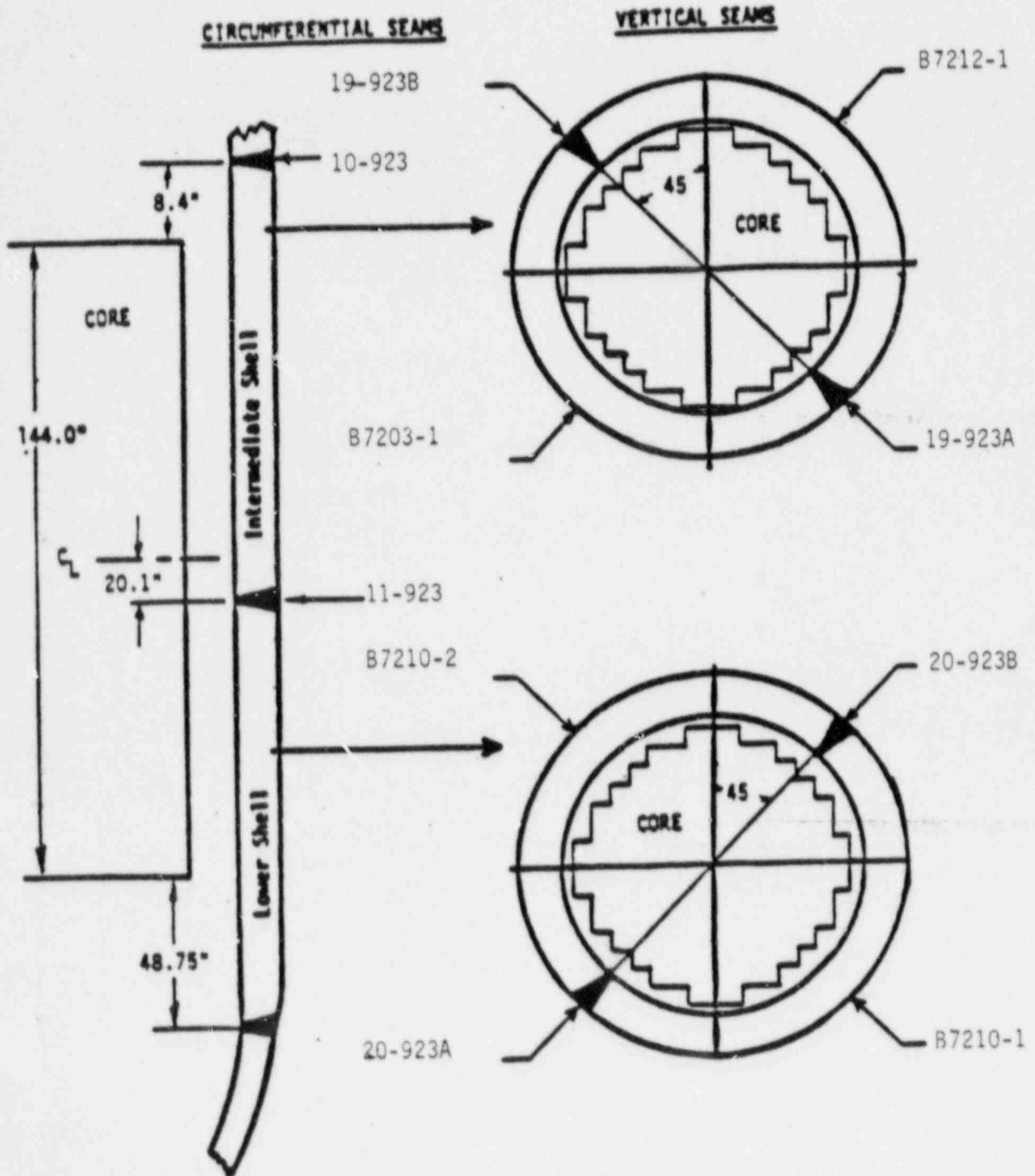


Figure 2-2. Identification and Location of Beltline Region Material for the Joseph Farley Unit No. 2 Reactor Vessel

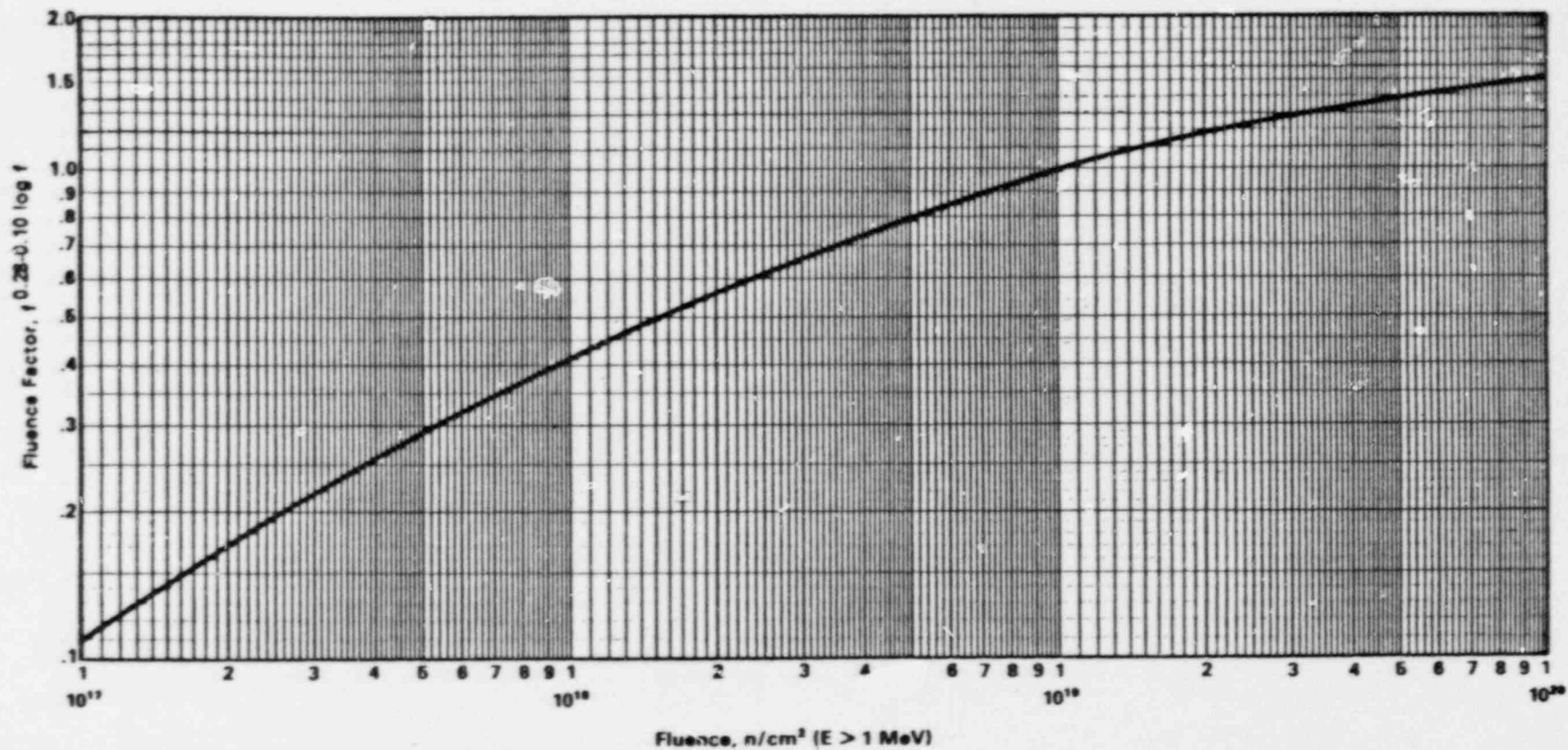


Figure 2-3. Fluence Factor For Use In The Expression for  $\Delta RT_{NDT}$

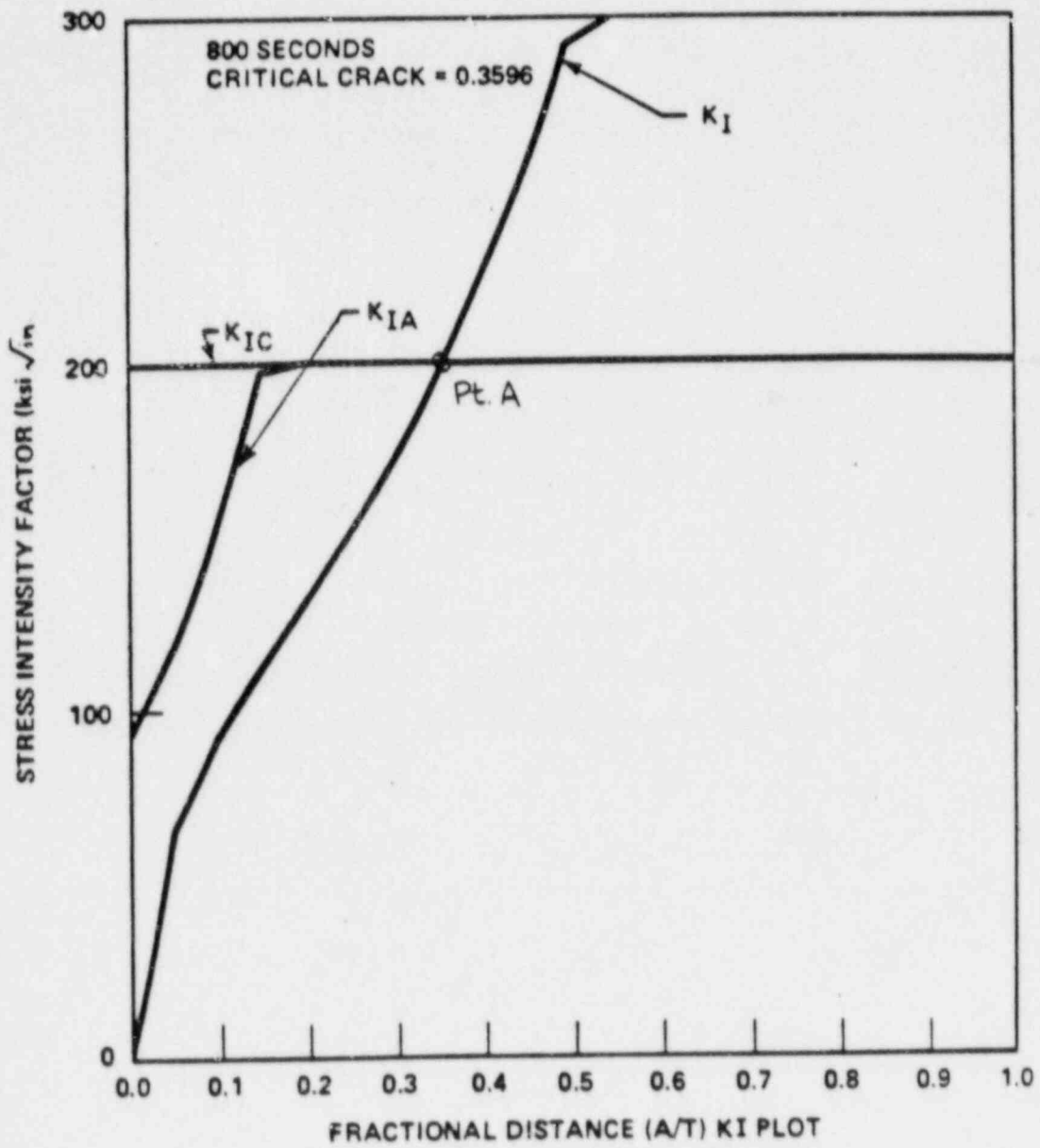


Figure 2-4. Example of Critical Flaw Size Determination

## SECTION 3

### FATIGUE CRACK GROWTH

In applying code acceptance criteria as introduced in Section 1, the final flaw size  $a_f$  used in criteria (1) is defined as the minimum flaw size to which the detected flaw is calculated to grow at the end of a specified period, or until the next inspection time. In this handbook, ten-, twenty- and thirty-year inspection periods are assumed.

These crack growth calculations have been carried out for all the regions in the Joseph Farley reactor vessels for which evaluation charts have been constructed. This section will examine each of the calculations, and provide the methodology used as well as the assumptions.

#### 3.1 ANALYSIS METHODOLOGY

The methods used in the crack growth analysis reported here are the same as those suggested by Section XI of the ASME Code. The analysis procedure involves postulating an initial flaw at specific regions and predicting the growth of that flaw due to an imposed series of loading transients. The input required for a fatigue crack growth analysis is basically the information necessary to calculate the parameter  $\Delta K_I$  which depends on crack and structure geometry and the range of applied stresses in the area where the crack exists. Once  $\Delta K_I$  is calculated, the growth due to that particular stress cycle can be calculated by equations given in Section 3.3 and Figure 3-1. This increment of growth is then added to the original crack size, and the analysis proceeds to the next transient. The procedure is continued in this manner until all the transients known to occur in the period of evaluation have been analyzed.

The transients considered in the analysis are all the design transients contained in the vessel equipment specification, as shown in Section 2, Table 2-1. These transients are spread equally over the design lifetime of the vessel, with the exception that the preoperational tests are considered first. Faulted conditions are not considered because their frequency of occurrence is too low to affect fatigue crack growth.

Crack growth calculations were carried out for a range of flaw depths, and three basic types. The first type was a surface flaw with length equal to six times its depth. The second was a continuous surface flaw, which represents a worst case for surface flaws, and the third was an embedded flaw, with length equal to three times its width. For all cases the flaw was assumed to maintain a constant shape as it grew.

### 3.2 STRESS INTENSITY FACTOR EXPRESSIONS

Stress intensity factors were calculated from methods available in the literature for each of the flaw types analyzed. The surface flaw with aspect ratio 6:1 was analyzed using an expression developed by McGowan and Raymond [2] where the stress intensity factor  $K$  is calculated from the actual stress profile through the wall at the location of interest.

The maximum and minimum stress profiles corresponding to each transient are represented by a third order polynomial, such that:

$$\sigma(x) = A_0 + A_1 \frac{x}{t} + A_2 \frac{x^2}{t^2} + A_3 \frac{x^3}{t^3} \quad (3-1)$$

The stress intensity factor  $K_I(\phi)$  can be calculated anywhere along the crack front. The point of maximum crack depth is represented by  $\phi = 0$ . The following expression is used for calculating  $K_I(\phi)$ .

$$K_I(\phi) = \left[ \frac{a}{Q} \right]^{0.5} (\cos^2 \phi + \frac{a^2}{c^2} \sin^2 \phi)^{1/4} (A_0 H_0 + \frac{2}{\pi} \frac{a}{t} A_1 H_1 + \frac{1}{2} \frac{a^2}{t^2} A_2 H_2 + \frac{4}{3\pi} \frac{a^3}{t^3} A_3 H_3) \quad (3-2)$$

The magnification factors  $H_0(\phi)$ ,  $H_1(\phi)$ ,  $H_2(\phi)$  and  $H_3(\phi)$  are obtained by the procedure outlined in reference [2].

The stress intensity factor for a continuous surface flaw was calculated using an expression for an edge cracked plate [20]. The stress distribution is linearized through the wall thickness to determine membrane and bending stress and the applied K is calculated from:

$$K_I = \sigma_m Y_m \sqrt{a} + \sigma_B Y_B \sqrt{a} \quad (3-3)$$

The magnification factors  $Y_m$  and  $Y_B$  are taken from [12] and  $a$  is the crack depth.

For an embedded flaw, the stress intensity factor expression provided in Appendix A of section XI was used directly, which again requires linearizing the stresses. The flaw shape was set with length equal to three times the width, and the eccentricity was set at 2.5, which corresponds to a flaw near the inside surface of the vessel, although still embedded. This flaw will provide a worst case calculation of stress intensity factor for embedded flaws. Since the calculated crack growth was very small for this case, no further consideration of other flaw shapes or locations was deemed necessary for an embedded flaw.

### 3.3 CRACK GROWTH RATE REFERENCE CURVES

The crack growth rate curves used in the analyses were taken directly from Appendix A of Section XI of the ASME Code. Water environment curves were used for all inside surface flaws, and the air environment curve was used for embedded flaws and outside surface flaws.

For water environments the reference crack growth curves are shown in Fig. 3-1, and growth rate is a function of both the applied stress intensity factor range, and the R ratio ( $K_{min}/K_{max}$ ) for the transient.

For  $R < 0.25$

$$(\Delta K_I < 19 \text{ ksi}\sqrt{\text{in}}) \frac{da}{dN} = (1.02 \times 10^6) \Delta K_I^{5.95} \quad (3-4)$$

$$(\Delta K_I > 19 \text{ ksi}\sqrt{\text{in}}) \frac{da}{dN} = (1.01 \times 10^{-3}) \Delta K_I^{1.95}$$

where  $\frac{da}{dN}$  = Crack Growth rate, micro-inches/cycle.

For  $R > 0.65$

$$(\Delta K_I < 12 \text{ ksi}\sqrt{\text{in}}) \frac{da}{dN} = (1.20 \times 10^{-5}) \Delta K_I^{5.95} \quad (3-5)$$

$$(\Delta K_I > 12 \text{ ksi}\sqrt{\text{in}}) \frac{da}{dN} = (2.52 \times 10^{-1}) \Delta K_I^{1.95}$$

For R ratio between these two extremes, interpolation is recommended.

The crack growth rate reference curve for air environments is a single curve, with growth rate being only a function of applied  $\Delta K$ . This reference curve is also shown in Figure 3-1.

$$\frac{da}{dN} = (0.0267 \times 10^{-3}) \Delta K_I^{3.726} \quad (3-6)$$

where,  $\frac{da}{dN}$  = Crack growth rate, micro-inches/cycle

$\Delta K_I$  = stress intensity factor range,  $\text{ksi}\sqrt{\text{in}}$

$$= (K_{I\text{max}} - K_{I\text{min}})$$

### 3.4 FATIGUE CRACK GROWTH RESULTS

The fatigue crack growth results for all locations for which handbook charts were developed are summarized in the tables which are included in Appendix C. An example is included in Table 3-1.

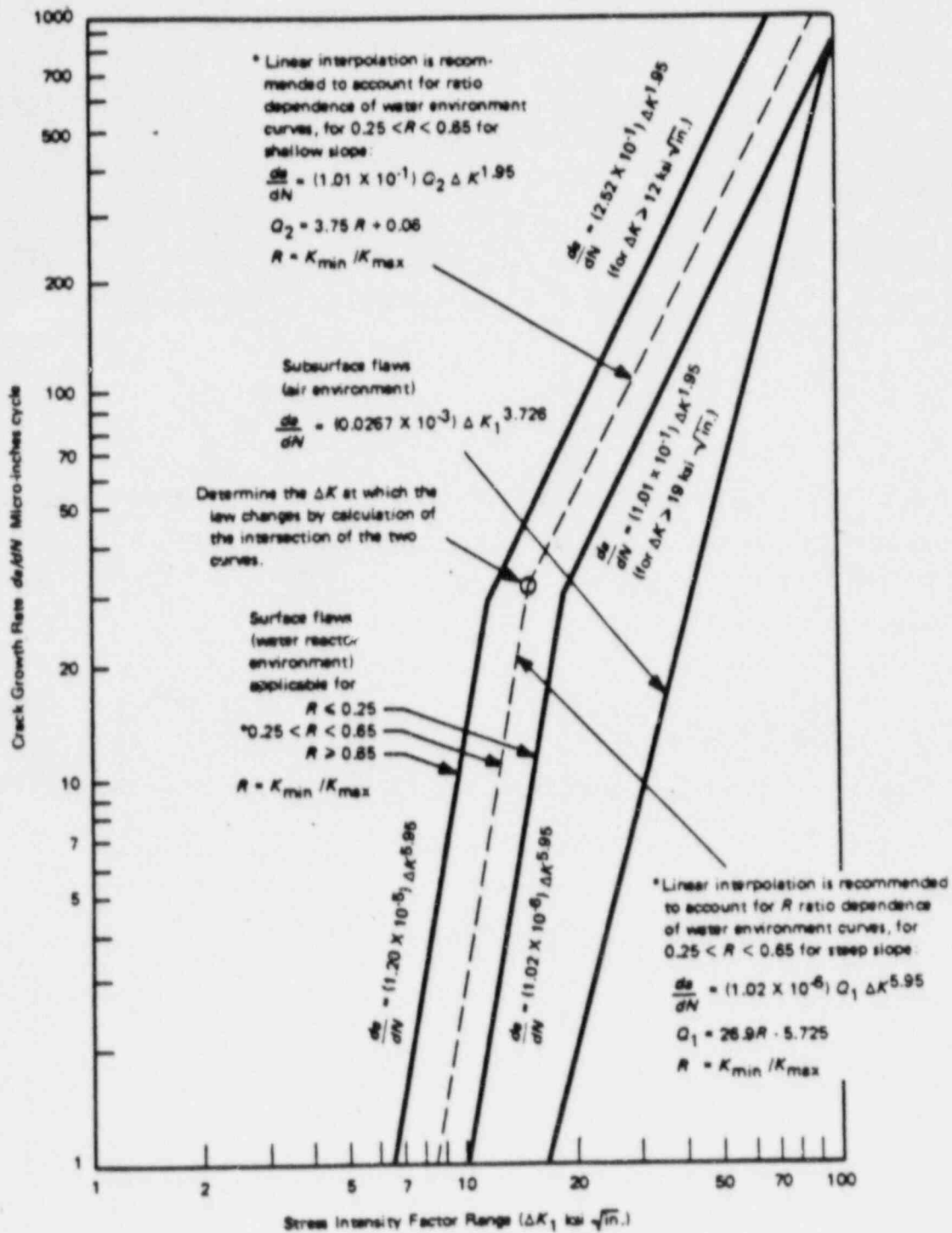


Figure 3-1. Reference Fatigue Crack Growth Curves for Carbon and Low Alloy Ferritic Steels

TABLE 3-1  
 BELTLINE REGION SURFACE FLAW FATIGUE CRACK GROWTH  
 - CIRCUMFERENTIAL FLAW

	INITIAL CRACK LENGTH	CRACK LENGTH AFTER YEAR			
		10	20	30	40
$a/t = 0.0$	0.100	0.10029	0.10051	0.10071	0.10093
	0.300	0.30559	0.30980	0.31392	0.31842
	0.500	0.51655	0.53068	0.54518	0.56063
	0.800	0.83247	0.86220	0.89248	0.92424
	1.000	1.04105	1.07914	1.11826	1.15934
	1.200	1.25608	1.30162	1.34794	1.39615
	1.300	1.35949	1.40802	1.45890	1.51202
	1.550	1.61870	1.67575	1.73367	1.79345
$a/t = 0.167$	0.100	0.10010	0.10018	0.10024	0.10032
	0.300	0.30188	0.30329	0.30463	0.30608
	0.500	0.50722	0.51287	0.51841	0.52425
	0.800	0.81267	0.82270	0.83265	0.84294
	1.000	1.01548	1.02830	1.04104	1.05429
	1.200	1.22245	1.23762	1.25260	1.26808
	1.300	1.32275	1.33802	1.35302	1.36841
	1.550	1.57467	1.59177	1.50868	1.62596

SECTION 4  
DETERMINATION OF LIMITING TRANSIENTS

#### 4.1 INTRODUCTION

The key parameters used in the evaluation of any indications discovered during inservice inspection are the critical flaw depths; first, that governing normal, upset, and test conditions and second, that governing emergency and faulted conditions.

The selection of the governing transient for normal, upset, and test conditions was done based on the highest surface stress for each location for which a chart was to be constructed. For emergency and faulted conditions, this choice was not as straightforward, as a result of developments on the pressurized thermal shock issue. This issue has resulted in a great deal of study of various transients which could occur in operating plants, including consideration of the overall frequency of each transient in addition to its severity. An extensive set of analyses have been carried out [13, 14] to consider other thermal shock transients in addition to the large loss of coolant accident (LOCA) and large steamline break (LSB) transients evaluated in previous reports [15, 16].

The following section will provide a summary of the generic work performed for PTS, along with a detailed comparison of the various emergency and faulted transients that are possible in the beltline region of the Joseph Farley Unit 1 and 2 reactor vessels.

#### 4.2 SELECTION OF GOVERNING EMERGENCY AND FAULTED TRANSIENTS

##### 4.2.1 BACKGROUND AND HISTORY

The issue of reactor vessel pressurized thermal shock (PTS) has focused significant attention to the evaluation of the vessel beltline location. Until early 1982 reactor vessel integrity was evaluated for PTS

events, which generally fall into the category of emergency and faulted conditions, usually using only design basis transient scenarios. For instance, a summary report on reactor vessel integrity for Westinghouse plants, WCAP-10019 [13], was submitted to the NRC staff in December 1981 and addressed the large LOCA and large steamline break transients along with a conservative evaluation of the small break LOCA and small steamline break events. The Joseph Farley Units 1 and 2 reactor vessels were evaluated as part of this generic evaluation supported by the Westinghouse Owners Group. Following the submittal of this information, the NRC was concerned, as a result of recent plant operating events, that other more likely events with dominating transient characteristics were not being addressed.

To respond to the above concern, an innovative methodology was developed that coupled probabilistic event sequence analysis results with thermal hydraulic and fracture mechanics analysis results to identify all potential transient scenarios of concern for reactor vessel PTS. This methodology efficiently evaluated over 8,000 possible transient scenarios on a generic basis and the results demonstrated adequate safety margin for the Westinghouse domestic operating plants. This work, which was submitted to the NRC via the Westinghouse Owners Group (WOG) in References [17, 18, 19] was extensively used by the NRC Staff in the development and improvement of their own position on PTS. The NRC used the Westinghouse probabilistic results to better quantify total plant risk from PTS and to support their licensing position as described in NRC Policy Issue SECY-82-465, November 1982 [20]. (This document provides the technical basis for the PTS Rule [21] that was issued in 1985.)

A key aspect of this work is that the principal contributors (dominating transients) to the total frequency of significant flaw extension in the vessel from PTS can be identified. However, this work was done in an approximate generic manner and both the Westinghouse Owners Group and the NRC agreed that more work should be done to investigate additional candidate transient sequences and characterizations and to validate some of the approximations made in the supporting analyses. For instance, the 2"-6" small LOCA results used detailed calculations of system response (including fluid mixing effect in the cold leg and vessel downcomer as predicted from experimental results, heat input from hot piping walls, and assumed benefits from the effect of warm

prestressing) whereas the extended high pressure injection category (i.e., events that could lead to extended high pressure safety injection operation with stagnated loop(s)) used very conservative transient characterizations. This approach lead to a conservative assessment of the total frequency of significant flaw extension.

#### 4.2.2 PTS RISK FOR A TYPICAL WESTINGHOUSE PWR

In order to address all candidate transient scenarios in a thorough manner, the Westinghouse Owners Group (WOG) undertook a Stagnant Loop Code Evaluation Program in late 1982. One key purpose of this program was to demonstrate that the overall risk from PTS on a typical Westinghouse plant is dominated by small steamline breaks, small LOCA's, and steam generator tube ruptures, as suggested in previous WOG work during 1982, and not by other transient scenarios, including those involving loop stagnation. WCAP-10319 [14] presents the results of this exhaustive study. The important results and the relationship of them to previous fracture analyses performed for the Joseph Farley Units 1 and 2 reactor vessels are discussed below.

The event sequence analysis performed in the WOG Stagnant Loop Code Evaluation resulted in the following broad categories of events that could potentially result in a pressurized thermal shock of the reactor vessel:

1. Secondary Depressurization (SD)
2. Loss of Coolant Accident (LOCA)
3. Steam Generator Tube Rupture (SGTR)
4. Loss of Secondary Heat Sink (LOHS)
5. Excessive Feedwater (EXFW)
6. Anticipated Transients Without SCRAM (ATWS)
7. Feedline Break (FB)

Combinations of these categories were also considered if they met certain criteria defined in WCAP-10319 [14]. Some of these PTS-categories were further subdivided into a number of small bins to offer greater resolution and accuracy in the risk assessment and in the identification of the dominating transient scenarios.

The summary results of the above WOG risk assessment for PTS (see Figure 4-1) showed that the key contributors to the total risk occur from the LOCA and SGTR categories because of the combination of severe transient characteristics with relatively high frequencies of transient occurrence. The LOHS transient, while much lower than LOCA or SGTR, was the third most dominating transient in terms of contributing to the total PTS risk. This is primarily because LOCA transient characteristics were conservatively used for the LOHS analysis. If the true LOHS transient results had been used, it is believed that the resulting transient characteristics would be less severe than those that were used. The other PTS transient scenarios, including those involving loop stagnation (i. e., SD, EXFW, ATWS, and FB), do not contribute significantly to the overall risk.

The ASME Code in its present form, however, does not take transient frequencies into consideration and requires an evaluation of flaw indications using the most limiting emergency/faulted condition transient. Therefore, the above PTS risk analysis results could not be used directly, but they were used to guide the determination of the key transients to be considered further, as will be seen in the next section.

#### 4.2.3 TREATMENT OF TRANSIENT SEVERITY

Probabilistic fracture mechanics (PFM) results, used in the above WOG risk assessment for PTS, were utilized to evaluate the severity of the transients used in the generic study that were major contributors to the risk of vessel failure.

Figure 4-2 shows an example of PFM results that quantify the conditional probability of reactor vessel failure (i. e., significant flaw extension) given that a PTS event occurs. The results shown in figure 4-2 were based upon the evaluation of stylized exponential cooldown transients characterized by three quantities: a final temperature ( $T_f$ ) reflecting the depth of the cooldown, a time constant ( $\beta$ ) reflecting the rate of the cooldown, and a characteristic pressure ( $P$ ) as described in figure 4-3. The curves in figure 4-2 were generated from PFM analyses using the Monte Carlo technique. A matrix of cases for given  $T_f$ ,  $\beta$ , and inner surface  $RT_{NDT}$  values were

evaluated to obtain results for generation of the curves. The  $RT_{NDT}$  values are calculated as a function of initial  $RT_{NDT}$ , material residual elements and fluence using the methodology discussed in Section 2. For each case, a large number of deterministic fracture mechanics analysis trials ( $\sim 10^6$ ) were simulated using random values selected by a random generator from distributions defined for the pertinent input properties. The input properties that have been treated as random variables include: initial crack depth, initial  $RT_{NDT}$ , copper content, fluence, and the critical stress intensity values for flaw initiation and arrest. The probability of vessel failure for each case was determined by dividing the number of failures by the number of trials. The curves in Figure 4-2 were plotted from the matrix of results by normalizing  $T_f$  against  $RT_{NDT}$  for assumed longitudinally oriented flaws.

The pertinent aspect of the PFM results for determining the governing transient(s) is that, at a given inner surface  $RT_{NDT}$  value, the higher the conditional probability of vessel failure, the more limiting the transient.

Using the stylized transient characteristics for the WOG generic transients within all of the various transient categories [14], the most limiting transients were determined from the WOG PFM results as shown in Table 4-1. The transients are shown in order of decreasing severity. The associated transient frequencies of occurrence are also given for the purpose of information.

The conditional probability of failure values ranged from  $1 \times 10^{-2}$  to  $5 \times 10^{-2}$  for the above transients at an inner surface  $RT_{NDT}$  value which is near the projected end-of-life (32 EFPY)  $RT_{NDT}$  value for the Joseph Farley 1 and 2 reactor vessels (see Section 2). For all other transient events, the conditional probability of failure values were much less than  $1 \times 10^{-2}$ . From the standpoint of statistics, however, the conditional probability of failure values were essentially the same for the above limiting transients, and any one of them could be the "governing" event. The fact that stylized transient characteristics were used in the evaluation rather than the actual transient histories lends further support to the above statement.

Although the large LOCA and LSB events are not significant contributors to the overall risk of failure because the frequency of occurrence for these events is negligible ( $\sim 1 \times 10^{-7}/r\text{-yr}$ ), the severity of these events still needs to be considered in the selection of the most limiting event for the flaw handbook. The plant specific results for these events from prior Joseph Farley analyses are considered as shown in the next section.

Therefore, we see that the large number of thermal shock and pressurized thermal shock transients (>8000) can be reduced to a list of a few key transients, as shown in Table 4-1. Fracture analysis was then concentrated on these transients, as discussed in the following section.

#### 4.2.4 EMERGENCY AND FAULTED CONDITIONS EVALUATION -- BELTLINE REGION

To determine the governing emergency and faulted conditions for the Joseph Farley reactor vessels, a series of transients were studied. These transients included the large LOCA and large steamline break (LSB) already analyzed [15, 16], and the dominating transients from the Westinghouse Owners Group pressurized thermal shock studies.

This work, which took into account the differences in plant system characteristics between Joseph Farley and the typical plant in the generic WOG evaluation, led to the conclusion that the following transients should be considered in the deterministic assessments for the beltline regions to be used for this handbook.

- o steam generator tube rupture (SGTR)
- o small LOCA
- o large LOCA
- o large steamline break (LSB)

The transient frequencies for these limiting events are also given in the table in Section 4.2.3.

Thermal, stress, and fracture analyses were performed for the beltline region, utilizing the characteristics of the above four transients, represented in the form of Figure 4-3. The limiting circumferential weld and the limiting longitudinal weld for both units were used in performing the fracture analyses. The resulting critical flaw depths for a range of shapes are shown in Table 4-1.

From this table it may be seen that the large steamline break transient evaluated previously is the governing transient for the beltline region. The detailed assessments performed for the tube rupture and small LOCA transients serve to verify this conclusion. Also, from the standpoint of total risk it is worthy of note that these latter two transients are the dominant ones. Section XI of the ASME Code presently requires that only the most severe transient be evaluated, regardless of its probability of occurrence, so the large steamline break is the governing transient for the handbook.

#### 4.2.5 FAULTED CONDITIONS EVALUATION FOR OTHER REGIONS

A number of analyses were performed by means of linear elastic fracture mechanics methods to determine the postulated minimum critical flaw size at which unstable flaw growth could occur in the Joseph Farley Units 1 and 2 reactor vessel beltline regions, as discussed above. The critical flaw size required for unstable flaw growth was determined from the intersection of the  $K_I$  curve with the  $K_{Ic}$  curve, as described in Section 2.

The conclusions reached as to the governing transients for the beltline region will not necessarily be applicable to the other regions, because the fracture toughness is not reduced from irradiation. The conditions which could lead to fracture in these other regions will be governed primarily by pressure stresses, while the conditions for the beltline regions are governed by thermal stresses. This conclusion is even more true for regions of stress discontinuity, where most of the welds are found. For this reason the severe thermal transient with the largest pressurization level was found to be generally the governing transient, i.e., the large steamline break (LSB). Although not true in general for all plants, this is the same transient found to be governing for the beltline region. The critical flaw size results for the regions analyzed are provided in Appendix B.

TABLE 4-1  
KEY PRESSURIZED THERMAL SHOCK TRANSIENTS

<u>Transient</u>	<u>WOG Frequency of Occurrence Per Reactor Year For Limiting Events</u>
o 3" Small Break LOCA in Hot Leg at Zero Power with Accumulator Injection Flow	$6.1 \times 10^{-5}$
o 3" Small Break LOCA in Hot Leg at Full Power	$4.6 \times 10^{-4}$
o Loss of Secondary Heat Sink	$1.0 \times 10^{-5}$
o Steam Generator Tube Rupture at Zero Power, 30 Minute Delay in SI Termination	$1.2 \times 10^{-5}$
o Steam Generator Tube Rupture at Moderate Decay Heat, 30 Minute Delay in SI Termination	$1.9 \times 10^{-5}$

TABLE 4-1  
CRITICAL FLAW SIZE SUMMARY FOR BELTLINE REGION

Condition	Flaw Orient.	Continuous Flow		Aspect Ratio = 6.0		Aspect Ratio = 2.0	
		inches	a/t	inches	a/t	inches	a/t
E/F (Steam Gen. Tube Rupture)	Long.	$a_i = 2.50$	(0.323)	$a_i = 5.51$	(0.711)	$a_i = 7.75$	(1.0)
	Circ.	$a_i = 7.75$	(1.0)	$a_i = 7.75$	(1.0)	$a_i = 7.75$	(1.0)
E/F (LSB)	Long.	$a_i = \text{N/A}$	N/A	$a_i = 3.39$	(0.44)	$a_i = \text{N/A}$	N/A
	Circ.	$a_i = 2.21$	(0.34)	$a_i = 7.75$	(1.00)	$a_i = 7.75$	(1.0)
E/F (Small LOCA)	Long.	$a_i = 2.25$	(0.33)	$a_i = 5.74$	(0.74)	$a_i = 7.75$	(1.0)
	Circ.	$a_i = 7.75$	(1.00)	$a_i = 7.75$	(1.00)	$a_i = 7.75$	(1.0)
E/F (Large LOCA)	Long.	$a_i = 7.75$	(1.00)	$a_i = 7.75$	(1.00)	$a_i = 7.75$	(1.0)
	Circ.	$a_i = 7.75$	(1.00)	$a_i = 7.75$	(1.00)	$a_i = 7.75$	(1.0)
N/U (Excessive Feedwater Flow)	Long.	$a_c = 3.83$	(0.494)	$a_c = 7.75$	(1.00)	$a_c = 7.75$	(1.0)
	Circ.	$a_c = 7.75$	(1.00)	$a_c = 7.75$	(1.00)	$a_c = 7.75$	(1.0)

6-4

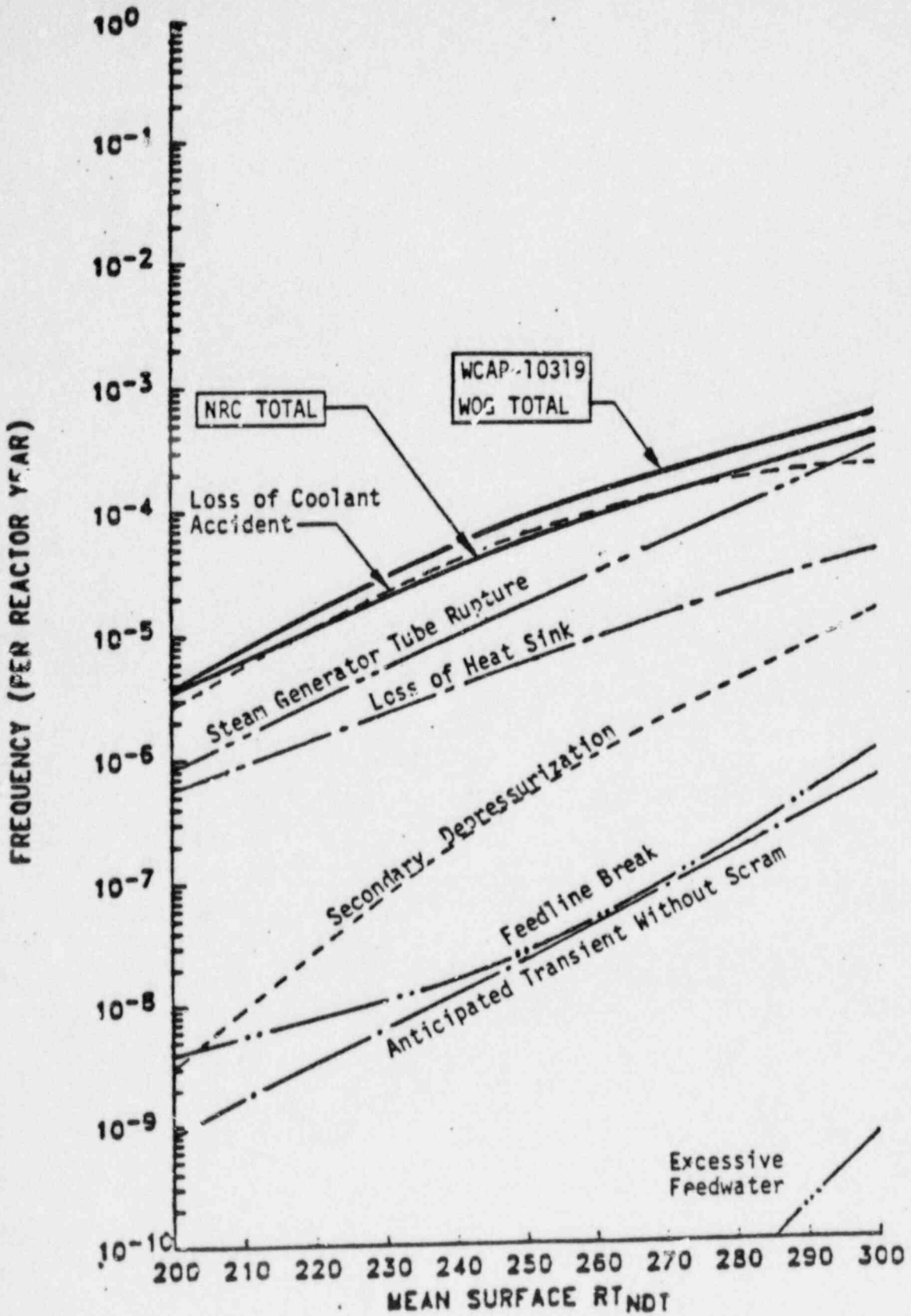


Figure 4-1. Frequency of Significant Flow Extension for Longitudinal Flaws in a Typical Westinghouse PWR

CONDITIONAL REACTOR VESSEL FAILURE PROBABILITIES FOR A SINGLE

LONGITUDINAL BELTLINE WELD-P=1500 psig

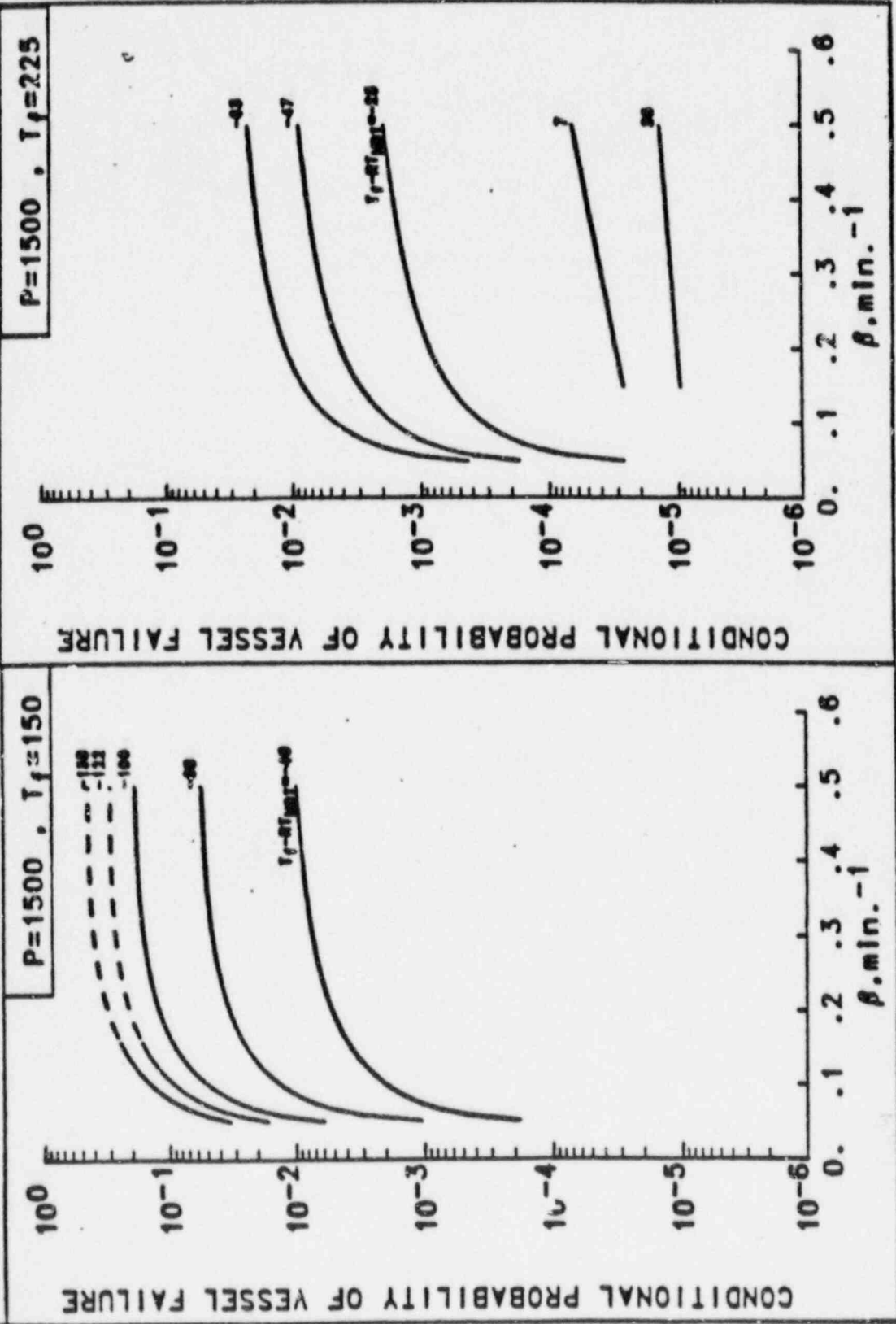
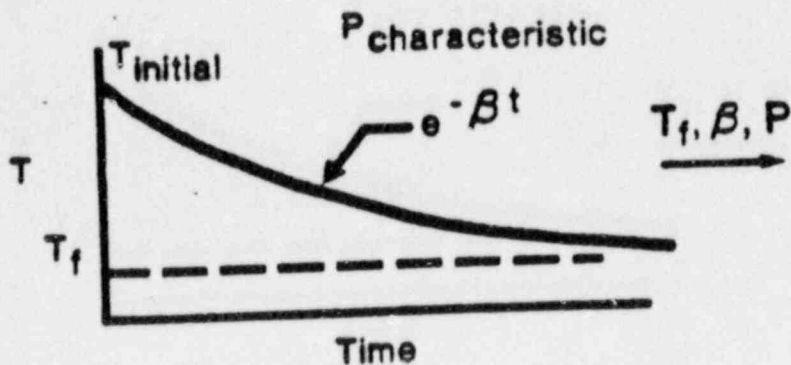


Figure 4-2



<u>PARAMETER</u>	<u>SMALL LOCA</u>	<u>LARGE LOCA</u>	<u>LARGE STEAM LINE BREAK</u>	<u>STEAM GEN. TUBE RUPTURE</u>
$\beta$	.1 $\text{Min}^{-1}$	-	0.25 $\text{min}^{-1}$	$\sim 0.10 \text{ min}^{-1}$
$T_F$	100°F	70°F	225°F	174°F
$T_I$	550°F	550°F	550°F	557°F
$P$	1000 psig	0 psig	1550 psig	1000-1800 psig

Figure 4-3. Schematic Representation of Emergency and Faulted Transients for Joseph Farley, along with actual values used for Transients Evaluated.

SECTION 5  
SURFACE FLAW EVALUATION

5.1 CODE CRITERIA

The acceptance criteria for surface flaws have been presented in paragraph 1.1. For convenience they are repeated as follows:

$$a_f \leq .1 a_c \quad \begin{array}{l} \text{For Normal Conditions} \\ \text{(Upset \& Test Conditions inclusive)} \end{array}$$

and

$$a_f \leq .5 a_i \quad \begin{array}{l} \text{For Faulted Conditions} \\ \text{(Emergency Condition inclusive)} \end{array}$$

where

$a_f$  = The maximum size to which the detected flaw is calculated to grow until the next inspection. 10, 20, and 30 year periods have been considered in this handbook.

$a_c$  = The minimum critical flaw size under normal operating conditions (upset and test conditions inclusive)

$a_i$  = The minimum critical flaw size for initiation of nonarresting growth under postulated faulted conditions. (emergency conditions inclusive)

Alternatively criteria based on applied stress intensity factors may be used:

$$K_I \leq \frac{K_{Ia}}{\sqrt{10}} \quad \text{For normal conditions (upset \& test conditions inclusive)}$$

$$K_I \leq \frac{K_{Ic}}{\sqrt{2}} \quad \text{For faulted conditions (emergency conditions inclusive)}$$

where

$K_I$  = The maximum applied stress intensity factor for the flaw size  $a_f$  to which a detected flaw will grow, during the conditions under consideration.

$K_{Ia}$  = Fracture toughness based on crack arrest for the corresponding crack tip temperature.

$K_{Ic}$  = Fracture toughness based on fracture initiation for the corresponding crack tip temperature.

## 5.2 LONGITUDINAL FLAWS VS. CIRCUMFERENTIAL FLAWS

Longitudinal flaws may be defined as flaws oriented in a radial plane, such that circumferential or hoop stresses would tend to open them. On the other hand, circumferential flaws would be oriented in a radial plane such that longitudinal or axial stresses would open them. These two types of flaws are portrayed graphically in the geometry figure of each section of Appendix A.

## 5.3 BASIC DATA

In view of the criteria, it is noticed that three groups of basic data are required for the construction of charts for surface flaw evaluation. Namely,  $a_f$ ,  $a_c$ , and  $a_i$ , respectively.

The preparation of these three groups of basic data will be discussed in the following paragraphs.

### 5.3.1 FATIGUE CRACK GROWTH

The first group of basic data required for surface flaw chart construction is the final flaw size  $a_f$  determined from fatigue crack growth. As defined in IWB-3611 of Code section XI,  $a_f$  is the maximum size resulting from growth during a specific time period, which is the next scheduled inspection of the

component. Therefore, the final depth,  $a_f$  after a specific service period of time must be used as the basis for evaluation. The charts have been constructed to allow the initial (measured) indication size to be used directly. Charts have been constructed for operational periods of 10, 20, and 30 years from the time of detection.

The final flaw size  $a_f$  can be calculated by fatigue crack growth analysis, which has been performed covering the range of postulated flaw sizes, and flaw shapes at various locations of the reactor vessel needed for the construction of surface flaw evaluation charts in this handbook. All crack growth results have been summarized in Appendix C.

Notice that all the finite surface flaws and embedded flaws analyzed are semi-elliptical in shape. Crack growth analyses for finite surface flaws with aspect ratio (length to depth) less than 6:1 have utilized the results of 6:1, and for any flaw with aspect ratio larger than 6:1, the results of the continuous flaw are used. This is conservative in both cases.

In some of the regions, it is noted that only the crack growth analysis for longitudinal flaws was performed. The crack growth results for the longitudinal flaws can be used for circumferential flaws at the same location with some slight conservatism. In regions where differences are significant, separate analyses have been done, as may be seen in the various sections of Appendix A.

### 5.3.2 MINIMUM CRITICAL FLAW SIZE $a_c$ and $a_f$

By definition  $a_c$  is the minimum critical flaw size for normal operating conditions. It is calculated based on the load of the most limiting transient for normal operating conditions. By the same token,  $a_f$  is defined as the minimum critical flaw size for faulted conditions. It is calculated based on the most governing transient of faulted conditions. The governing transients are often different for different regions, and those for each category of load conditions have been identified in tables in Appendix B. The theory and methodology for the calculation of  $a_f$  and  $a_c$  has been provided in Section 2.

#### 5.4 TYPICAL SURFACE FLAW EVALUATION CHART

Two basic dimensionless parameters can fully address the characteristics of a surface flaw, and are used for the evaluation chart construction, Namely:

- o Flaw Shape Parameter  $a/\ell$
- o Flaw Depth Parameter  $a/t$

where,

- t - wall thickness, in.
- a - flaw depth, in.
- $\ell$  - flaw length, in.

A typical chart was chosen for illustration purpose as follows: (Refer to Figure 5-1)

- o the flaw shape parameter  $a/\ell$  was plotted as the abscissa from 0 (continuous flaw) to .5 (AR = 2.0)
- o The flaw depth parameter  $a/t$  in % was plotted as the ordinate.
- o The lower curves were the Code acceptable flaw depth tabulated in Table IWB-3510-1 of ASME Section XI. These curves indicate the acceptance standards of the Code, below which analytical evaluation is not required. Two curves are provided, since the code acceptance standards were revised with the Winter Addendum of the 1983 Code. The revised curves remain in effect through the present time (1986 Code, 1988 Addenda).
- o The upper boundary curve shows the maximum acceptable flaw depth beyond which no surface flaw is acceptable for continued service without repair. This upper bound curve has been determined by the fracture and fatigue evaluations described herein.

- o Any surface indication which falls between the two boundary curves will be acceptable by the Code, with the analytical justification provided herein. However, IWB-2420 of ASME Section XI requires future monitoring of such indications.

The surface flaw evaluation charts constructed for various locations of the reactor vessel are presented in Appendix A.

### 5.5 PROCEDURE FOR THE CONSTRUCTION OF A SURFACE FLAW EVALUATION CHART

A numerical example is used here to show how a surface flaw evaluation chart was constructed.

#### Example

Required: To construct a surface flaw evaluation chart for the longitudinal flaws at the beltline region, at the inside surface.

#### Step 1

Determine the critical flaw sizes from Table 4-1. These flaw sizes are used to determine allowable flaw sizes per IWB-3611.

Load Condition	Flaw Orientation	Critical Flaw Depth (in.)		
		$a/\ell = 0.0$	$a/\ell = 0.167$	$a/\ell = 0.5$
N/U/T*	Circumferential	$a_c = 7.75$	$a_c = 7.75$	$a_c = 7.75$
E/F*	Circumferential	$a_i = 2.21$	$a_i = 7.75$	$a_i = 7.75$

Note that in some cases here the critical flaw depth is set equal to the wall thickness. This is for the case where the stress intensity factor for postulated flaws never exceeds the fracture toughness, regardless of flaw depth.

\* N/U/T normal, upset, and test conditions  
E/F emergency and faulted conditions

The maximum code allowable flaw depths using the criteria of IWB-3611 are then determined, using a factor of 10 for normal upset and test conditions and a factor of 2 for emergency and faulted conditions. The results are presented below:

Load Condition	Allowable Flaw Depth (in)		
	a/l = 0.0	a/l = 0.167	a/l = 0.5
N/U/T	0.775	0.775	0.775
E/F	1.105	3.875	3.875

Therefore, the allowable flaw depth for the normal and upset conditions is more limiting, and the governing transient can be considered as the excessive feedwater flow transient. This is because much larger safety factors are applied to the normal/upset conditions than to the emergency and faulted conditions.

### Step 2

Determine the maximum Code allowable flaw depth per IWB-3612, which is based on allowable stress intensity factor criteria.

Load Condition	Flaw Orientation	Code Criteria	Allowable Flaw Depth (in)		
			a/l = 0.0	a/l = 0.167	a/l = 0.5
N/U/T	Circumferential	$K_{Ia}/\sqrt{10}$	3.18	3.84	4.078

### Step 3

The allowable flaw depth is then determined from the Step 1 and Step 2 allowable flaw depths. The most liberal results are taken for each set of criteria, and this becomes the final allowable. Thus, from the results of Step 2 we find:

$a/l = 0.0$	allowable $a = 3.18$ in.
$a/l = 0.167$	$a = 3.84$ in.
$a/l = 0.5$	$a = 4.078$ in.

#### Step 4

Determine the corresponding initial flaw sizes which will grow to the above critical flaw sizes after 10, 20, and 30 years of service.

We define the above limiting critical flaw depth as  $a_f$ . The initial flaw size  $a_o$  can be found from the fatigue crack growth results of Table 3-1.

The values of  $a_o$  which are applicable to 10 years of service, for example, are listed as follows:

	Continuous Flaw	$a/l = 0.167$	$a/l = 0.5$
$a_f$	3.18	3.84	4.078
$a_o$	3.056	3.80	4.034

This shows that the effect of fatigue crack growth in this region is very small.

#### Step 5

Determine  $a/l$  vs.  $a/t$  in the beltline region where  $t = 7.75$ ", and  $a = a_o$ . For 10 years of service, the values are:

	Continuous Flaws	Finite Surface Flaws, $a/l = 0.167$	Finite Semicircular Surface Flaws
$a/l$	0	.167	.5
$a/t$	0.394	0.490	0.5205

Note that the allowable flaw depths here exceed 20 percent of the wall thickness, which has been set as an arbitrary limit, based on engineering judgement. The charts therefore refer to this value as an upper limit.

#### Step 6

The upper bound curves result from the plots of  $a/\ell$  vs.  $a/t$  for 10, 20, 30 years of service, as obtained from the crack growth results. These curves are shown in Figure 5-2.

#### Step 7

Plot  $a/\ell$  vs.  $a/t$  data from the standards tables of Section XI as the lower curve of Figure 5-2.

For example, the values of Table IWB-3510-1 for Code editions up until the Winter '83 addendum are:

<u>Aspect Ratio, <math>a/\ell</math></u>	<u>Surface Indication, <math>a/t, \%</math></u>
0.00	1.8
0.05	2.0
0.10	2.2
0.15	2.4
0.20	2.7
0.25	3.1
0.30	3.5
0.35	3.5
0.40	3.5
0.45	3.5
0.50	3.5

The above seven steps would complete the procedure for the construction of the surface flaw evaluation charts for 10 years, 20 years, or 30 years of operating life.

In the interest of prudence, Figure 5-2 only shows the allowable flaw depths for these inside surface flaws up to 20 percent of the section thickness.

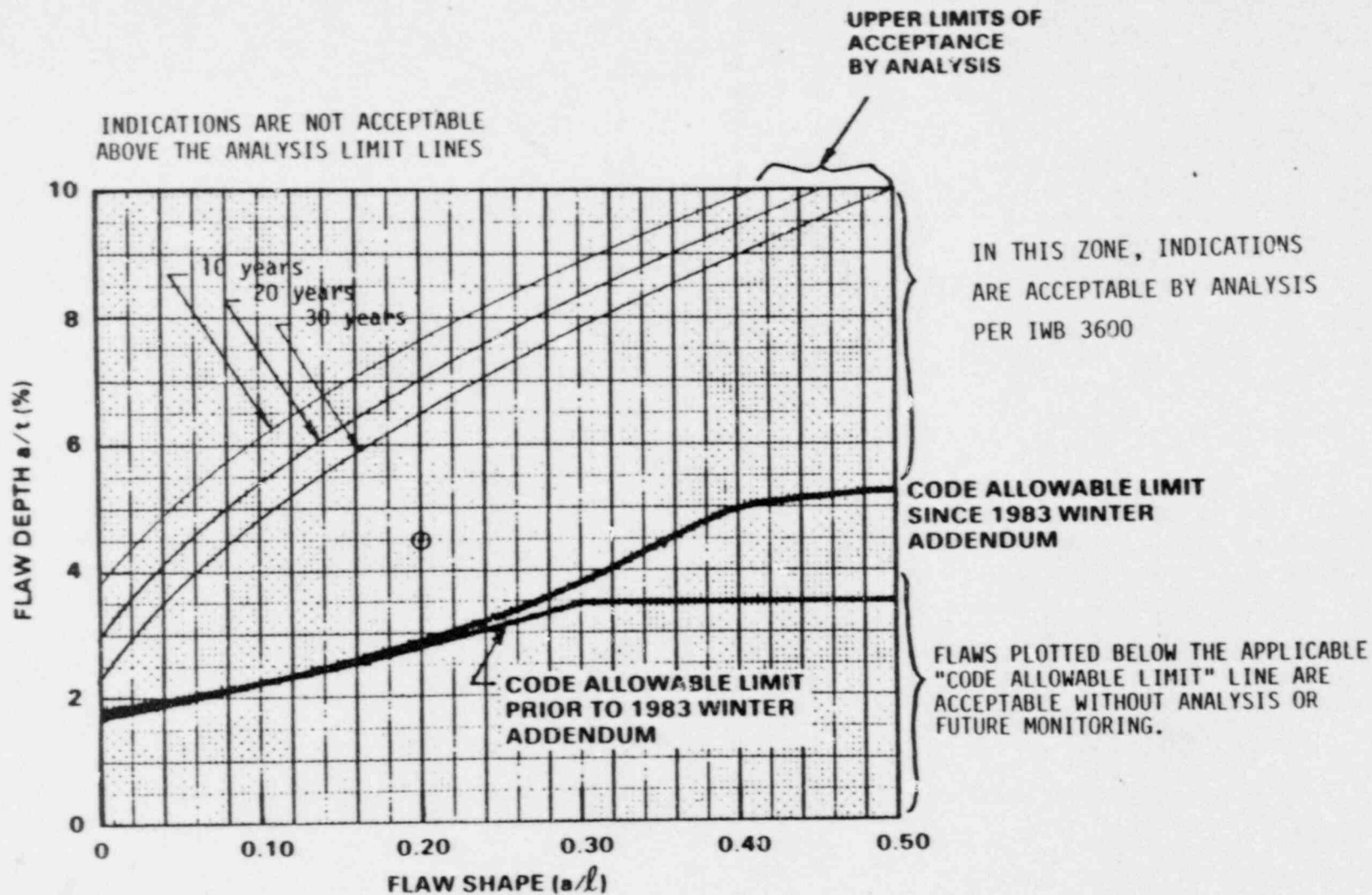


Figure 5-1. Sample Surface Flaw Evaluation Chart

LEGEND

- A - The 10, 20, 30 year acceptable flaw limits.
- B - Within this zone, the surface flaw is acceptable by ASME Code analytical criteria in IMB-3600.
- C - ASME Code allowable since 1983 Winter Addendum.
- D - ASME Code allowable prior to 1983 Winter Addendum.

© Westinghouse 1987

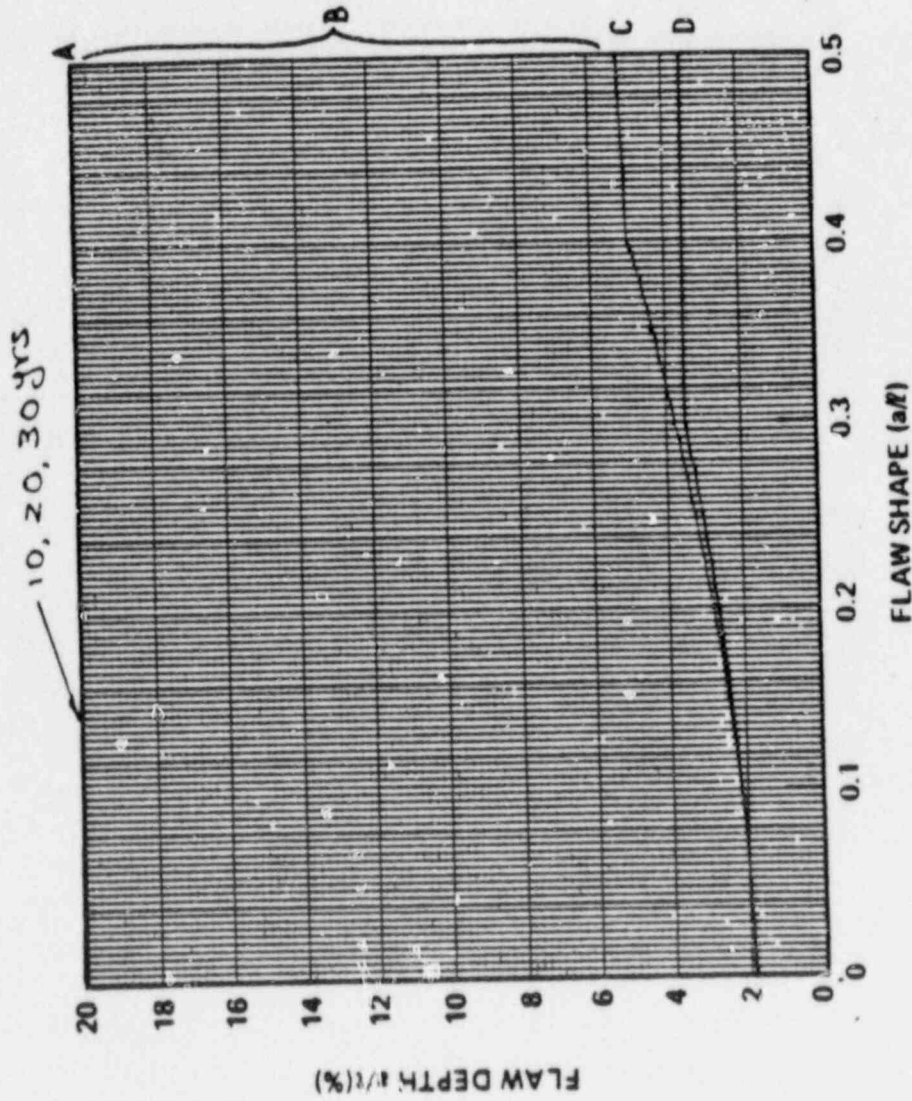


Figure 5-2 Evaluation Chart for Reactor Vessel Beltline  
 X Inside Surface X Surface Flaw X Longitudinal Flaw  
 — Outside Surface — Embedded Flaw X Circumferential Flaw

SECTION 6  
EMBEDDED FLAW EVALUATION

6.1 EMBEDDED VS. SURFACE FLAWS

According to IWA-3300 of the ASME Code Section XI, a flaw is defined as embedded, as shown in Figure 6-1, whenever,

$$S \geq a \text{ [For Editions prior to 1980]}$$

or

$$S \geq 0.4 a \text{ [For Editions of 1980 and thereafter]}$$

where

S - the minimum distance from the flaw edge to the nearest vessel wall surface (clad-base metal interface for flaws near the inside of the vessel)

a - the embedded flaw depth, (defined as the semi-minor axis of the elliptical flaw.)

Surface Proximity Rules

The surface proximity rules were liberalized with the 1980 Code, allowing flaws as near the surface as four-tenths their width to be considered embedded. This change resulted from the finding that the original proximity rules had been more restrictive for near-surface embedded flaws than for known surface flaws, which is clearly not technically correct. Specifically, the criterion for a flaw to be considered embedded was changed to  $S \geq 0.4 a$ , so substituting into the definition for  $\delta$  we now find:

WESTINGHOUSE CLASS 3  
CUSTOMER DESIGNATED DISTRIBUTION

$$a \leq \delta - S$$

$$\delta \geq 1.4 a$$

Therefore, the limit for a flaw to be considered embedded is  $a_o = 0.714 \delta$  for Code editions of 1980 and thereafter. This more accurate criterion has been used throughout this handbook, and is recommended for all inspections, regardless of the edition of the Code which is used for the inspection.

A flaw lying within the embedded flaw domain is to be evaluated by the embedded flaw evaluation charts generated in this section of the handbook. On the other hand, a flaw lying beyond this domain should be evaluated as a surface flaw using the charts developed in Section 5 of the handbook instead. The demarcation lines between the two domains are shown graphically in Figure 6-3, for both earlier and later Code editions.

In other words, for any flaw indication detected by inservice inspection, the first step of evaluation is to define the category to which the flaw actually belongs, then, choose the appropriate charts for evaluation.

## 6.2 CODE CRITERIA

As mentioned in Section 1, the criteria used for all the embedded flaws are from IWB-3612 of ASME Code Section XI. Namely,

$$K_I \leq \frac{K_{Ia}}{\sqrt{10}} \text{ For normal conditions (upset \& test conditions inclusive)}$$

$$K_I \leq \frac{K_{Ic}}{\sqrt{2}} \text{ For faulted conditions (emergency conditions inclusive)}$$

where

$K_I$  = The maximum applied stress intensity factor for the flaw size  $a_f$  to which a detected flaw will grow, during the conditions under consideration.

$K_{Ia}$  = Fracture toughness based on crack arrest for the corresponding crack tip temperature.

$K_{Ic}$  = Fracture toughness based on fracture initiation for the corresponding crack tip temperature.

The above two criteria must be met simultaneously. In this handbook only the most limiting results have been used as the basis of the flaw evaluation charts.

### 6.3 BASIC DATA

In view of the criteria based on stress intensity factor, three basic groups of data are needed for construction of embedded flaw evaluation charts. They are:  $K_{Ic}$ ,  $K_{Ia}$ , and  $K_I$ , respectively. The units used herein for all these three parameters are  $\text{ksi}\sqrt{\text{in}}$ .

$K_{Ic}$  and  $K_{Ia}$  are the initiation and arrest fracture toughness values (respectively) of the vessel material at which the flaw is located. They can be calculated by formulae:

$$K_{Ic} = 33.2 + 2.806 \exp[.02(T - RT_{NDT} + 100^\circ\text{F})] \quad (6-1)$$

and

$$K_{Ia} = 26.8 + 1.233 \exp[.0145(T - RT_{NDT} + 160^\circ\text{F})] \quad (6-2)$$

$K_I$  is the maximum stress intensity factor for the embedded flaw of interest. The methods used for determining the stress intensity factors for embedded flaws have been referenced in Section 2.

Notice that both  $K_{Ic}$  and  $K_{Ia}$  are a function of crack tip temperature  $T$ , and the material property of  $RT_{NDT}$  at the tip of the flaw. The upper shelf fracture toughness of the reactor vessel steel is assumed to be 200  $\text{ksi}\sqrt{\text{in}}$  in all regions.

$K_I$  used in the determination of the flaw evaluation charts is the maximum stress intensity factor of the embedded flaw under evaluation. It is important to note that the flaw size used for the calculation of  $K_I$  is not the flaw size detected by inservice inspection. Instead, it is the calculated flaw size which will have grown from the flaw size detected by inservice inspection. That means that the embedded flaw size used for the calculation of  $K_I$  had to be determined by using fatigue crack growth results, similar to the approach used for surface flaw evaluation, as illustrated in the previous section.

#### 6.4 FATIGUE CRACK GROWTH FOR EMBEDDED FLAWS

Unlike the surface flaw case, the fatigue crack growth for an embedded flaw (even after 40 years of service life) is very small in comparison with that of a surface flaw with the same initial depth. Consequently, in the handbook evaluations, the detected flaw size has been used for evaluation by the charts without any appreciable error.\* This simplifies the evaluation procedure without sacrificing the accuracy of the results. A detailed justification of this conclusion is provided in this section.

The environment of an embedded flaw is considered to be inert, or air. The crack growth rate for air environment is far smaller than that of the water environment, to which the surface flaw is conservatively considered to be exposed. Consequently, the fatigue crack growth for an embedded flaw must be far smaller than that of an inside surface flaw (of the same size and under

---

\* This conclusion holds for the range of flaw sizes acceptable by the rules of section XI, IWB-3600. It would not necessarily hold for very large flaws of the order of 50 percent of the vessel wall thickness.

the same transient conditions). Numerically, the fatigue crack growth of an embedded flaw is so low that the difference between the initial flaw depth and its final crack depth is negligible.

This engineering judgment has been demonstrated by an illustrative example, as follows:

Example

The beltline region of the Joseph Farley reactor vessels was used as a demonstration. The crack growth results for circumferential inside surface flaws ( $a/t = 0.167$ ) are as follows, as also shown in Appendix C. These flaws were assumed exposed to the water environment.

<u>Postulated Initial Crack Depth</u>	<u>Crack Depth (in.) After Year</u>			
	<u>10</u>	<u>20</u>	<u>30</u>	<u>40</u>
0.80	.813	0.823	0.833	0.843
1.00	1.015	1.028	1.041	1.054
1.20	1.222	1.237	1.253	1.268
1.30	1.323	1.338	1.353	1.368
1.550	1.575	1.592	1.609	1.626

A similar crack growth analysis was performed for an embedded flaw, using the same set of transients\* and the number of cycles\* as the surface flaw run, and the results follow. The air crack growth reference law was used.

\* As specified in Table 2-1.

<u>Initial Crack Depth</u>	<u>Crack Depth (in.) After Year</u>			
	<u>10</u>	<u>20</u>	<u>30</u>	<u>40</u>
0.90	0.900	0.900	0.901	0.901
1.050	1.050	1.051	1.051	1.051
1.200	1.200	1.201	1.201	1.201
1.350	1.351	1.351	1.352	1.352

In comparing the results of the two types of flaws under the same service conditions, it is seen that the final crack growth for an embedded flaw is less than 1% of that for a surface flaw under the same operating conditions as tabulated below:

<u>Postulated Initial Crack Depth, (in)</u>	<u>Final Crack Depth (in) After 40 Years Embedded Flaws</u>	<u>Crack Growth for Embedded Flaws, in (%)</u>
0.90	0.90075	0.1%
1.050	1.05108	0.1%
1.200	1.20149	0.1%
1.350	1.35202	0.15%

In conclusion: in the construction of the evaluation charts for the embedded flaws, the accuracy of the charts would not be impaired using the flaw size found by inservice inspection directly.

## 6.5 TYPICAL EMBEDDED FLAW EVALUATION CHART

The details of the procedures for the construction of an embedded flaw evaluation chart are provided in the next section.

In this section, instructions for reading a chart are provided by going through construction of a typical chart, Figure 6-3, step by step. This will help the users to become familiar with the characteristics of each part of the chart, and make it easier to apply. This example utilizes the surface/embedded flaw demarkation criteria of the 1980 Code, and later editions.

Following are the highlights of a typical embedded flaw evaluation chart. (Refer to Figures 6-2 and 6-3).

1. The abscissa of the chart in Figure 6-2 represents the flaw depth  $a$ , of the embedded flaw.
2. As defined by the Code, the embedded flaws with a depth less than  $a_0 = 0.714 \delta$  should be considered as embedded flaws. Any embedded flaws beyond the domain of  $a_0 = 0.714 \delta$ , should be evaluated by means of surface flaw charts instead.
3. A key parameter for evaluating an embedded flaw is  $\delta$ , the distance between the flaw centerline and the nearest surface of the vessel wall (clad-base metal interface for the inside surface).

A range of  $\delta$  between  $\frac{1}{16}t$  and  $\frac{1}{4}t$  have been considered in constructing Figure 6-2.

4. For each specific value of  $\delta$ , such as  $\frac{1}{16}t$ ,  $\frac{3}{32}t$ ,  $\frac{1}{8}t$ , etc., a family of curves were plotted for a range of aspect ratios\*, for 3:1 through 10:1. This corresponds to  $a/\ell$  values ranging from 0.333 to 0.1. For any specific flaw depth  $a$  at the abscissa, a corresponding value  $K_I$  at the ordinate can be found in Figure 6-2, for any distance to the surface,  $\delta$ .

---

\*Note that aspect ratio  $AR = \ell/a$

5. The range of aspect ratios from 3:1 to 10:1 was chosen to encompass the range of flaws which might be detected. Within this range, interpolation can be used for any other aspect ratio. Use the 3:1 curve as a lower bound and the 10:1 curve as an upper bound.
6. In this specific chart, the Code acceptance limit line was

$$\frac{K_{Ia}}{\sqrt{10}} = \frac{200}{\sqrt{10}} = 63.3 \text{ ksi in}$$

because governing condition was an upset

condition, and the operating temperature of the transient was over 500°F across the wall thickness at all times. The shelf value of 200 ksi√in for  $K_{Ia}$  was used.

7. The intersection of the  $K_I$  curve with the code acceptance limit line is the maximum flaw size acceptable by Code for the specific curve.
8. In view of Figure 6-2, it is seen that only the curves for  $\delta = \frac{1}{4}t$  intersect with the code acceptance limit line. That means that, up to a distance of  $\delta = \frac{3}{16}t$  (= 1.453"), all embedded flaws are acceptable by code criterion so long as their depth is within the domain of  $a_o = 0.714 \delta$ . On the other hand, for flaws located at a distance up to  $\delta = \frac{1}{4}t$  (= 1.938"), the maximum acceptable flaw sizes for various aspect ratios are less than the domain of  $a_o = .714 \delta$ . Therefore, for flaws centered at this depth, separate allowable flaw lines are produced in the evaluation charts, as shown in Figure 6-3.
9. The maximum acceptable flaw size can be found from the chart by determining the abscissa of the intersection points. Namely, for  $\delta = 0.25 t$ ,

<u>Aspect Ratio of the Flaw</u>	<u>a/l</u>	<u>Maximum Acceptable Flaw Size (in)</u>
10:1	0.1	0.968
6:1	0.167	0.968 (< a <sub>o</sub> = 0.969)
3:1	0.333	0.968

10. The maximum acceptable embedded flaw size for  $\delta = \frac{1}{4}t$  has been depicted in Figure 6-3. This simpler flaw evaluation chart, described in the following paragraph, is the type included in the handbook, as may be seen in Appendix A.

These embedded flaw evaluation charts, constructed for various locations of the reactor vessel, are presented in Appendix A.

#### 6.6 PROCEDURES FOR THE CONSTRUCTION OF EMBEDDED FLAW EVALUATION CHARTS

A numerical example was used in this section to show how an embedded flaw evaluation chart was constructed step by step as follows:

##### Example

To construct an embedded flaw evaluation chart for circumferential flaws at the beltline. The excess feedwater flow transient was determined to be the governing condition for this example.

##### Step 1

Calculate  $K_{Ia}$  for various distances underneath the inside vessel wall surface (clad-base metal interface) (in). The procedures of the calculation are as follows:

- o Plot the temperature across the wall thickness during the worst time step (610.86 sec.) of the excess feedwater flow transient. The minimum temperature is 472.5°F for this transient.
- o Calculate the corresponding  $K_{Ia}$  by the formula given in equation (6-1). The values of  $RT_{NDT}$  at various  $\delta$  locations were also determined.
- o Calculate the values of  $\frac{K_{Ia}}{\sqrt{10}}$

### Step 2

Calculate  $K_I$  values for embedded flaws of various sizes, various aspect ratios, and at various distances underneath the surface. In total, 141 cases were analyzed by closed form stress intensity factor expressions [5].

The 141 analyzed cases are tabulated in Table 6-1.

### Step 3

The  $K_I$  results of the 141 cases were plotted in Figure 6-2. These curves were combined into one single plot as the final chart, as shown in Figure 6-3.

The Code acceptance limit of  $\frac{K_{Ia}}{\sqrt{10}}$  was plotted on all these figures as a guideline for evaluation.

### Step 4

Determine the maximum acceptable flaw size:

The basic concept of the evaluation is that the part of the curves under the  $\frac{K_{Ia}}{\sqrt{10}}$  line are acceptable by the Code criteria. Therefore, the intersection of a curve  $\frac{K_{Ia}}{\sqrt{10}}$  with the driving force  $K_I$  curve indicates the maximum flaw depth acceptable by the Code criteria.

The acceptable maximum flaw sizes for various distances of flaws beneath the vessel surface,  $\delta$ , were plotted as shown in Figure 6-3, which is the final flaw evaluation chart. By examining Figure 6-4 for instance, for a flaw located at  $\delta = \frac{1}{8}t$  with an aspect ratio of 3:1, the maximum flaw size acceptable is .0.692". For an aspect ratio of 10:1, a maximum flaw depth of 0.692" is acceptable.

The above four steps have completely described the procedures of the construction of an embedded flaw evaluation chart for circumferential flaws at the inlet nozzle to shell weld.

The basic concept for the interpretation of the curves in a typical evaluation chart is that any flaw size which lies on the curve above the Code acceptance limit line is not acceptable for continued service without repair. The intersection of a curve with the Code acceptance limit line is therefore, the maximum acceptable flaw size for that particular case.

#### 6.7 COMPARISON OF EMBEDDED FLAW CHARTS WITH ACCEPTANCE STANDARDS OF IWB-3510

The handbook charts for embedded flaws do not show the acceptance standards of Section XI, as the surface flaw charts do. Therefore, it is not clear from the charts themselves how much is gained from the analysis process over the standards tables contained in IWB-3510. Such a comparison cannot be made directly on the embedded flaw handbook charts, because the charts are applicable for a full range of sizes, shapes and locations. The purpose of this section is to provide such comparisons, and to discuss the results of those comparisons.

The example will be for the inlet nozzle to shell weld, whose handbook chart is provided in the appendix, and also in Figure 6-3. The handbook chart values have been compared with the acceptance standards tables in Figure 6-4. This example is applicable to the cases where all flaws which are embedded are acceptable, up to a depth of  $2a/t = 0.25$ . Again it can be seen that the advantage gained by use of the analysis is greater for flaws located further from the inside surface. The largest allowable flaw shown here is centered at one quarter the wall thickness from the surface. Note that the allowable depth for this type of embedded flaw is  $a/t = 0.125$ , or a total flaw width ( $2a/t$ ) equal to 25 percent of the wall thickness. Carrying the calculations further would result in an allowable flaw depth for a mid-wall flaw ( $\delta = 1/2t$ ) equal to 50 percent of the wall thickness, but it is clearly not prudent to allow flaws of this size to remain. Therefore, the allowable flaw depths for embedded flaws have been limited to 25 percent of the wall thickness in total depth, and the upper curve of Figure 6-3 has been labelled accordingly.

TABLE 6-1  
EMBEDDED FLAW CASES ANALYZED FOR THE INLET NOZZLE  
TO SHELL WELD

Distance of Flaw To Surface	Embedded Flaw Depth(in.)					
	A.R. 10:1		A.R. 6:1		A.R. 3:1	
T/16 $\delta = 0.658$	0.05	0.10	0.05	0.10	0.05	0.10
	0.15	0.20	0.15	0.20	0.15	0.20
	0.25	0.30	0.25	0.30	0.25	0.30
	0.35	0.40	0.35	0.40	0.35	0.40
	0.450	0.470	0.450	0.470	0.450	0.470
3T/32 $\delta = 0.987$	0.1	0.2	0.1	0.2	0.1	0.2
	0.3	0.4	0.3	0.4	0.3	0.4
	0.5	0.6	0.5	0.6	0.5	0.6
	0.7	0.70504	0.7	0.70504	0.7	0.70504
T/8 $\delta = 1.316$	0.1	0.2	0.1	0.2	0.1	0.2
	0.3	0.4	0.3	0.4	0.3	0.4
	0.5	0.6	0.5	0.6	0.5	0.6
	0.7	0.8	0.7	0.8	0.7	0.8
	0.9	0.9400	0.9	0.9400	0.9	0.9400
3T/16 $\delta = 1.974$	0.15	0.30	0.15	0.30	0.15	0.30
	0.45	0.60	0.45	0.60	0.45	0.60
	0.75	0.90	0.75	0.90	0.75	0.90
	1.05	1.20	1.05	1.20	1.05	1.20
	1.35	1.410 1.40	1.35	1.410 1.40	1.35	1.410 1.40
T/4 $\delta = 2.632$	0.2	0.4	0.2	0.4	0.2	0.4
	0.6	0.8	0.6	0.8	0.6	0.8
	1.0	1.2	1.0	1.2	1.0	1.2
	1.4	1.6	1.4	1.6	1.4	1.6
	1.8	1.8801	1.8	1.8801	1.8	1.8801

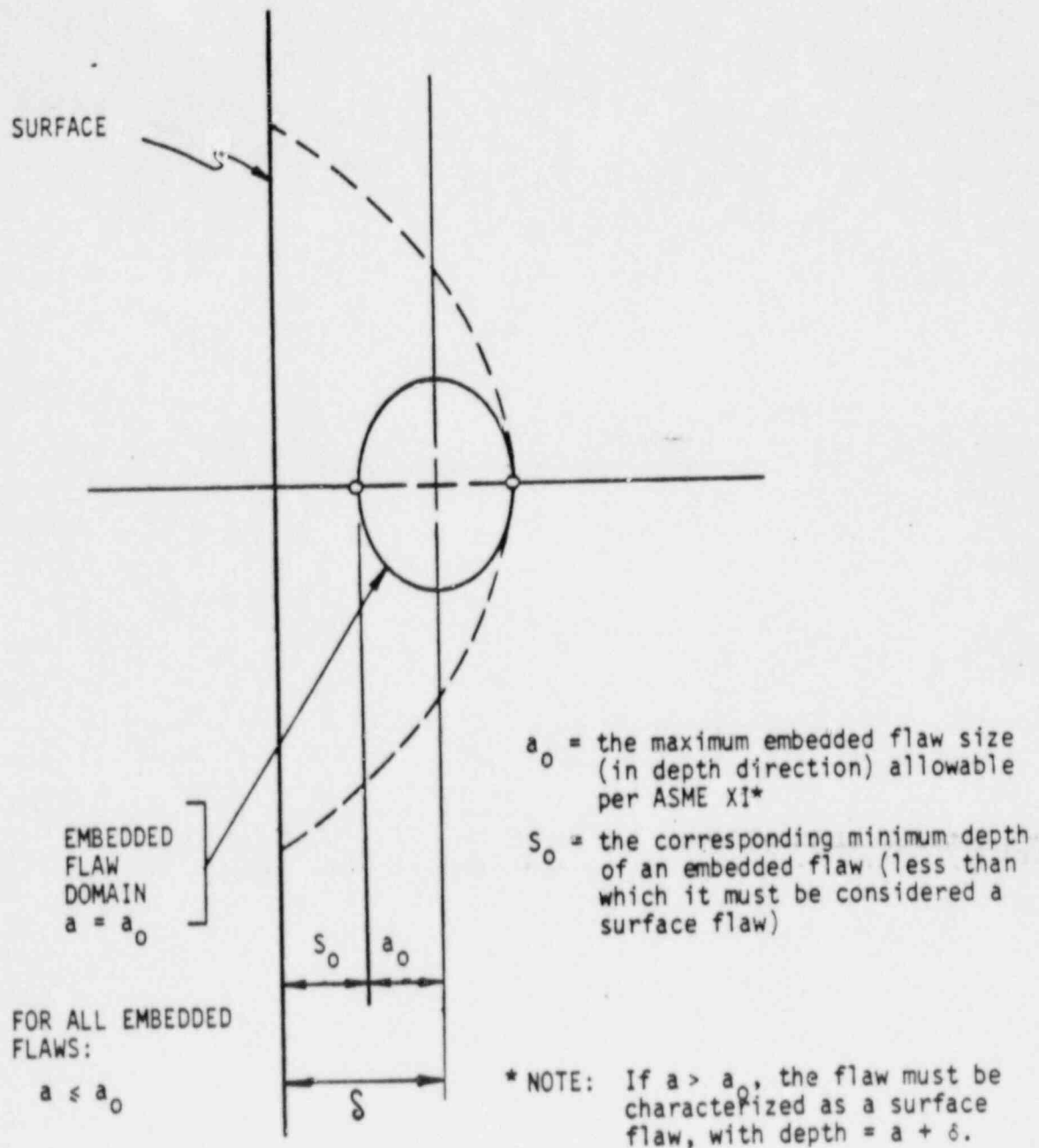


Figure 6-1. Embedded vs. Surface Flaw

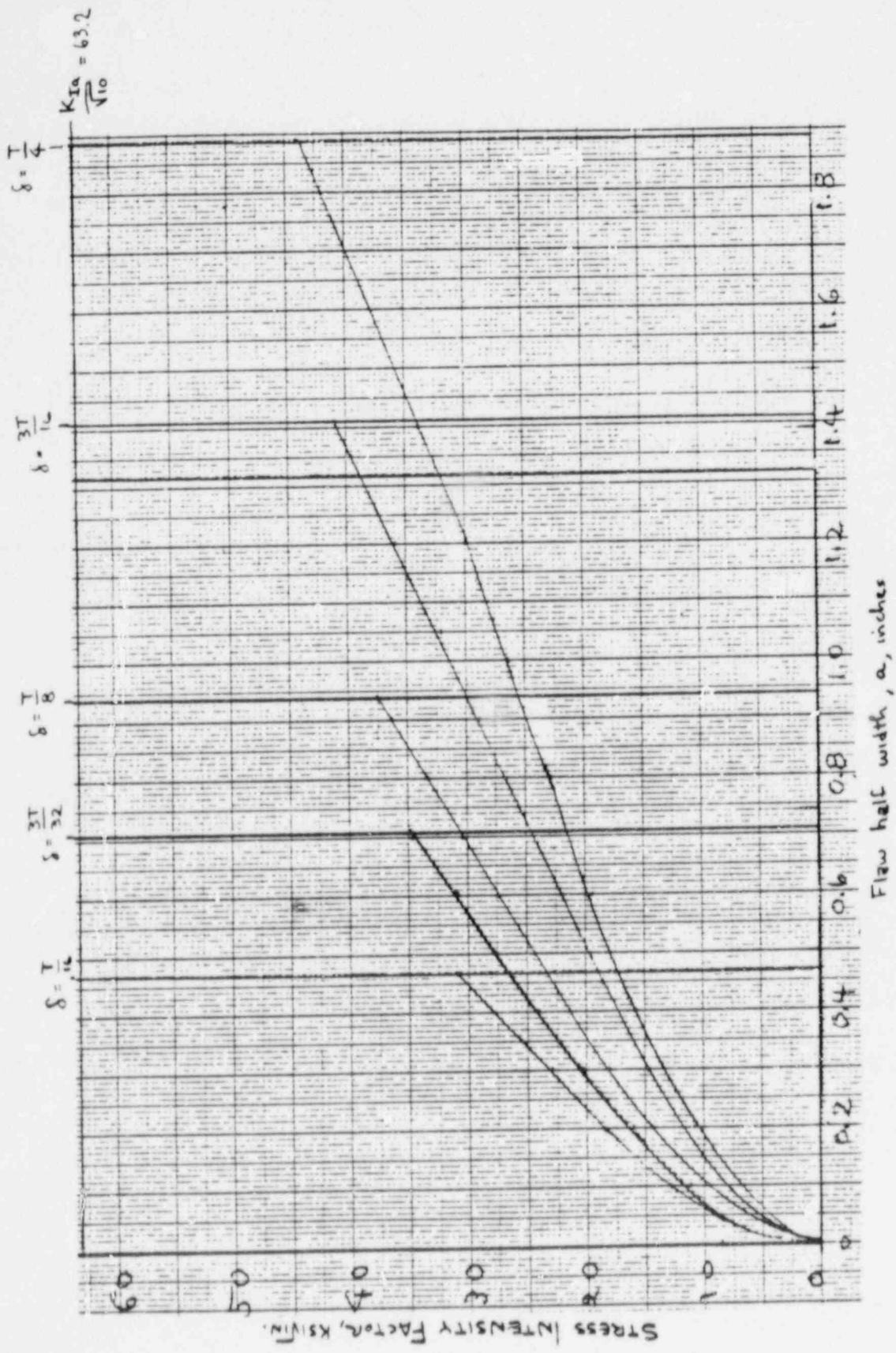
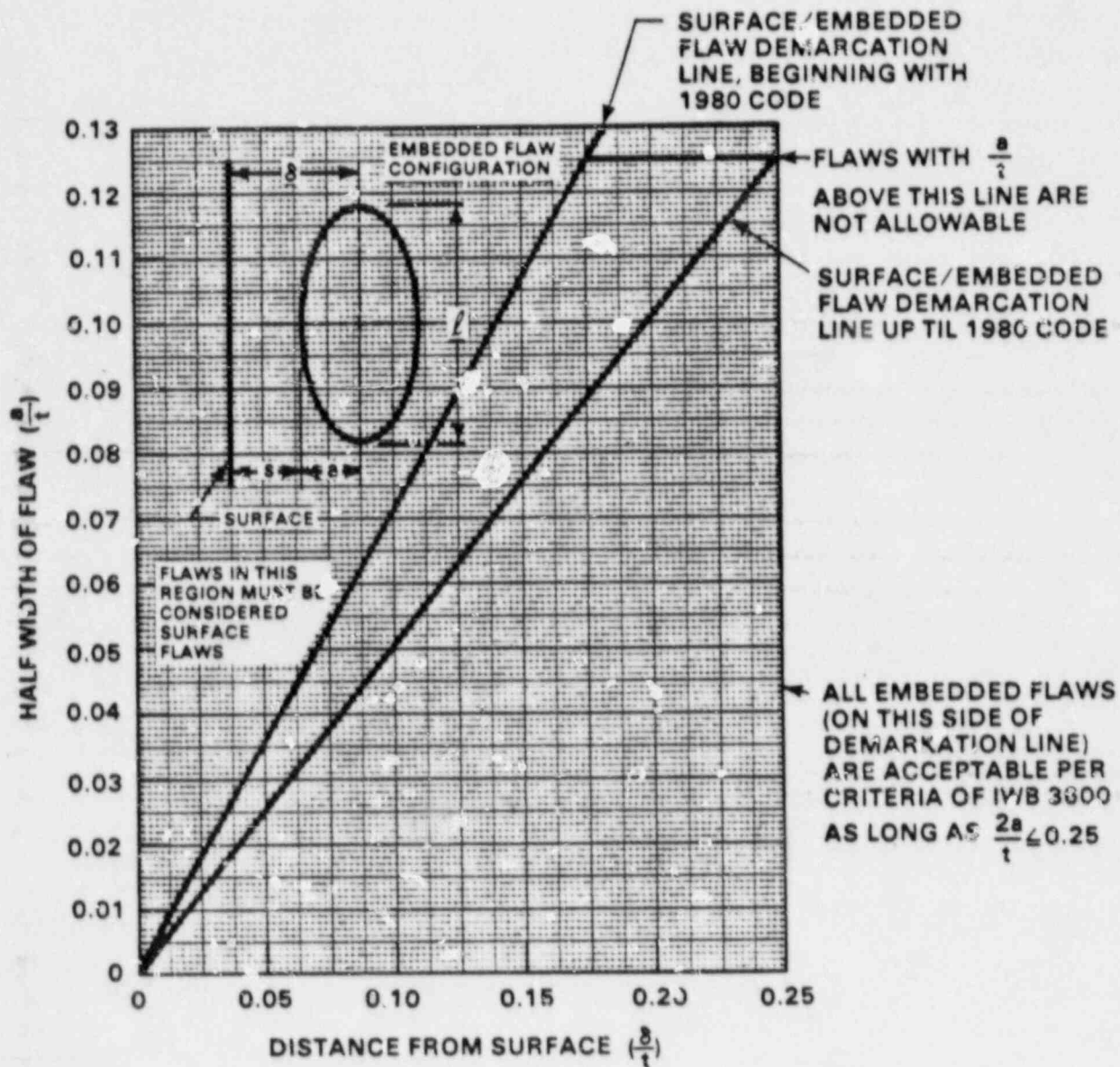


Figure 6-2. Illustrative Embedded Flaw Evaluation Chart for Longitudinal Flaws at Inlet Nozzle to Shell Weld

Z8924/030198 10



Embedded Flaw Evaluation Chart for Inlet Nozzle to Shell Weld  
(for Longitudinal and Circumferential Flaws)

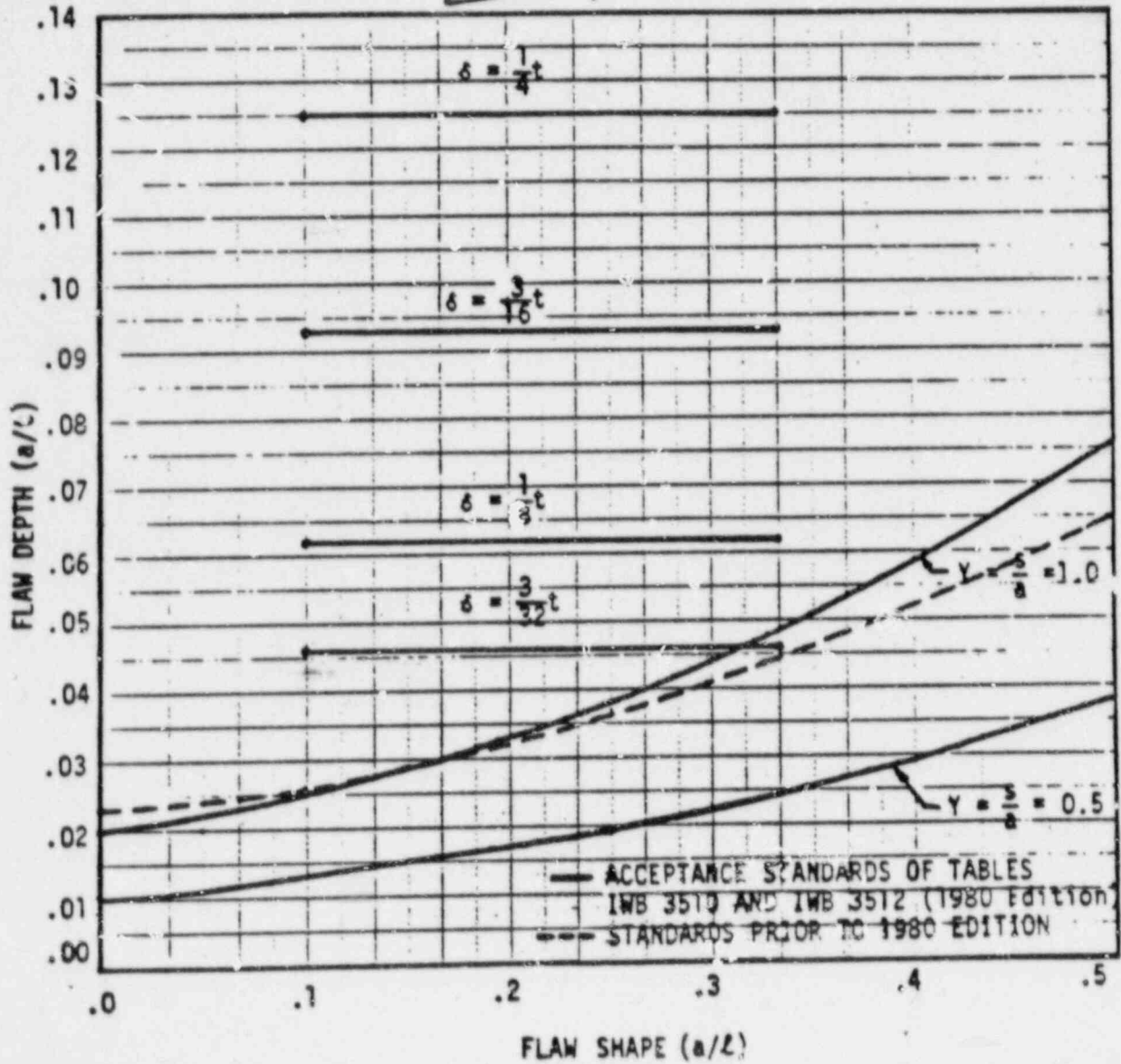
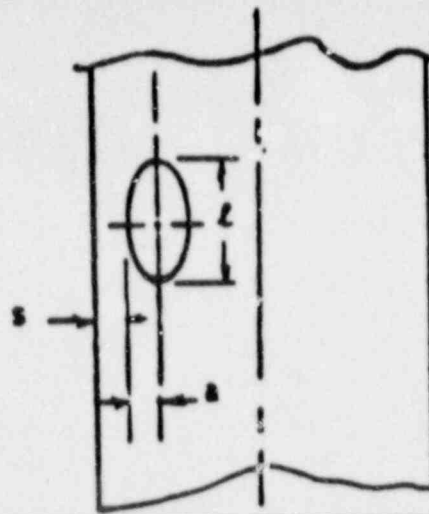


Figure 6-4. Illustration of Advantages gained by Analysis for Embedded Flaws at the Inlet Nozzle to Vessel Weld

SECTION 7  
REFERENCES

1. ASME Code Section XI, "Rules for Inservice Inspection of Nuclear Power Plant Components", 1974 Edition [Summer 75 Addendum] and 1983 Edition [Summer 83 Addendum]; In addition these specific addenda contain updates in standards and data used for the evaluation charts: 1983 edition (used for updated standards tables, and 1980 edition [Winter 1981 Addendum] (for revised reference crack growth curves).
2. McGowan, J. J. and Raymond, M., "Stress Intensity Factor Solutions for Internal Longitudinal Semi-Elliptic Surface Flaws in a Cylinder Under Arbitrary Loading," ASTM STP-677, 1979, pp. 365-380.
3. Newman, J. C. Jr. and Raju, I. S., "Stress Intensity Factors for Internal Surface Cracks in Cylindrical Pressure Vessels", ASME Trans., Journal of Pressure Vessel Technology, Vol. 102, 1980, pp. 342-346.
4. Buchalet, C. B. and Bamford, W. H., "Stress Intensity Factor Solutions for Continuous Surface Flaws in Reactor Pressure Vessels", in Mechanics of Crack Growth, ASTM, STP 590, 1976, pp. 385-402.
5. Shah, R. C. and Kobayashi, A. S., "Stress Intensity Factor for an Elliptical Crack Under Arbitrary Loading", Engineering Fracture Mechanics, Vol. 3, 1981, pp. 71-96.
6. Lee, Y. S. and Bamford, W. H., "Stress Intensity Factor Solutions for a Longitudinal Buried Elliptical Flaw in a Cylinder Under Arbitrary Loads", presented at ASME Pressure Vessel and Piping Conference, Portland Oregon, June 1983. Paper 93-PVP-92.
7. Marston, T. U. et. al. "Flaw Evaluation Procedures: ASME Section XI" Electric Power Research Institute Report EPRI-NP-719-SR, August 1978.

8. Congedo, T. V., et. al. "Heatup and Cooldown Limit Curves for the Alabama Power Co. Joseph M. Farley Unit 2 Reactor Vessel," Westinghouse Electric Co. WCAP 10910 Rev. 1, February 1986.
9. Congedo, T. V., et. al. "Heatup and Cooldown Limit Curves for the Alabama Power Co. Joseph M. Farley Unit 1 Reactor Vessel," Westinghouse Electric WCAP 10934, April 1986.
10. USNRC Regulatory Guide 1.99, Effects of Residual Elements on Predicting Radiation Damage to Reactor Vessel Materials, July 1975; Rev. 1: April 1977; Rev. 2 (in printing) 1988.
11. USNRC Standard Review Plan, NUREG 0800.
12. Plane Strain Crack Toughness Testing of High Strength Metallic Materials, ASTM STP 410, March 1969.
13. WCAP-10019, "Summary Report on Reactor Vessel Integrity for Westinghouse Operating Plants," December, 1981.
14. WCAP-10319, "A Generic Assessment of Risk from Pressurized Thermal Shock of Reactor Vessels on Westinghouse Nuclear Power Plants," July, 1983.
15. Meyer, T. A., et. al. "Fracture Mechanics Evaluation of the Farley Unit 1 Reactor Vessel" Westinghouse Report WCAP-9623, Nov. 1979.
16. Schmertz, J. C., et. al. "Fracture Mechanics Evaluation of the Farley Unit 2 Reactor Vessel," Westinghouse Electric WCAP 9641, Dec. 1979.
17. "Summary of Evaluations Related to Reactor Vessel Integrity report performed for the Westinghouse Owner's Group, Westinghouse Electric Corporation, May, 1982.
18. Letter O. D. Kingsley, WOG, to H. Denton, NRC, "Westinghouse Owner's Group Activities Related to Pressurized Thermal Shock," OG-73, July 15, 1982.

19. Letter from O. D. Kingsley, WOG, to H. Denton, NRC, "Westinghouse Owner's Group Activities Related to Pressurized Thermal Shock," OG-79, September 2, 1982.
20. SECY-82-465, United States Nuclear Regulatory Commission Policy Issue, "Pressurized Thermal Shock (PTS)," November 23, 1982.
21. U. S. Nuclear Regulatory Commission, 10CFR50, "Analysis of Potential Pressurized Thermal Shock Events," Federal Register Vol. 50. No. 141, July 23, 1985.

APPENDIX A  
FLAW EVALUATION

A-1 INTRODUCTION TO EVALUATION PROCEDURE

The evaluation procedures contained in ASME Section XI are clearly specified in paragraph IWB-3600. Use of the evaluation charts herein follows these procedures directly, but the steps are greatly simplified.

Once the indication is discovered, it must be characterized as to its location, length ( $l$ ) and depth dimension ( $a$ ) for surface flaws, ( $2a$ ) for embedded flaws, including its distance from the clad-base metal interface ( $S$ ) for embedded indications. This characterization is discussed in further detail in paragraph IWA-3000 of Section XI.

The following parameters must be calculated from the above dimensions to use the charts (see Figure 1-5 in the main text):

- o Flaw shape parameter,  $\frac{a}{r}$
- o Flaw depth parameter,  $\frac{a}{t}$
- o surface proximity parameter (for embedded flaws only),  $\frac{\delta}{t}$

where

- t = wall thickness of region where indication is located (not including clad thickness)
- l = length of indication

- a = depth of surface flaw; or half depth of embedded flaw in the width direction
- $\delta$  = distance from flaw centerline to surface (for embedded flaws only,  $\delta = S - a$ )
- S = smallest distance from edge of embedded flaw to surface

Once the above parameters have been determined and the determination made as to whether the indication is embedded or surface, then the two parameters may be plotted directly on the appropriate evaluation chart. Its location on the chart determines its acceptability immediately.

#### Important Observations on the Handbook Charts

Although the use of the handbook charts is conceptually straight forward, experience in their development and use has led to a number of observations which will be helpful.

#### Surface Flaws

An example handbook chart for surface flaws is shown in Figure A-1.1. The flaw indication parameters (whose calculation is described above) may be plotted directly on the chart to determine acceptability. The lower two curves shown (labelled code allowable limit) are simply the acceptance standards from IWB-3500, which are tabulated in Section XI. If the plotted point falls below these lines, the indication is acceptable without analytical justification having been required. If the plotted point falls between the Code allowable limit lines and the lines labelled "upper limits of acceptance by analysis" it is acceptable by virtue of its meeting the requirements of IWB-3600, which allow acceptance by fracture analysis. (Flaws between these lines would, however, require future monitoring per IWB-2420 of Section XI.) The analysis used to develop these lines is documented in the main body of this report. There are three of these lines shown in the charts, labelled 10, 20 and 30 years. The years indicate for how long the acceptance limit applies, from the date that a flaw indication is discovered, based on fatigue crack growth calculations.

As may be seen in Figure A-1.1, the chart gives results for surface flaw shapes up to a semi-circular flaw ( $a/\ell = 0.5$ ). For the unlikely occurrence of flaws which the value of  $a/\ell$  exceeds 0.5, the limits on acceptance for  $a/\ell = 0.5$  should be used, according to ASME Code requirements.

### Embedded flaws

An example chart for embedded flaws is shown in Figure A-1.2. The heavy diagonal line in the figure can be used directly to determine whether the indication should be characterized as an embedded flaw or whether it is sufficiently close to the surface that it must be considered as a surface flaw (by the rules of Section XI). If the flaw parameters produce a plotted point below the heavy diagonal line, it is acceptable by analysis if the point is below the appropriate  $a/\ell$  limit line. If it is above the line, it cannot be justified by analysis, and is, therefore, not acceptable.

For cases where there are several acceptance limit lines, interpolation between adjacent lines is recommended. A worked example is provided as embedded flaw Example 5. The outermost lines should be used as the limits, with no interpolation beyond them. For example, for  $a/\ell$  values greater than 0.333, use the line for  $a/\ell = 0.333$  in the figure, and for  $a/\ell$  values less than 0.167, use the line for  $a/\ell = 0.167$ . Beyond these outer limits, the analyses have shown that the sensitivity to flaw shape is small.

For cases where there are no branching limit lines below the heavy diagonal line (see Figure A-2.6 for example) then all flaws classified as embedded are acceptable. The only limitation is, as discussed in Section 6.5:

$$\frac{2a}{t} < 0.25$$

Note that the embedded flaw evaluation charts are applicable for flaws near either the inner or outer vessel surface, and the parameters "S" and "δ" are defined from the nearest surface.

Another important observation is the procedure to be used for an embedded flaw whose plotted point falls above the heavy diagonal line, and must therefore be considered a surface flaw. An example of this is provided in "Embedded Flaw Example 1" below, but it is important to note that when this must be done, the depth of the flaw is redefined. The new depth is equal to  $2a + S$ , as shown in the example, which becomes the effective crack depth  $a^*$  to be used in the surface flaw chart in such cases.

#### Surface Flaw Example 1

Suppose an indication has been discovered which is a surface flaw, and has the following characterized dimensions:

$$\begin{aligned} a &= 0.357 \text{ in.} \\ \ell &= 1.783 \text{ in.} \\ t &= 7.75 \text{ in.} \end{aligned}$$

The flaw parameters for the use of the charts are

$$\frac{a}{t} = 0.046$$

$$\frac{a}{\ell} = 0.20$$

Plotting these parameters on Figure A-1.1 it is quickly seen that the indication is acceptable by analysis. To justify operation without repair it is necessary to submit this plot along with this technical basis document to the regulatory authorities.

#### Embedded Flaw Example 1

A longitudinal\* embedded flaw of 2.0" x 5.00", located within 0.10" from the surface, was detected. Determine whether this flaw should be considered as an embedded flaw.

$$\begin{aligned}
2a &= 2.0'' \\
S &= 0.16'' \\
\delta &= S + a = 0.16 + 1/2 (2.0) = 1.16 \\
t &= 7.75'' \\
\ell &= 5.0''
\end{aligned}$$

\*Note: longitudinal herein means relative to the vessel or nozzle centerline, not the weld length. For the nozzle inner radius, and other regions of a nozzle, longitudinal is relative to the nozzle centerline.

and,

$$\begin{aligned}
a &= 1/2 \times 2.0'' \\
&= 1.0''
\end{aligned}$$

Using Figure A-1.2:

$$\frac{a}{t} = \frac{1.0}{7.75} = 0.13$$

$$\frac{\delta}{t} = \frac{1.16}{7.75} = 0.15$$

Since the plotted point (X) is above the diagonal line, the flaw must be considered a surface flaw instead.

Now, since the flaw must be considered as a surface flaw, the depth must be redefined as the distance from the surface to the deepest point of the flaw. This is equivalent to circumscribing the embedded flaw with a semi-elliptical surface flaw. Operationally, the parameters are recalculated as follows. Defining  $a^*$  as the corrected crack depth for the surface flaw,

$$c^* = 2a + S = 2.16''$$

$$\ell = 5.0''$$

$$\frac{a^*}{t} = 0.278$$

$$\frac{a^*}{\ell} = 0.432$$

Referring to Figure A-1.1 for the surface flaw, it is quickly seen that this flaw is much too large to be acceptable, and must be repaired.

#### Embedded Flaw Example 2 (Point A)

Suppose an indication has been discovered which is embedded, and has the following characterized dimensions:

$$\begin{aligned} 2a &= 1.15 \text{ in.} \\ \ell &= 1.72 \text{ in.} \\ t &= 10.53 \text{ in.} \\ S &= 0.86 \text{ in.} \end{aligned}$$

Calculating the flaw parameters, we have:

$$\frac{a}{t} = 0.0545$$

$$\frac{a}{\ell} = 0.333$$

$$\delta = S + a = 1.43 \text{ in.} \quad \frac{\delta}{t} = 0.136$$

Plotting these parameters on the embedded flaw evaluation chart, Figure A-1.2 it may be quickly seen that the indication is embedded, and is acceptable by analysis (point A), since it lies below the  $a/\ell = 0.333$  limit case.

Embedded Flaw Example 3 (Point B)

Suppose an indication has been discovered which is embedded, and has the following characterized dimensions:

$$\begin{aligned}2a &= 1.68 & a &= 0.84 \\ \ell &= 2.55 \\ t &= 10.53 \\ S &= 1.52\end{aligned}$$

Calculating the flaw parameters, we have:

$$\begin{aligned}\frac{a}{t} &= 0.08 \\ \frac{a}{\ell} &= 0.33 \\ \delta &= S + a = 2.37 \\ \frac{\delta}{t} &= 0.225\end{aligned}$$

Plotting these parameters on Figure A-1.2 (point B) we see that the indication is acceptable, since it falls below the line which is applicable to  $a/\ell = 0.333$ . (Note that if  $a/\ell = 0.167$ , for example, the indication would not be acceptable, since point B would lie above that line, as may be seen in the figure.)

Embedded Flaw Example 4 (Point C)

A longitudinal embedded flaw of 1.15" x 5.38" was detected at a distance  $S = 1.075$  in. underneath the surface. Evaluate the flaw for code acceptance for continued service without repair.

The flaw geometry parameters are determined as follows:

$$\begin{aligned}t &= 7.75" \\S &= 1.24" \\ \delta &= S + a = 1.937" \\ \ell &= 6.52"\end{aligned}$$

and

$$\begin{aligned}a &= 1/2 \times 1.395" \\ &= .698"\end{aligned}$$

$$\frac{\delta}{t} = \left(\frac{1.937}{7.75}\right) = 0.25$$

$$\frac{a}{\ell} = \frac{.698}{6.52} = 0.107$$

$$\frac{a}{t} = \frac{.698}{7.75} = 0.09$$

Evaluate the flaw by referring to Fig. A-1.2 and plotting the point (as point C). This is above the code acceptance limit line for  $a/\ell = 0.167$ , which should also be used for  $a/\ell < 0.167$ ; therefore, the flaw is not acceptable, and must be repaired.

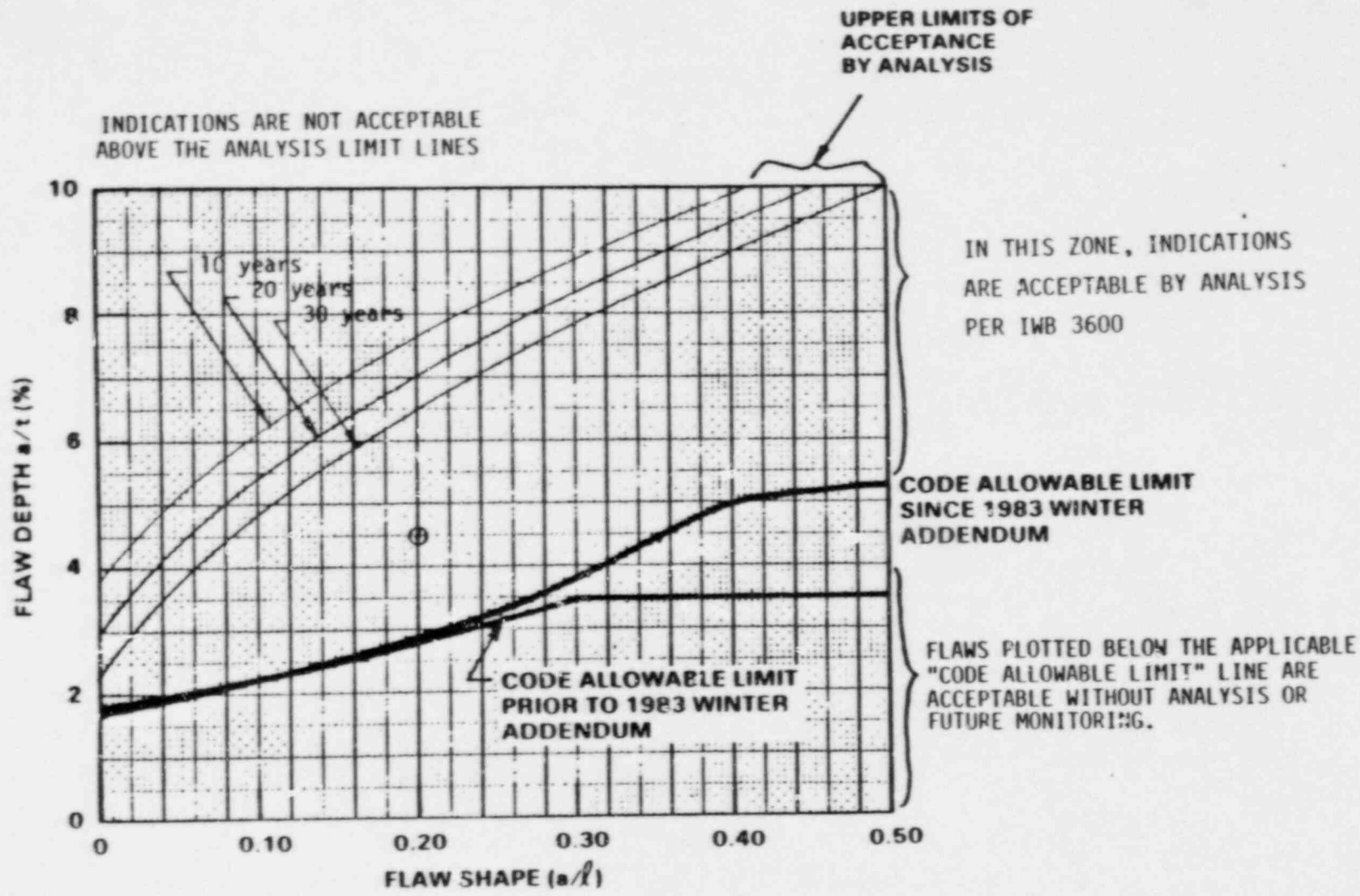


Figure A-1.1 Example of Surface Flaw Evaluation

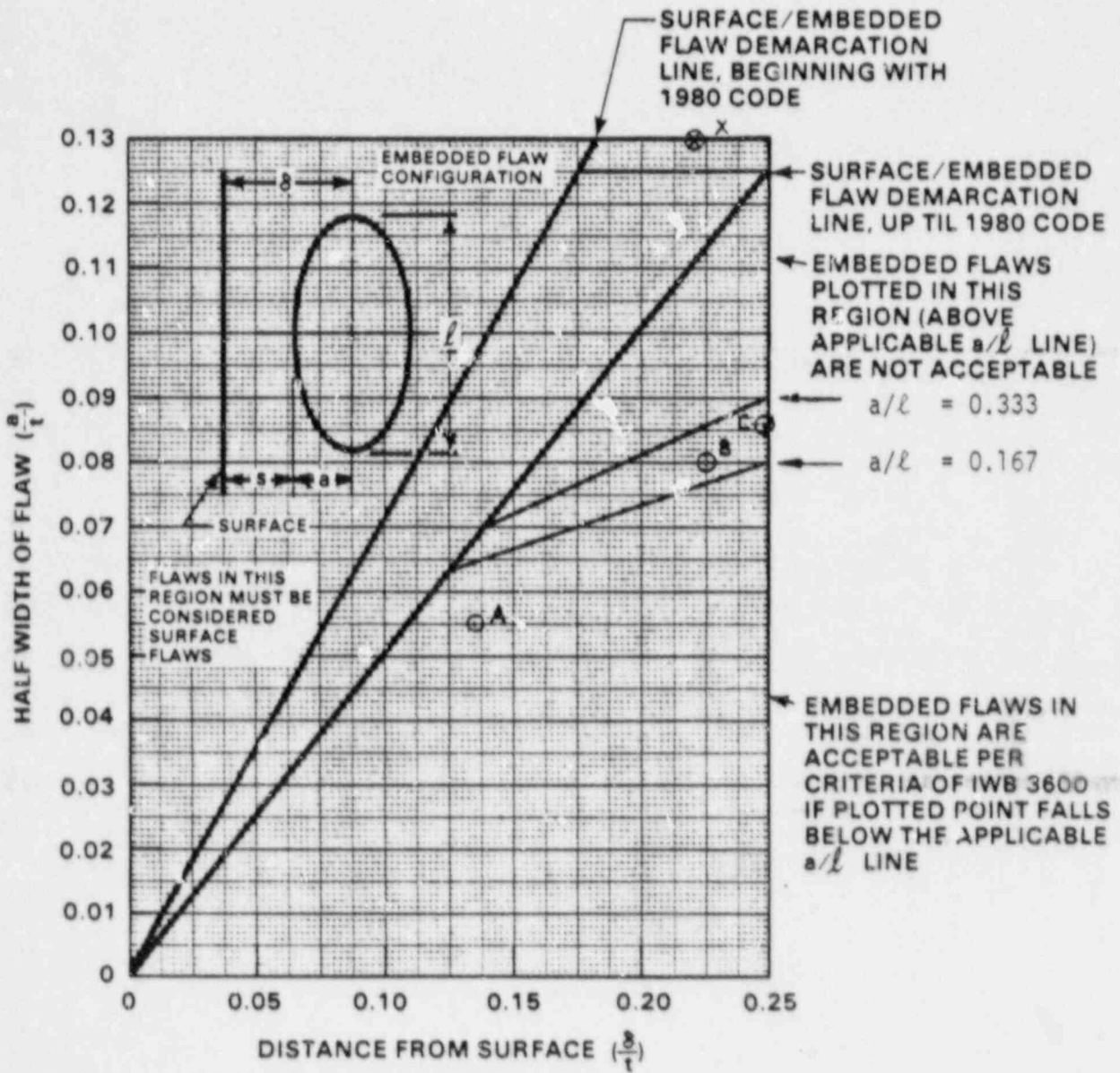


Figure A-1.2 Example of Embedded Flaw Treatment

A-2 BELTLINE (INCLUDING MIDDLE-TO-UPPER SHELL CIRCUMFERENTIAL WELD, AND LOWER-TO- MIDDLE SHELL CIRCUMFERENTIAL WELDS, AND LONGITUDINAL SEAM WELDS)

A-2.1 SURFACE FLAWS

The geometry and terminology used for flaws in the beltline region is depicted in Figure A-2.1. The following parameters must be determined for surface flaw evaluation with the charts.

- o Flaw shape parameter  $\frac{a}{l}$
- o Flaw depth parameter  $\frac{a}{t}$

where     a - the surface flaw depth detected, (in.)  
           l - the surface flaw length detected, (in.)  
           t - wall thickness at the beltline (t = 7.75")

The surface evaluation charts for the beltline are listed below:

- o Figure A-2.2 Evaluation Chart for Reactor Vessel Beltline
 

<u>X</u>	Inside Surface	<u>X</u>	Surface Flaw	<u>X</u>	Longitudinal Flaw
---	Outside Surface	---	Embedded Flaw	---	Circumferential Flaw
  
- o Figure A-2.3 Evaluation Chart for Reactor Vessel Beltline
 

<u>X</u>	Inside Surface	<u>X</u>	Surface Flaw	---	Longitudinal Flaw
---	Outside Surface	---	Embedded Flaw	<u>X</u>	Circumferential Flaw
  
- o Figure A-2.4 Evaluation Chart for Reactor Vessel Beltline
 

---	Inside Surface	<u>X</u>	Surface Flaw	<u>X</u>	Longitudinal Flaw
<u>X</u>	Outside Surface	---	Embedded Flaw	---	Circumferential Flaw
  
- o Figure A-2.5 Evaluation Chart for Reactor Vessel Beltline
 

---	Inside Surface	<u>X</u>	Surface Flaw	---	Longitudinal Flaw
<u>X</u>	Outside Surface	---	Embedded Flaw	<u>X</u>	Circumferential Flaw

## A-2.2 EMBEDDED FLAWS

The geometry and terminology used for embedded flaws at beltline is depicted in Figure A-1.1.

### Basic Data:

- t = 7.75 in.
- $\delta$  = Distance of the centerline of the embedded flaw to the surface (in.)
- a = Flaw depth (Defined as one half of the minor diameter) (in.)
- l = Flaw length (Major diameter) (in.)
- $a_0$  = Maximum embedded flaw size in depth direction, beyond which it must be considered a surface flaw, per Section XI characterization criteria.

The following parameters must be calculated from the above dimensions to use the charts for evaluating the acceptability of an embedded flaw

- o Flaw shape parameter,  $\frac{a}{l}$
- o Flaw depth parameter,  $\frac{a}{t}$
- o surface proximity parameter,  $\frac{\delta}{t}$

The evaluation chart for embedded flaws in the beltline is shown in Figure A-2.6. Any embedded flaw in this region will be acceptable regardless of its size, shape and location (as long as  $\frac{c}{t} < 0.125$ ) as shown in Figure A-2.6 and discussed in Section A-1. This determination can be easily made by plotting the indication parameters on the figure, to determine if it lies below the appropriate demarcation line (i.e. embedded not surface).

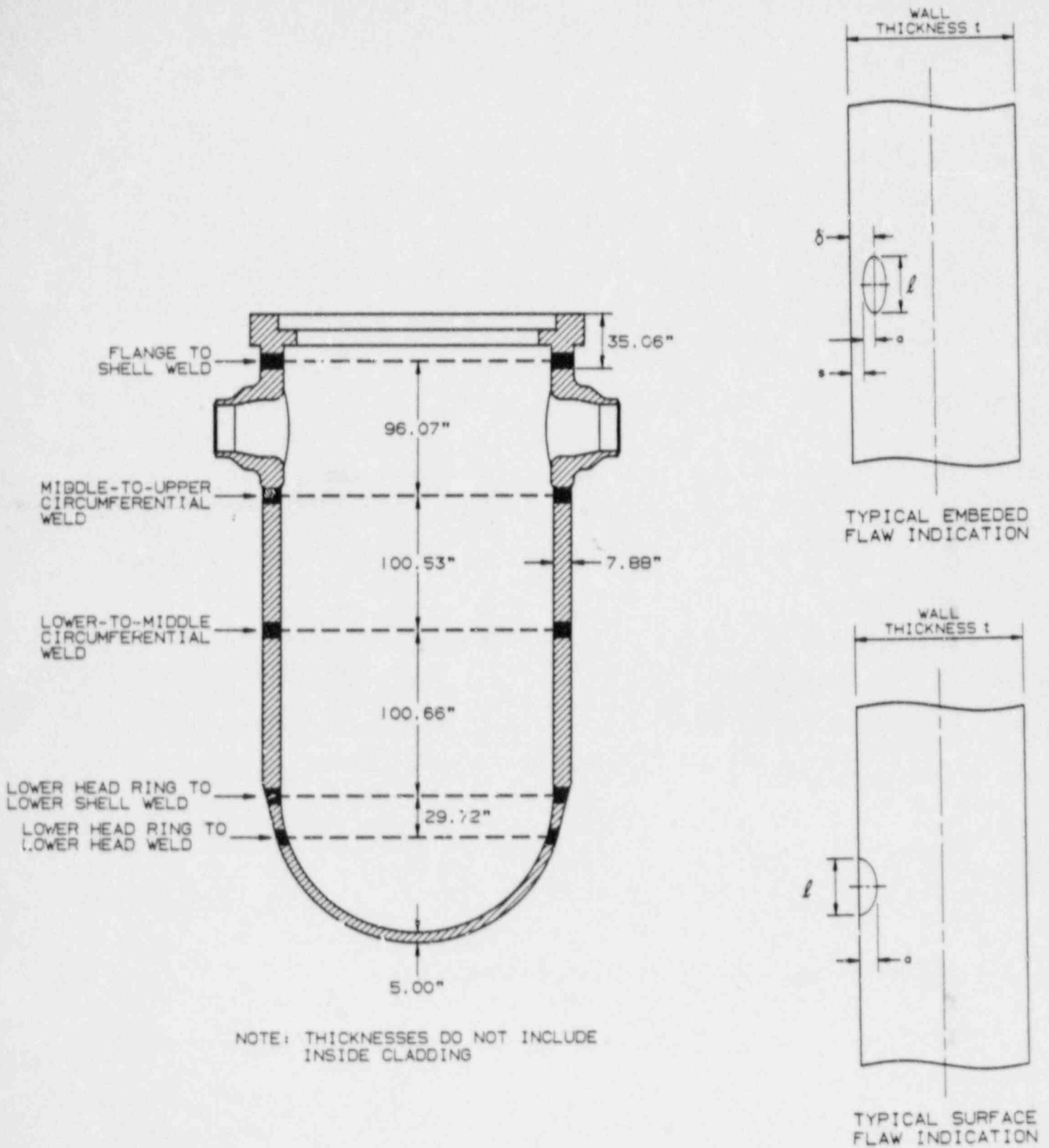
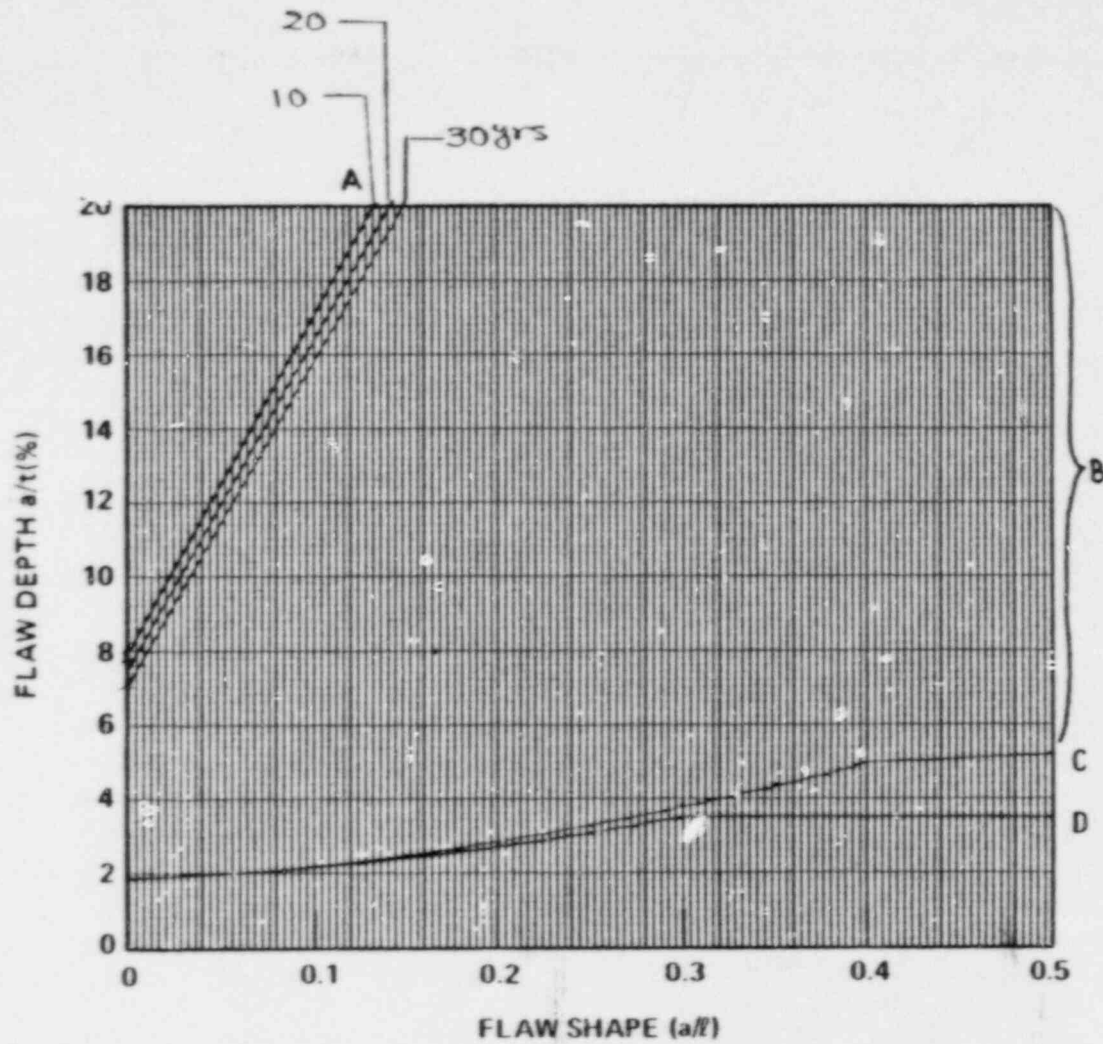


Figure A-2.1 Geometry and Terminology for Flaws at the Beltline



LEGEND

- A - The 10, 20, 30 year acceptable flaw limits.
- B - Within this zone, the surface flaw is acceptable by ASME Code analytical criteria in IWB-3600.
- C - ASME Code allowable since 1983 Winter Addendum.
- D - ASME Code allowable prior to 1983 Winter Addendum.

© Westinghouse 1987

Figure A-2.2 Evaluation Chart for Reactor Vessel Beltline ( $RT_{NDT} < 270^{\circ}F$ )

<u>X</u>	Inside Surface	<u>X</u>	Surface Flaw	<u>X</u>	Longitudinal Flaw
—	Outside Surface	—	Embedded Flaw	—	Circumferential Flaw

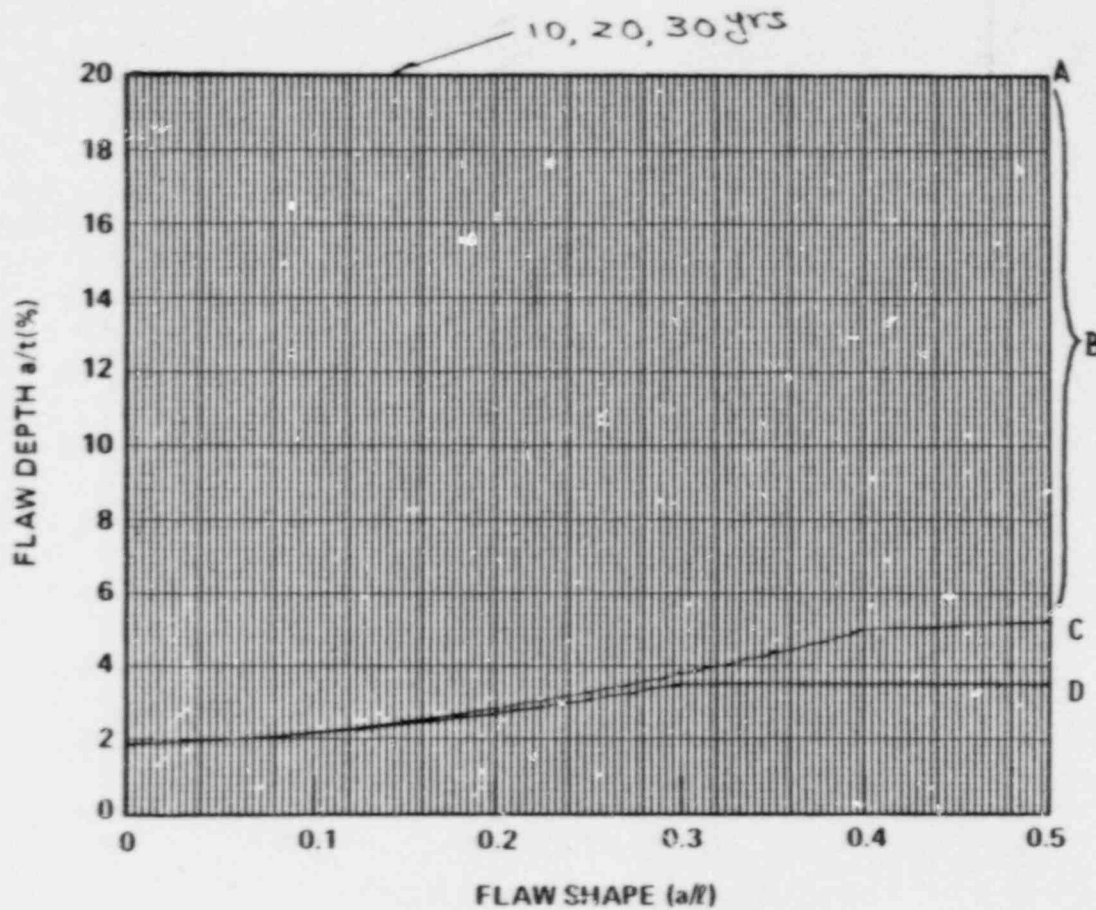
LEGEND

A - The 10, 20, 30 year acceptable flaw limits.

B - Within this zone, the surface flaw is acceptable by ASME Code analytical criteria in IWB-3600.

C - ASME Code allowable since 1983 Winter Addendum.

D - ASME Code allowable prior to 1983 Winter Addendum.



© Westinghouse 1987

Figure A-2.3 Evaluation Chart for Reactor Vessel Beltline ( $RT_{NDT} < 220^{\circ}F$ )

<u>X</u>	Inside Surface	<u>X</u>	Surface Flaw	<u>    </u>	Longitudinal Flaw
<u>    </u>	Outside Surface	<u>    </u>	Embedded Flaw	<u>X</u>	Circumferential Flaw

LEGEND

- A - The 10, 20, 30 year acceptable flaw limits.
- B - Within this zone, the surface flaw is acceptable by ASME Code analytical criteria in IWB-3600.
- C - ASME Code allowable since 1983 Winter Addendum.
- D - ASME Code allowable prior to 1983 Winter Addendum.

© Westinghouse 1987

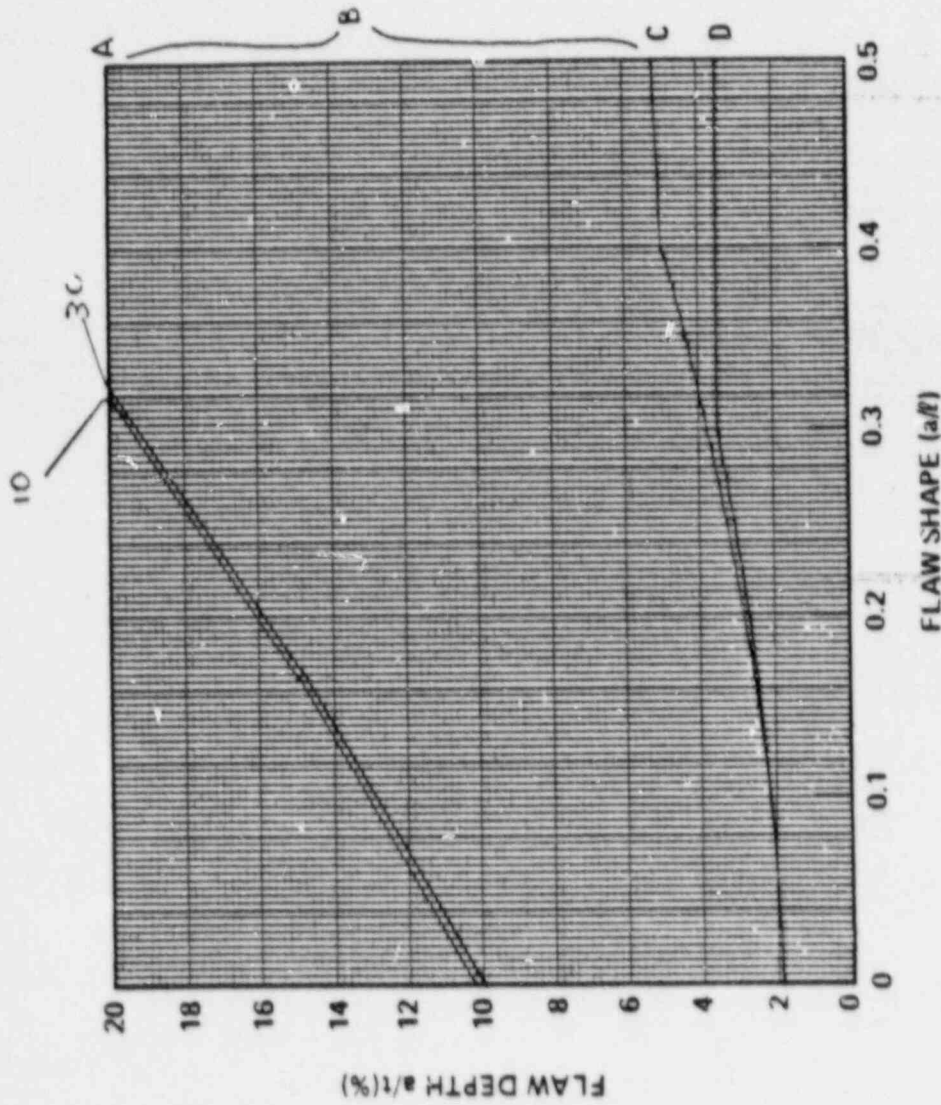
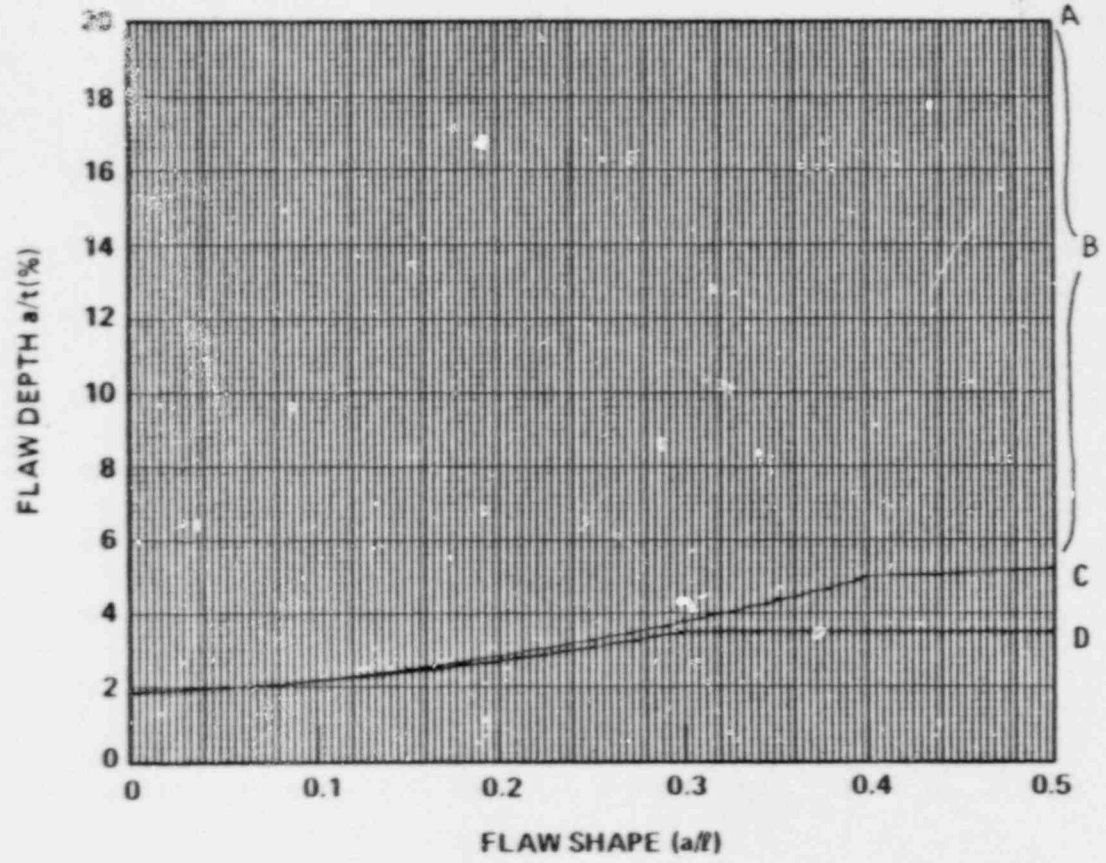


Figure A-2.4 Evaluation Chart for Reactor Vessel Beltline  
 Inside Surface X Surface Flaw X Longitudinal Flaw  
 Outside Surface Embedded Flaw Circumferential Flaw

A-17



LEGEND

- A - The 10, 20, 30 year acceptable flaw limits.
- B - Within this zone, the surface flaw is acceptable by ASME Code analytical criteria in IWB-3600.
- C - ASME Code allowable since 1983 Winter Addendum.
- D - ASME Code allowable prior to 1983 Winter Addendum.

© Westinghouse 1987

Figure A-2.5 Evaluation Chart for Reactor Vessel Bellline

—	Inside Surface	X	Surface Flaw	—	Longitudinal Flaw
X	Outside Surface	—	Embedded Flaw	X	Circumferential Flaw

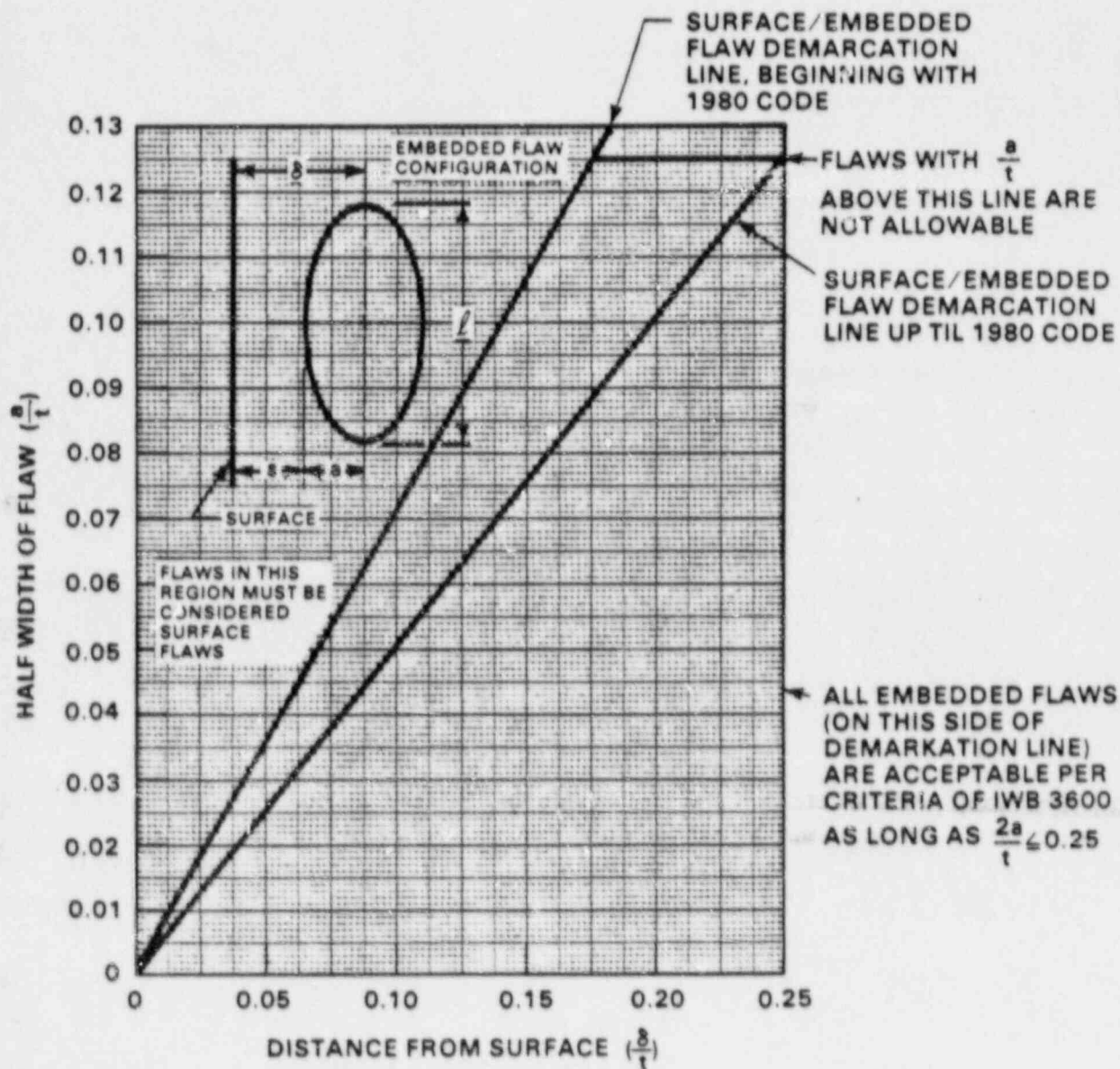


Figure A-2.6 Evaluation Chart for Reactor Vessel Beltline

<u>X</u>	Inside Surface	<u>—</u>	Surface Flaw	<u>X</u>	Longitudinal Flaw
<u>X</u>	Outside Surface	<u>X</u>	Embedded Flaw	<u>X</u>	Circumferential Flaw

## A-3 INLET NOZZLE TO SHELL WELD (PENETRATION)

### A-3.1 SURFACE FLAWS

The geometry and terminology for surface flaws at the inlet nozzle to shell weld is depicted in figure A-3.1. The following parameters must be determined for surface flaw evaluation with the charts

- o Flaw shape parameter  $\frac{a}{l}$
- o Flaw depth parameter  $\frac{a}{t}$

where  $a$  = The surface flaw depth detected (in.)  
 $l$  = The surface flaw length detected (in.)  
 $t$  = Wall thickness at the inlet nozzle to vessel weld ( $t = 10.53$ " )

The surface flaw evaluation charts for the inlet nozzle to vessel weld are listed below:

- o Figure A-3.2 Evaluation Chart for Inlet Nozzle to Shell Weld  

<u>X</u>	Inside Surface	<u>X</u>	Surface Flaw	<u>X</u>	Longitudinal Flaw
___	Outside Surface	___	Embedded Flaw	___	Circumferential Flaw
- o Figure A-3.3 Evaluation Chart for Inlet Nozzle to Shell Weld  

<u>X</u>	Inside Surface	<u>X</u>	Surface Flaw	___	Longitudinal Flaw
___	Outside Surface	___	Embedded Flaw	<u>X</u>	Circumferential Flaw
- o Figure A-3.4 Evaluation Chart for Inlet Nozzle to Shell Weld  

___	Inside Surface	<u>X</u>	Surface Flaw	<u>X</u>	Longitudinal Flaw
<u>X</u>	Outside Surface	___	Embedded Flaw	<u>X</u>	Circumferential Flaw

### A-3.2 EMBEDDED FLAWS

The geometrical description of an embedded flaw at the inlet nozzle to shell weld is depicted in Figure A-3.1.

#### Basic Data:

- t = 10.53 in.
- $\delta$  = Distance of the centerline of the embedded flaw to the surface (in.)
- a = Flaw depth (defined as one half of the minor diameter) (in.)
- l = Flaw length (major diameter) (in.)
  
- $a_o$  = Maximum embedded flaw size in depth direction, beyond which it must be considered a surface flaw, per Section XI characterization rules.

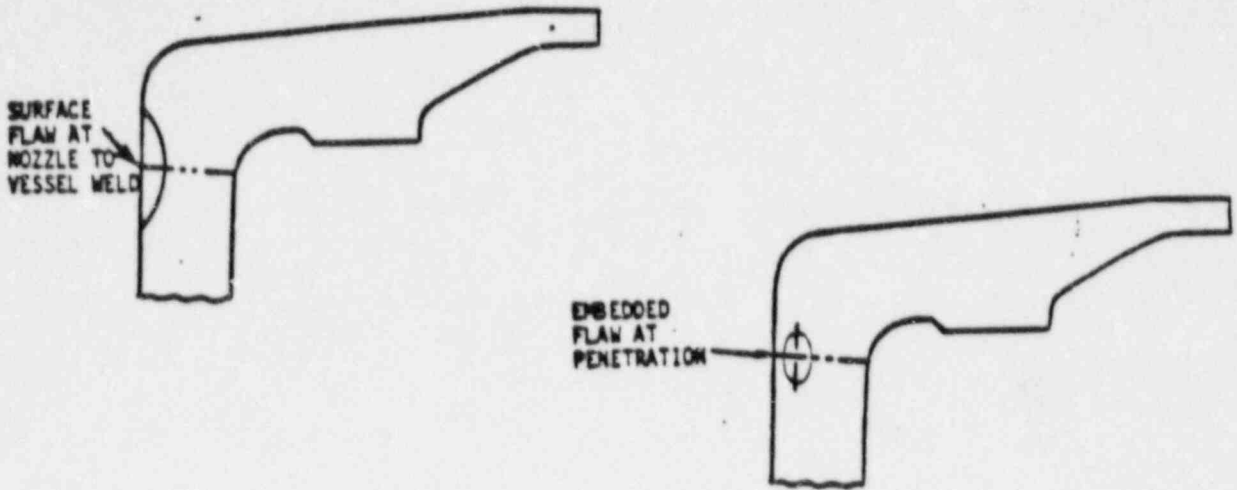
The following parameters must be calculated from the above dimensions to use the charts for evaluating the acceptability of an embedded flaw

- o Flaw shape parameter,  $\frac{a}{l}$
- o Flaw depth parameter,  $\frac{a}{t}$
- o surface proximity parameter,  $\frac{\delta}{t}$

The evaluation chart for embedded flaws:

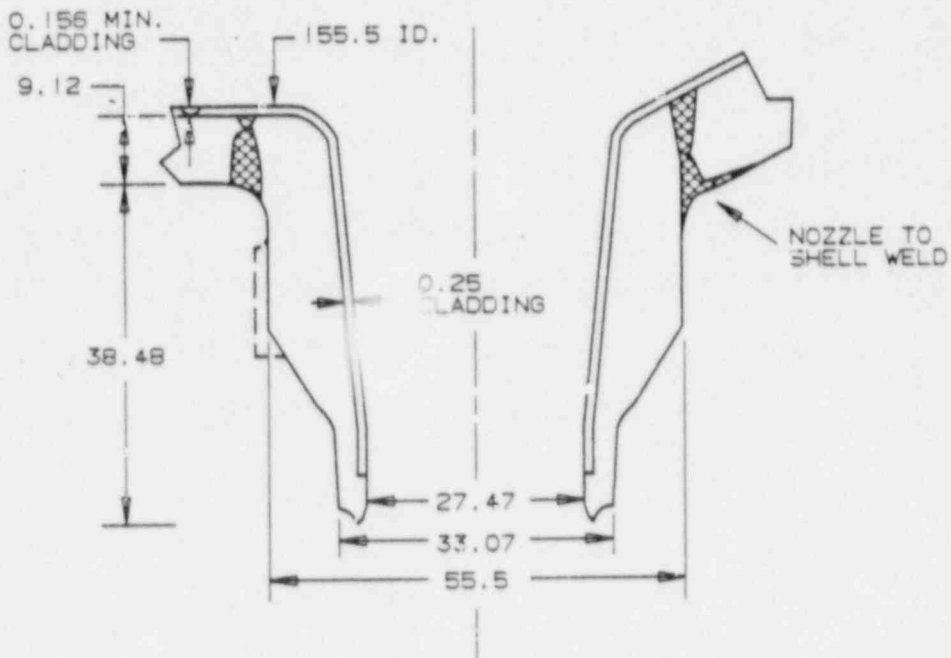
- o Figure A-3.5 Evaluation Chart for Inlet Nozzle to Shell Weld

<u>X</u>	Inside Surface	—	Surface Flaw	<u>X</u>	Longitudinal Flaw
<u>X</u>	Outside Surface	<u>X</u>	Embedded Flaw	<u>X</u>	Circumferential Flaw



SIDE VIEW

TOP VIEW



NOTES:

1. DIMENSIONS DO NOT INCLUDE CLAD
2. ALL DIMENSIONS ARE IN INCHES

Figure A-3.1 Geometry and Terminology for Flaws at the Inlet Nozzle to Shell Weld (Penetration)

LEGEND

- A - The 10, 20, 30 year acceptable flaw limits.
- B - Within this zone, the surface flaw is acceptable by ASME Code analytical criteria in IWB-3600.
- C - ASME Code allowable since 1983 Winter Addendum.
- D - ASME Code allowable prior to 1983 Winter Addendum.

© Westinghouse 1987

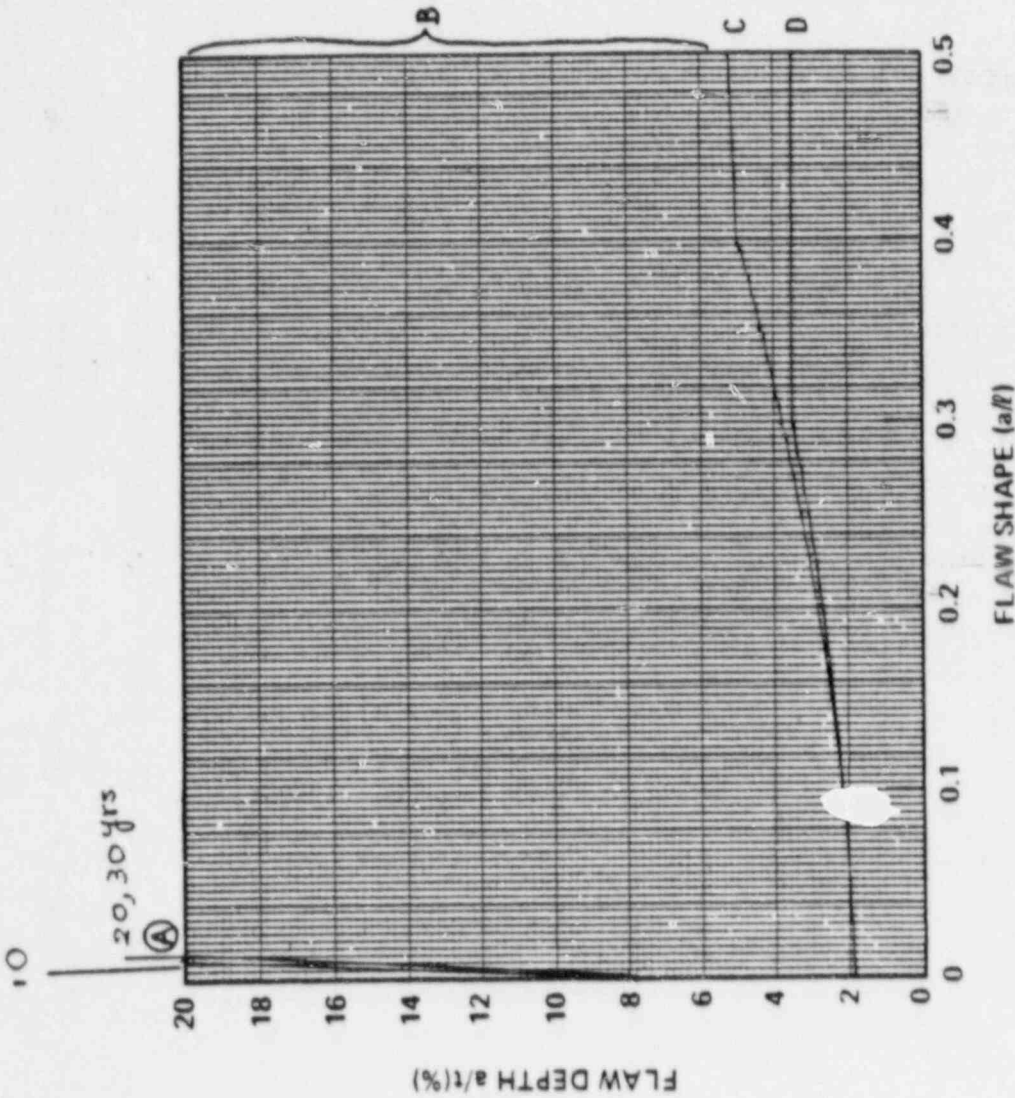


Figure A-3.2 Evaluation Chart for Inlet Nozzle to Shell Weld

- X Inside Surface
- \_\_\_ Outside Surface
- X Surface Flaw
- \_\_\_ Embedded Flaw
- X Longitudinal Flaw
- \_\_\_ Circumferential Flaw

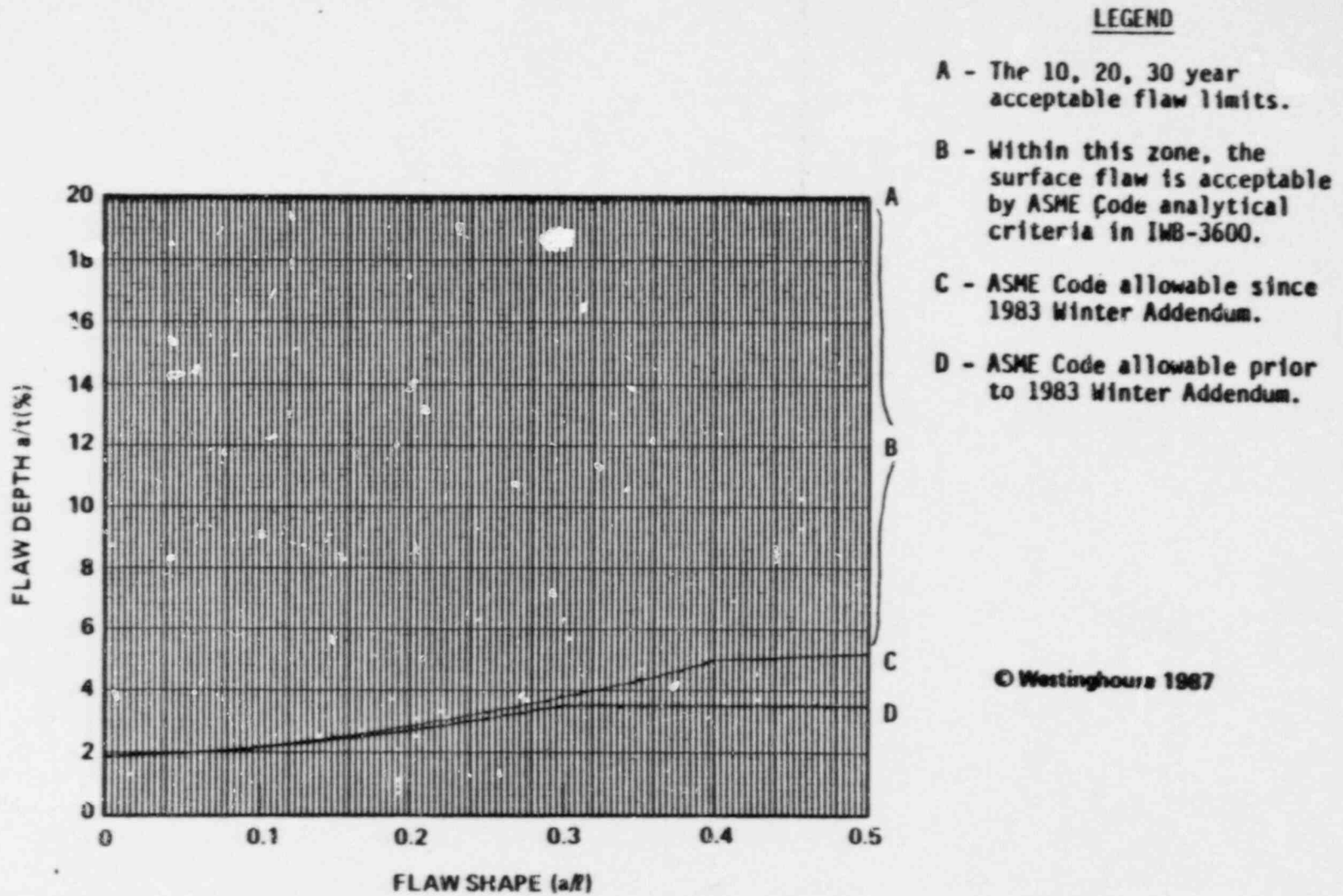
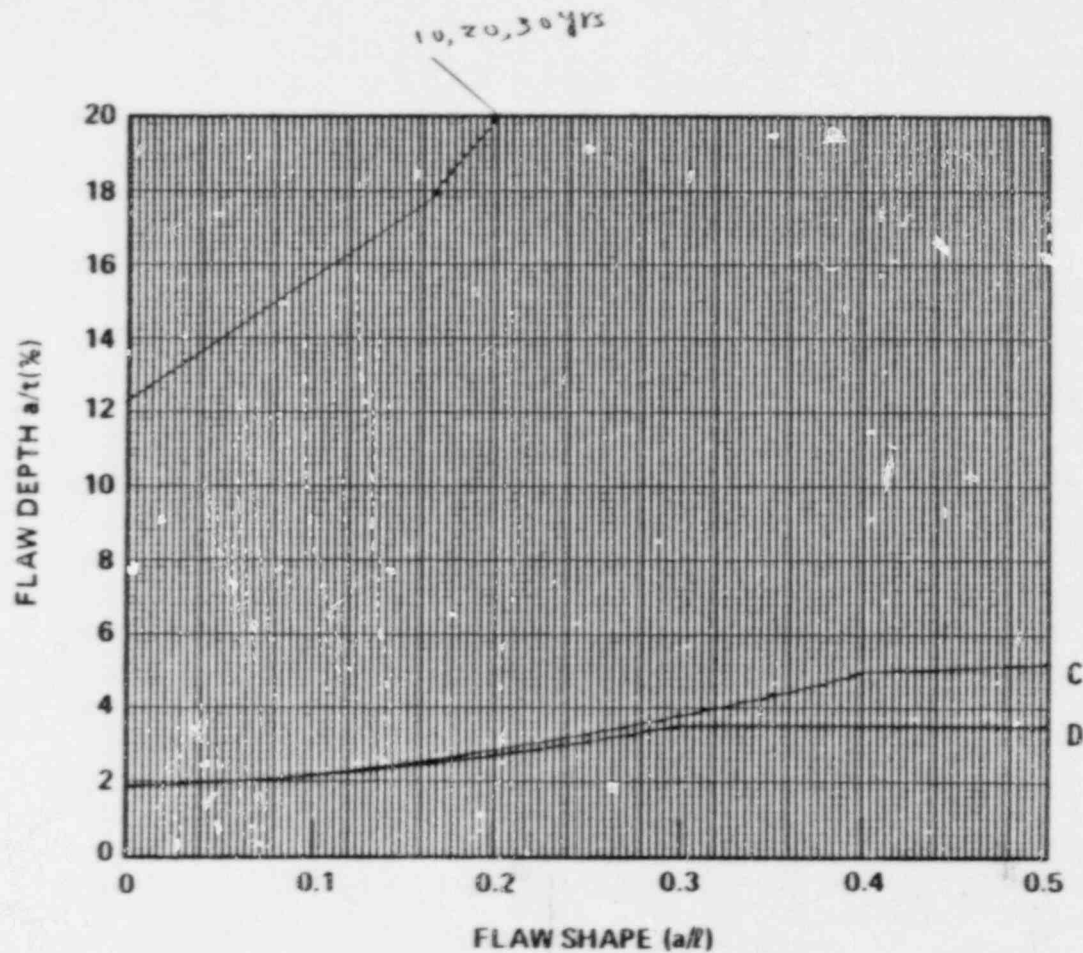


Figure A-3.3 Evaluation Chart for Inlet Nozzle to Shell Weld

<u>X</u> Inside Surface	<u>X</u> Surface Flaw	<u>—</u> Longitudinal Flaw
<u>—</u> Outside Surface	<u>—</u> Embedded Flaw	<u>X</u> Circumferential Flaw



LEGEND

- A - The 10, 20, 30 year acceptable flaw limits.
- B - Within this zone, the surface flaw is acceptable by ASME Code analytical criteria in IWB-3600.
- C - ASME Code allowable since 1983 Winter Addendum.
- D - ASME Code allowable prior to 1983 Winter Addendum.

© Westinghouse 1987

Figure A-3.4 Evaluation Chart for Inlet Nozzle to Shell Weld

—	Inside Surface	X	Surface Flaw	X	Longitudinal Flaw
X	Outside Surface	—	Embedded Flaw	X	Circumferential Flaw

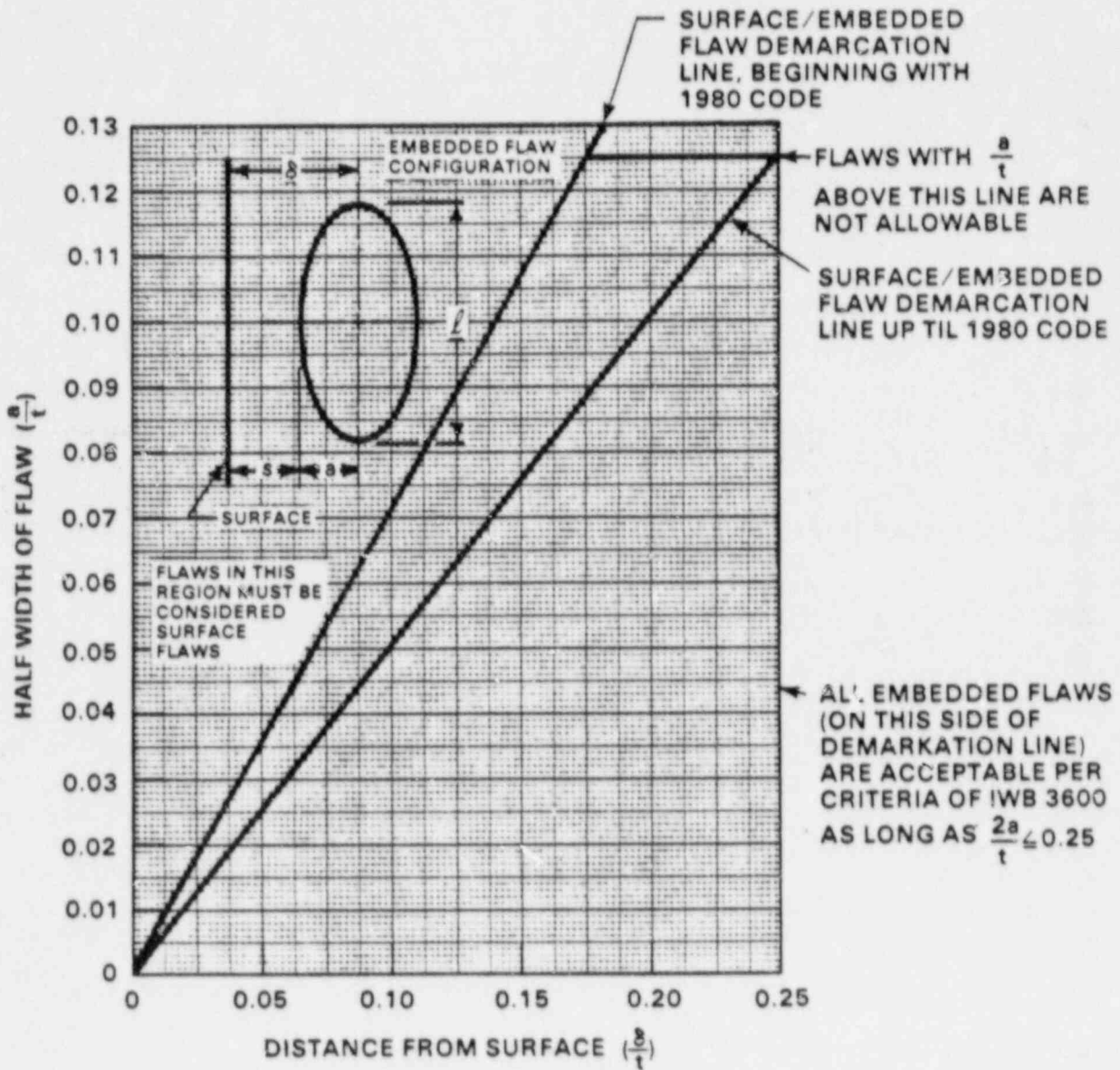


Figure A-3.5 Evaluation Chart for Inlet Nozzle to Shell Weld

<u>X</u>	Inside Surface	<u>—</u>	Surface Flaw	<u>X</u>	Longitudinal Flaw
<u>X</u>	Outside Surface	<u>X</u>	Embedded Flaw	<u>X</u>	Circumferential Flaw

#### A-4 OUTLET NOZZLE TO SHELL WELD

The analyses of the outlet nozzle to vessel weld showed a very complex stress state in this region. Consequently two separate sets of evaluation charts were constructed. The geometry most nearly corresponding to the angle of the indication should be used, or if there is some doubt, use both sets of charts, and take the most limiting result.

##### A-4.1 SURFACE FLAWS

The geometry and terminology for surface flaws at the Outlet Nozzle Penetration is depicted in figure A-4.1. The following parameters must be prepared for surface flaw evaluation with charts.

- o Flaw shape parameter  $\frac{a}{l}$
- o Flaw depth parameter  $\frac{a}{t}$

where

- a - the surface flaw depth detected (in.)
- l - the surface flaw length detected (in.)
- t - wall thickness (t = 11.11)

The surface flaw evaluation chart for the Outlet Nozzle Penetration, is listed below:

- o Figure A-4.2 Evaluation Chart for Outlet Nozzle to Shell Weld  

<u>X</u>	Inside Surface	<u>X</u>	Surface Flaw	<u>X</u>	Longitudinal Flaw
___	Outside Surface	___	Embedded Flaw	___	Circumferential Flaw
  
- o Figure A-4.3 Evaluation Chart for Outlet Nozzle to Shell Weld  

<u>X</u>	Inside Surface	<u>X</u>	Surface Flaw	___	Longitudinal Flaw
___	Outside Surface	___	Embedded Flaw	<u>X</u>	Circumferential Flaw

- o Figure A-4.4: Outside Surface Flaw Evaluation Chart - outlet nozzle full penetration, (longitudinal and circumferential)

#### A-4.2 EMBEDDED FLAWS

The geometry of embedded flaws at the Outlet Nozzle to Shell Weld is depicted in Figure A-4.1.

##### Basic Data:

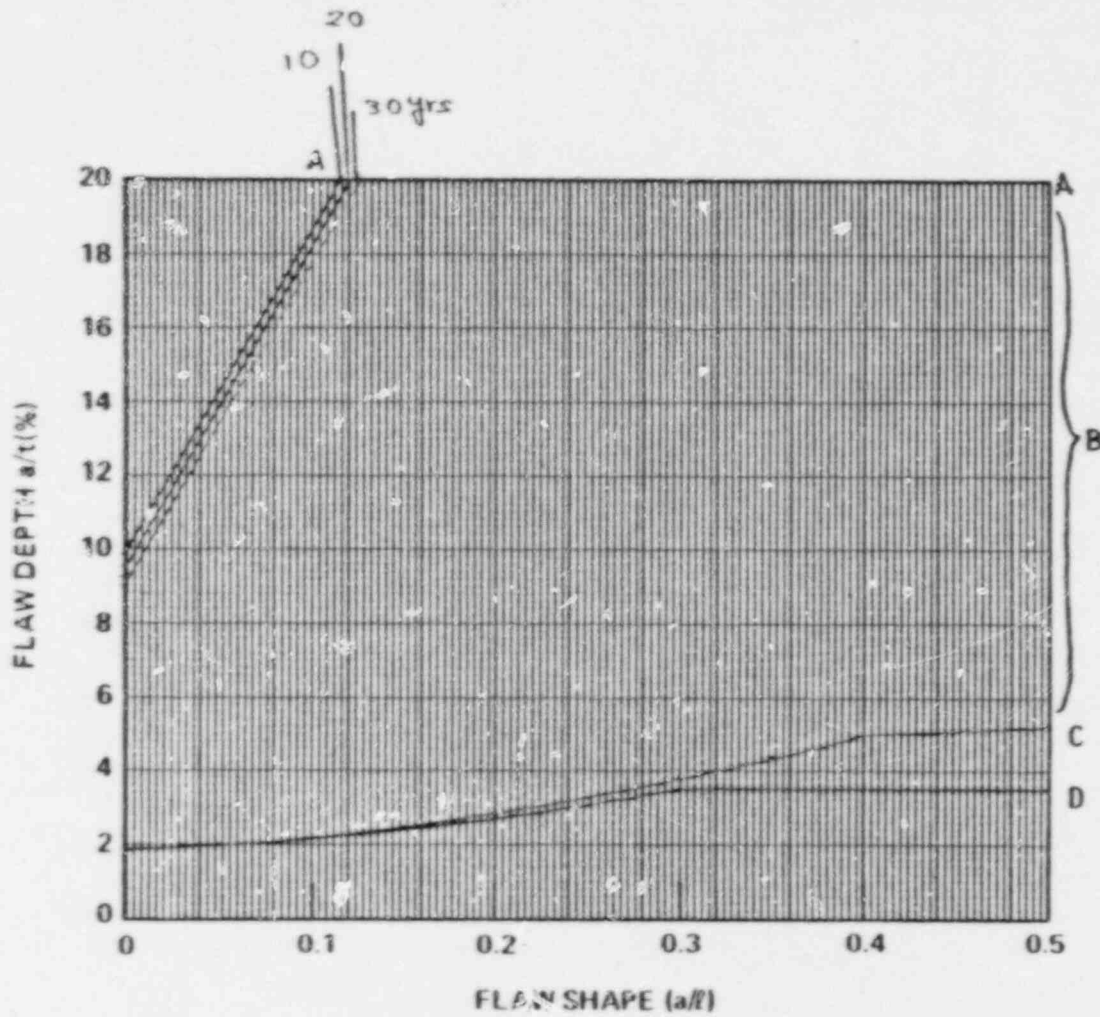
- t = 11.11 in.
- $\delta$  = Distance from the centerline of the embedded flaw to the surface (in.)
- a = Flaw depth (Defined as one half of the minor diameter) (in.)
- l = Flaw length (Major diameter) (in.)
- $\delta$  = Distance of the flaw to surface. (in terms of wall thickness e.g.  $\delta = 1/8 T$ , etc.)
- $a_0$  = Maximum embedded flaw size in depth direction, beyond which it must be considered a surface flaw, per Section XI characterization rules.

The following parameters must be calculated from the above dimensions to use the charts for evaluating the acceptability of an embedded flaw

- o Flaw shape parameter,  $\frac{a}{l}$
- o Flaw depth parameter,  $\frac{a}{t}$
- o surface proximity parameter,  $\frac{\delta}{t}$

Evaluation chart for embedded flaws: Figure A-4.5





LEGEND

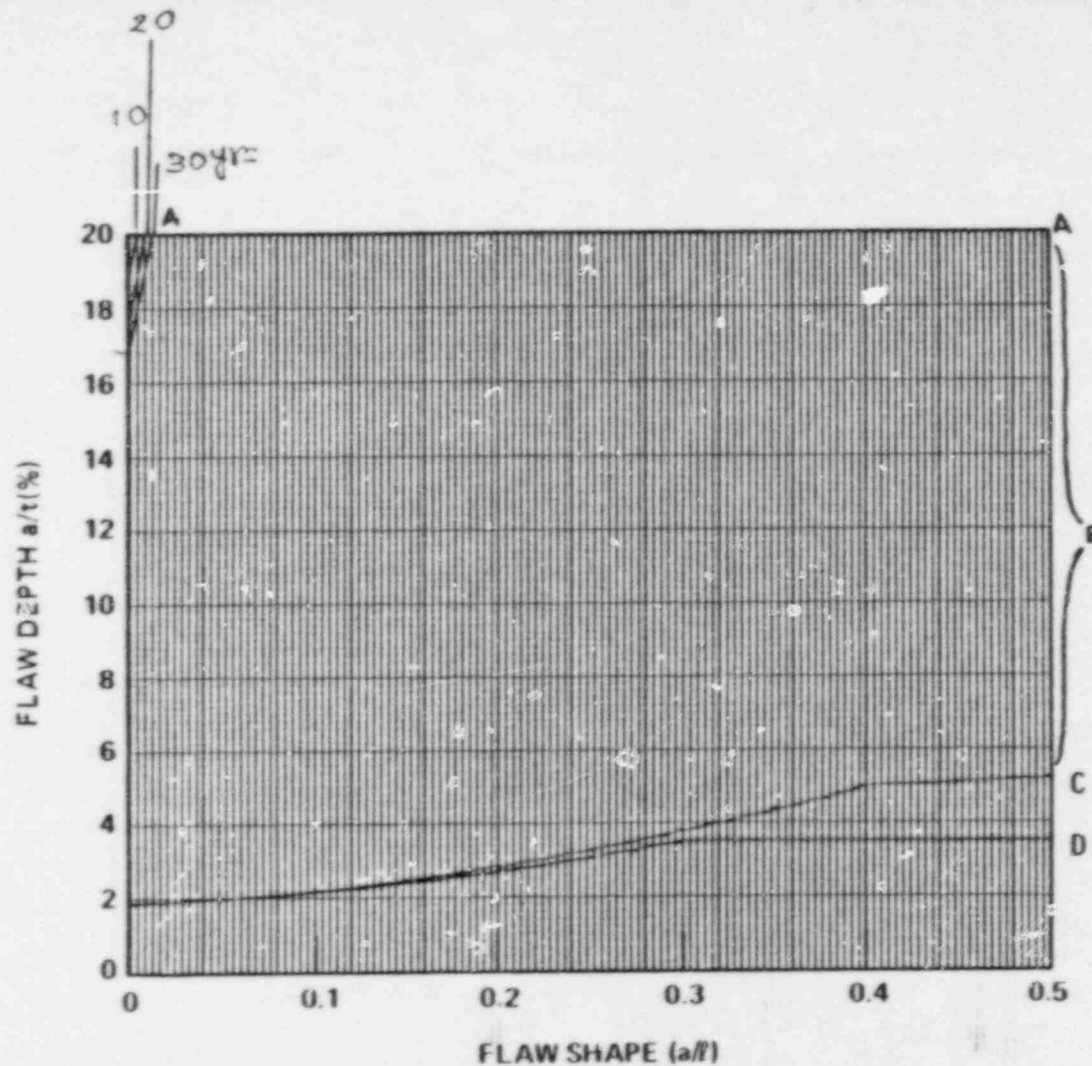
- A - The 10, 20, 30 year acceptable flaw limits.
- B - Within this zone, the surface flaw is acceptable by ASME Code analytical criteria in IWB-3600.
- C - ASME Code allowable since 1983 Winter Addendum.
- D - ASME Code allowable prior to 1983 Winter Addendum.

© Westinghouse 1987

Figure A-4.2 Evaluation Chart for Outlet Nozzle to Shell Weld

<u>X</u> Inside Surface	<u>X</u> Surface Flaw	<u>X</u> Longitudinal Flaw
<u>—</u> Outside Surface	<u>—</u> Embedded Flaw	<u>X</u> Circumferential Flaw

A-30



LEGEND

- A - The 10, 20, 30 year acceptable flaw limits.
- B - Within this zone, the surface flaw is acceptable by ASME Code analytical criteria in IWB-3600.
- C - ASME Code allowable since 1983 Winter Addendum.
- D - ASME Code allowable prior to 1983 Winter Addendum.

© Westinghouse 1987

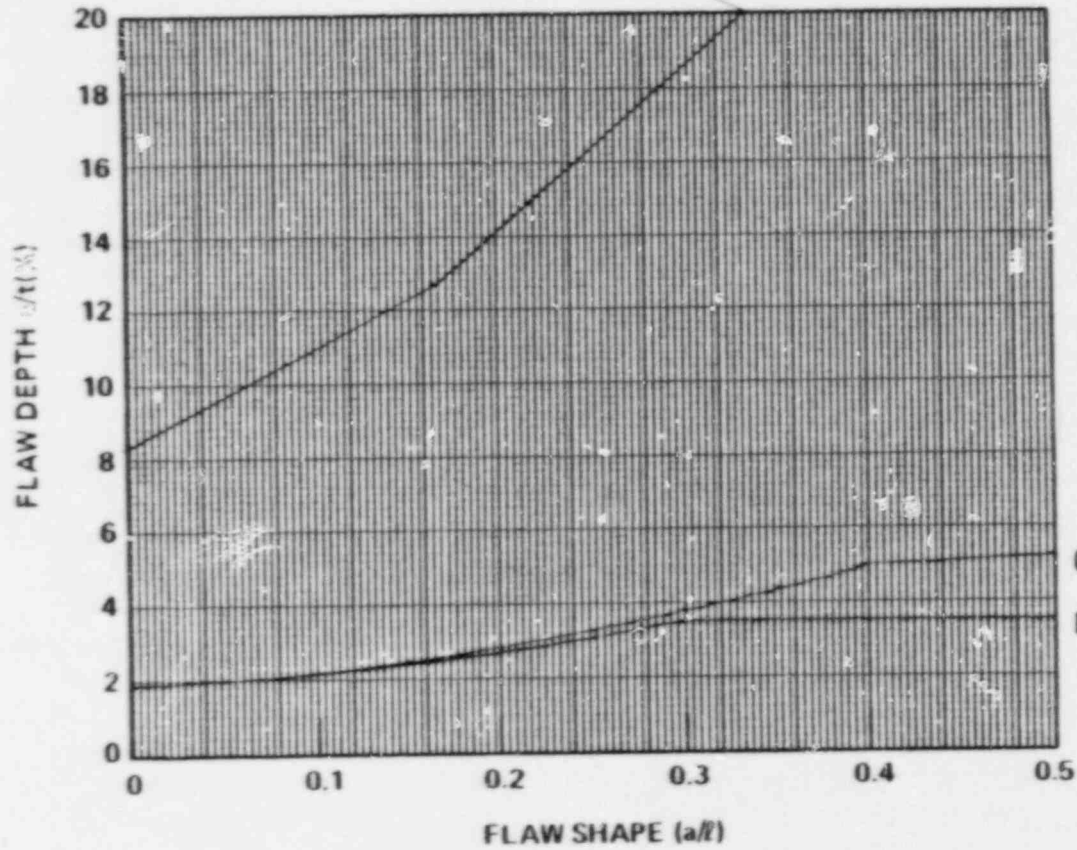
Figure A-4.3 Evaluation Chart for Outlet Nozzle to Shell Weld

- |          |                 |          |               |          |                      |
|----------|-----------------|----------|---------------|----------|----------------------|
| <u>X</u> | Inside Surface  | <u>X</u> | Surface Flaw  | <u>X</u> | Longitudinal Flaw    |
| —        | Outside Surface | —        | Embedded Flaw | <u>X</u> | Circumferential Flaw |

10, 20, 30 yrs

LEGEND

- A - The 10, 20, 30 year acceptable flaw limits.
- B - Within this zone, the surface flaw is acceptable by ASME Code analytical criteria in IWB-3500.
- C - ASME Code allowable since 1983 Winter Addendum.
- D - ASME Code allowable prior to 1983 Winter Addendum.



© Westinghouse 1987

Figure A-4.4 Evaluation Chart for Reactor Vessel Bellline

—	Inside Surface	X	Surface Flaw	X	Longitudinal Flaw
X	Outside Surface	—	Embedded Flaw	X	Circumferential Flaw

A-31

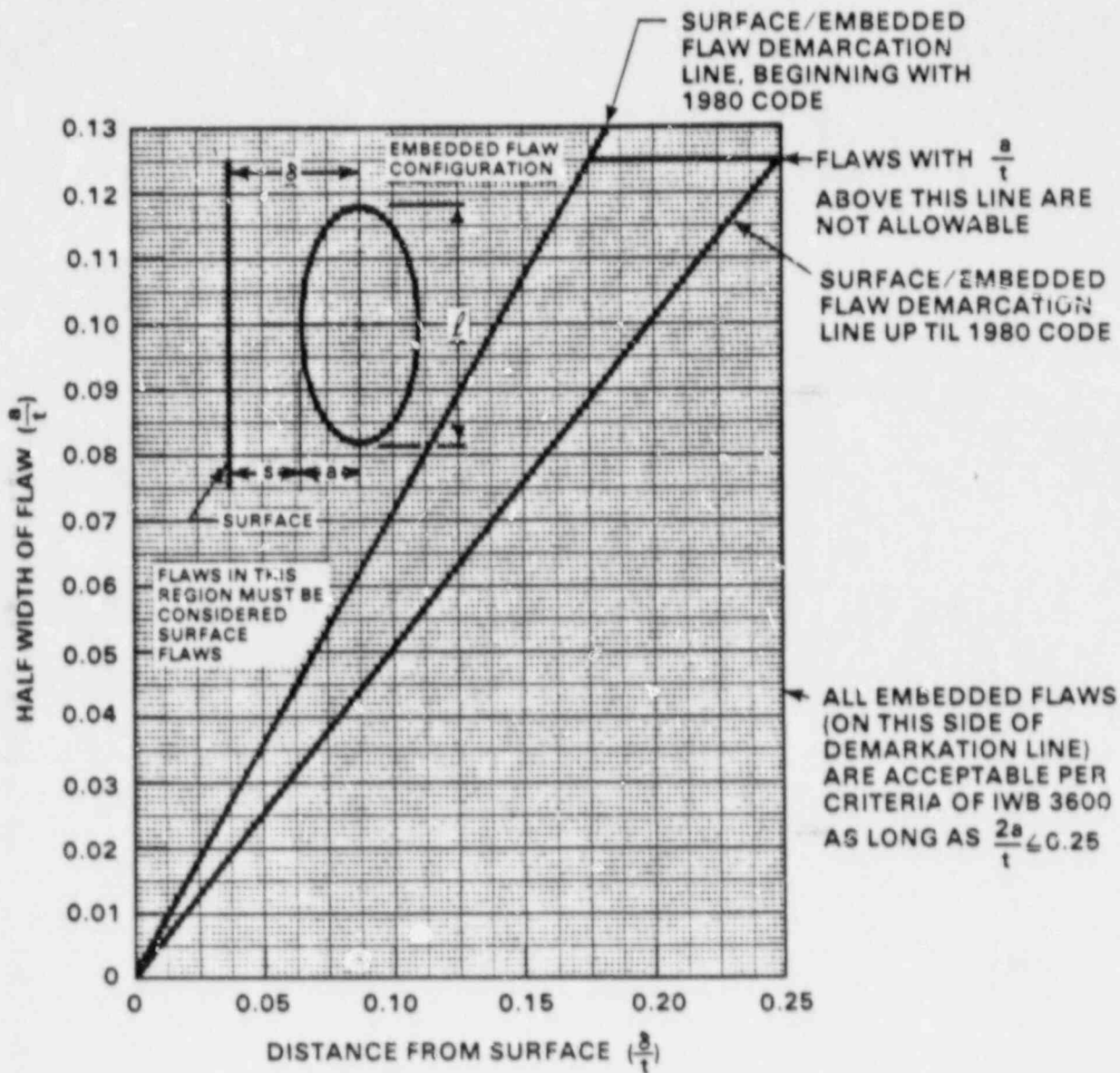


Figure A-4.5 Evaluation Chart for Outlet Nozzle to Shell Weld

<u>X</u> Inside Surface	<u>—</u> Surface Flaw	<u>X</u> Longitudinal Flaw
<u>X</u> Outside Surface	<u>X</u> Embedded Flaw	<u>X</u> Circumferential Flaw

## A-5 LOWER HEAD RING TO LOWER SHELL WELD

### A-5.1 SURFACE FLAWS

The geometry and terminology for surface flaws at the Lower Head Ring to Lower Head Weld is depicted in figure A-5.1. The following parameters must be prepared for surface flaw evaluation with charts.

- o Flaw shape parameters  $\frac{a}{l}$
- o Flaw depth parameter  $\frac{a}{t}$

where

- a - the surface flaw depth detected (in.)
- l - the surface flaw length detected (in.)
- t - wall thickness (t = 4.875")

The surface flaw evaluation charts for the Lower Head Ring to Lower Head Weld are listed below:

- o Figure A-5.2 Evaluation Chart for Lower Head Ring to Lower Head Weld

<u>X</u>	Inside Surface	<u>X</u>	Surface Flaw	<u>X</u>	Longitudinal Flaw
___	Outside Surface	___	Embedded Flaw	___	Circumferential Flaw

- o Figure A-5.3 Evaluation Chart for Lower Head Ring to Lower Head Weld

<u>X</u>	Inside Surface	<u>X</u>	Surface Flaw	___	Longitudinal Flaw
___	Outside Surface	___	Embedded Flaw	<u>X</u>	Circumferential Flaw

- o Figure A-5.4 Evaluation Chart for Lower Head Ring to Lower Head Weld

___	Inside Surface	<u>X</u>	Surface Flaw	<u>X</u>	Longitudinal Flaw
<u>X</u>	Outside Surface	___	Embedded Flaw	<u>X</u>	Circumferential Flaw

## A-5.2 EMBEDDED FLAWS

The geometry of embedded flaws at the Lower Head Ring to Lower Head Weld is depicted in figure A-5.1.

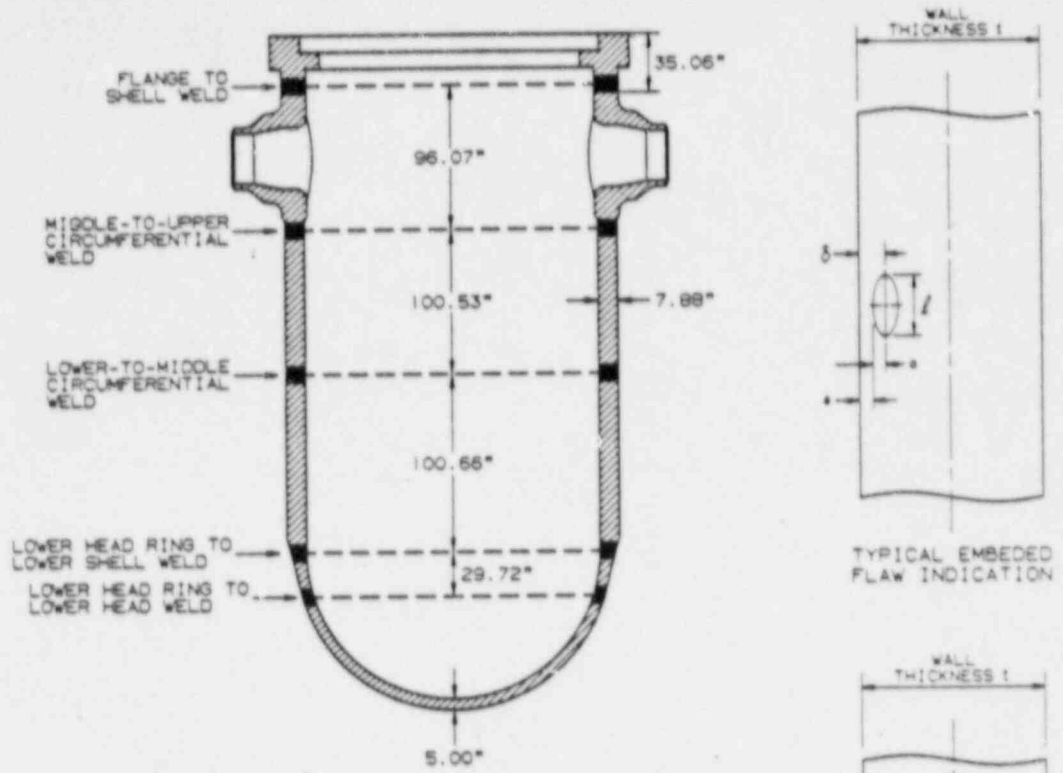
### Basic Data:

- t = 4.875 in.
- $\delta$  = Distance from the centerline of the embedded flaw to the surface (in.)
- a = Flaw depth (Defined as one half of the minor diameter) (in.)
- l = Flaw length (Major diameter) (in.)
- $a_o$  = Maximum embedded flaw size in depth direction, beyond which it must be considered a surface flaw, per Section XI characterization rules.

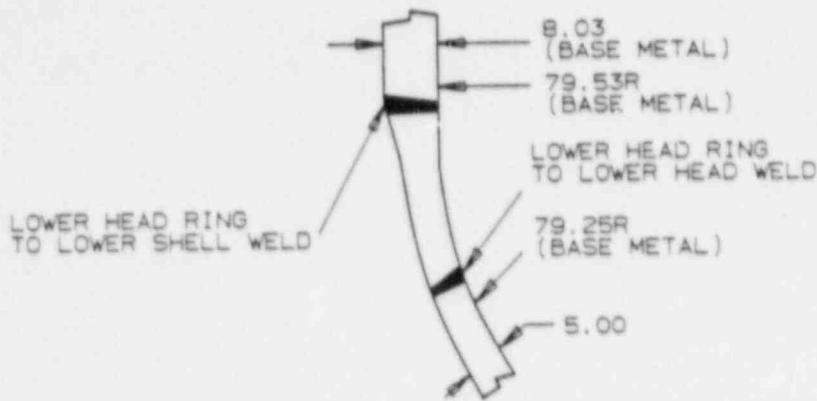
The following parameters must be calculated from the above dimensions to use the charts for evaluating the acceptability of an embedded flaw

- o Flaw shape parameter,  $\frac{a}{r}$
- o Flaw depth parameter,  $\frac{a}{t}$
- o surface proximity parameter,  $\frac{\delta}{t}$

Evaluation chart for embedded flaws: Figure A-5.5.



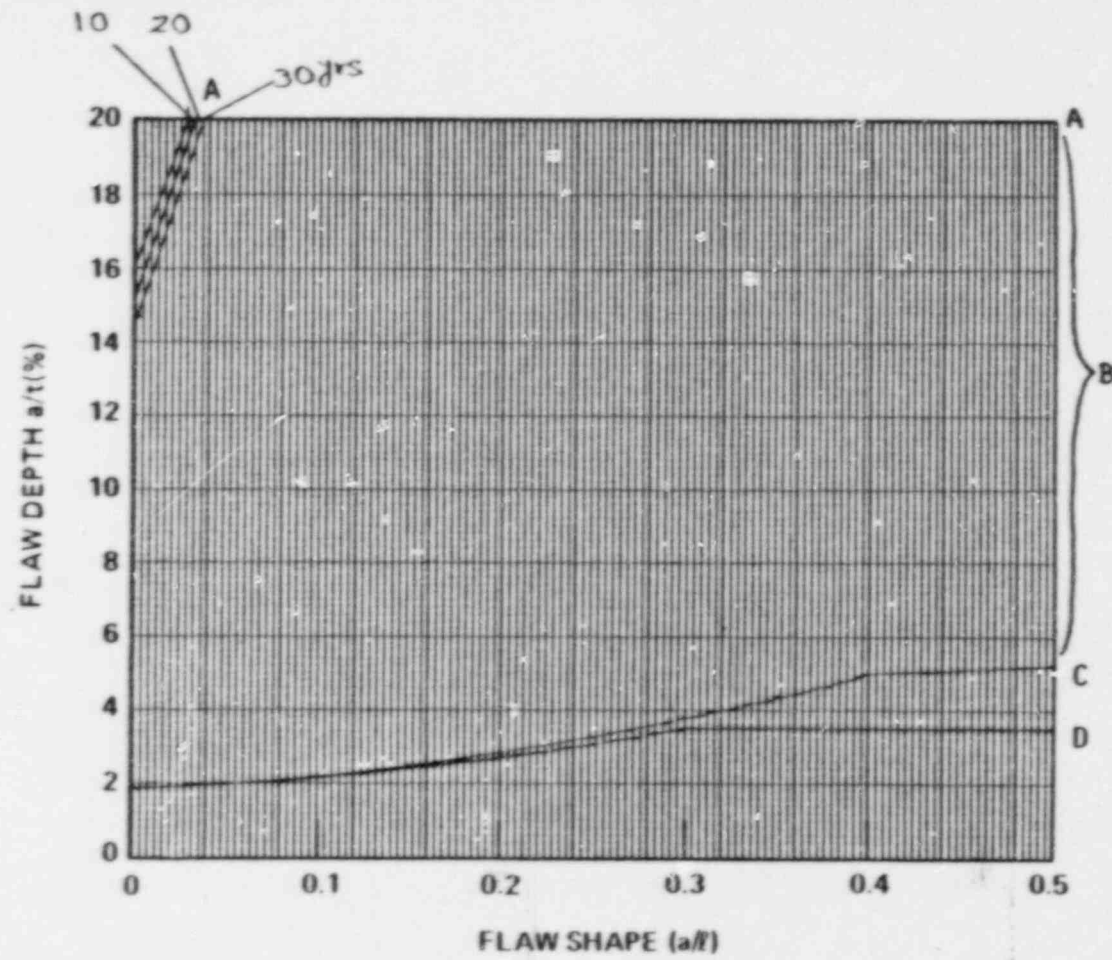
NOTE: THICKNESSES DO NOT INCLUDE INSIDE CLADDING



BELTLINE AND LOWER HEAD REGIONS

- NOTES: 1. DIMENSIONS DO NOT INCLUDE CLADDING  
 2. ALL DIMENSIONS ARE IN INCHES

Figure A-5.1 Geometry and Terminology for Flaws at the Lower Head Ring to Lower Head Weld



LEGEND

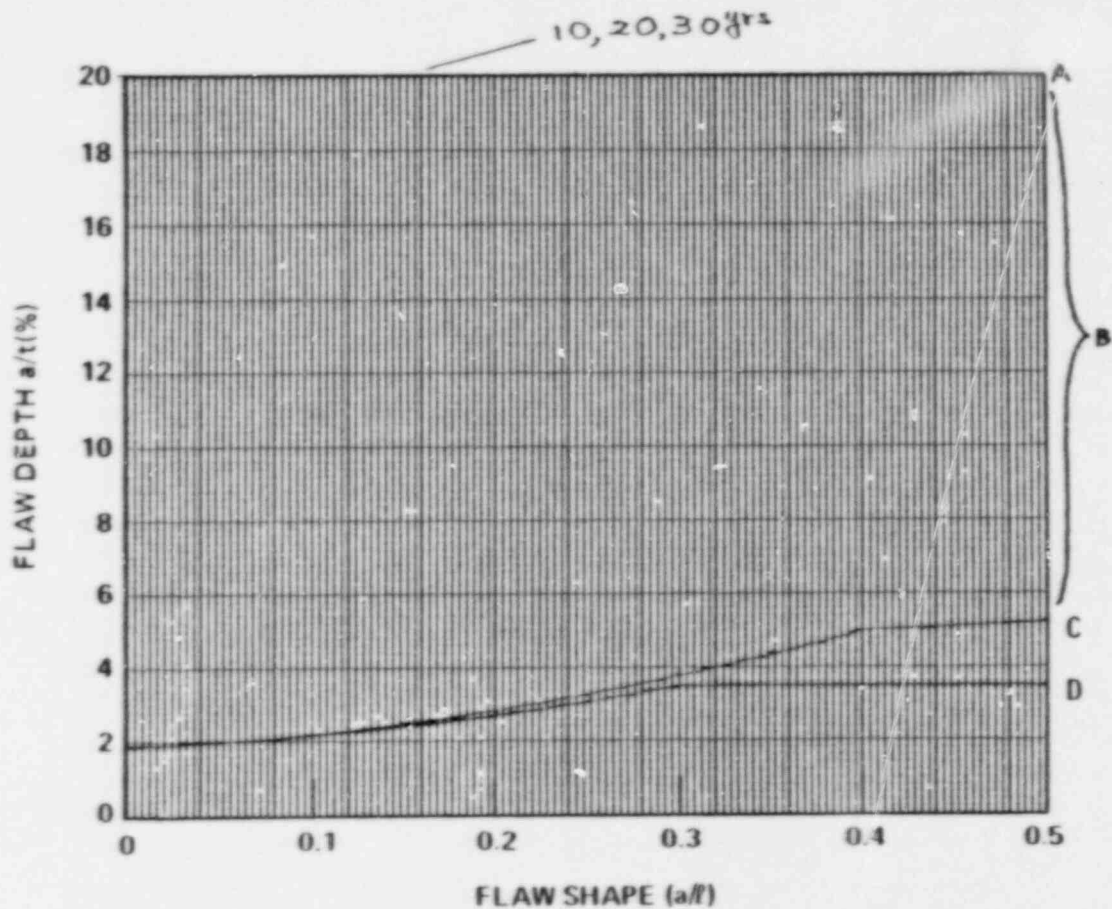
- A - The 10, 20, 30 year acceptable flaw limits.
- B - Within this zone, the surface flaw is acceptable by ASME Code analytical criteria in IWB-3600.
- C - ASME Code allowable since 1983 Winter Addendum.
- D - ASME Code allowable prior to 1983 Winter Addendum.

© Westinghouse 1987

Figure A-5.2 Evaluation Chart for Lower Head Ring to Lower Head Weld

- X Inside Surface    X Surface Flaw    X Longitudinal Flaw
- Outside Surface    — Embedded Flaw    — Circumferential Flaw

A-37



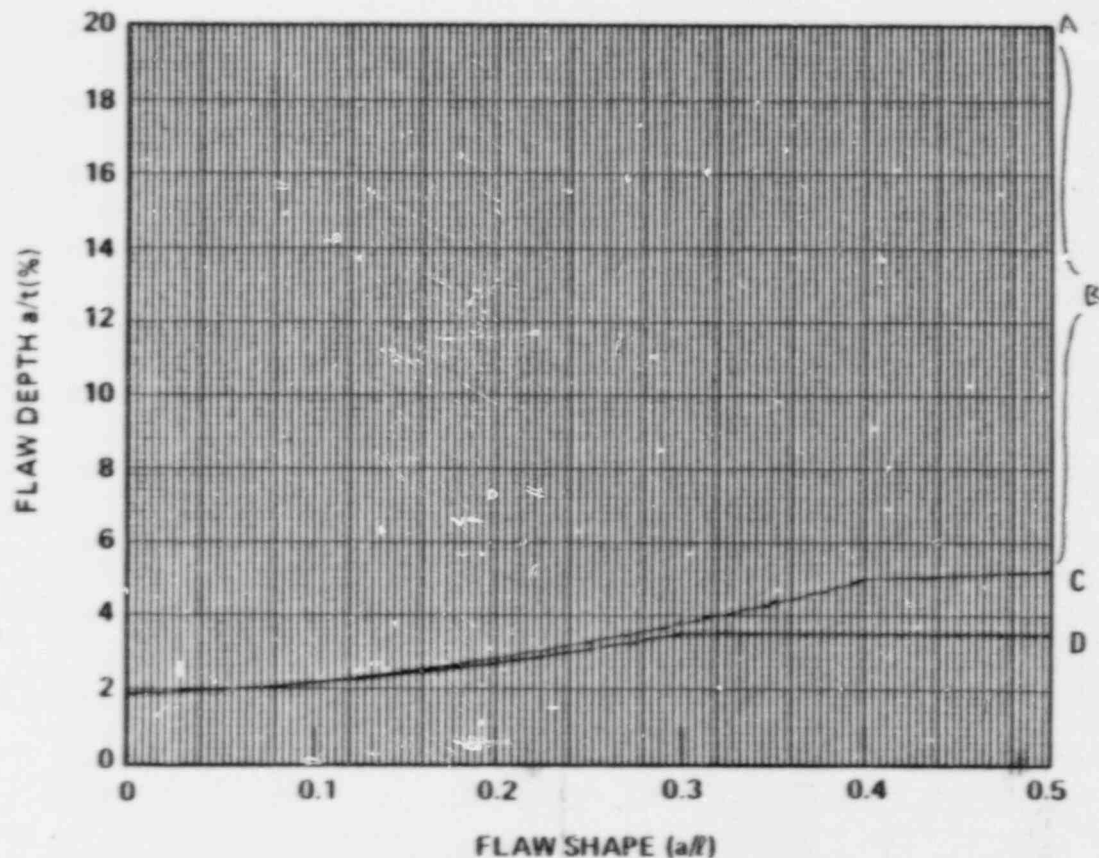
LEGEND

- A - The 10, 20, 30 year acceptable flaw limits.
- B - Within this zone, the surface flaw is acceptable by ASME Code analytical criteria in IWB-3600.
- C - ASME Code allowable since 1983 Winter Addendum.
- D - ASME Code allowable prior to 1983 Winter Addendum.

© Westinghouse 1987

Figure A-5.3 Evaluation Chart for Lower Head Ring to Lower Head Weld

<u>X</u>	Inside Surface	<u>X</u>	Surface Flaw	<u>    </u>	Longitudinal Flaw
<u>    </u>	Outside Surface	<u>    </u>	Embedded Flaw	<u>X</u>	Circumferential Flaw



### LEGEND

- A - The 10, 20, 30 year acceptable flaw limits.
- B - Within this zone, the surface flaw is acceptable by ASME Code analytical criteria in IWB-3600.
- C - ASME Code allowable since 1983 Winter Addendum.
- D - ASME Code allowable prior to 1983 Winter Addendum.

© Westinghouse 1987

Figure A-5.4 Evaluation Chart for Lower Head Ring to Lower Head Weld

—	Inside Surface	X	Surface Flaw	X	Longitudinal Flaw
X	Outside Surface	—	Embedded Flaw	X	Circumferential Flaw

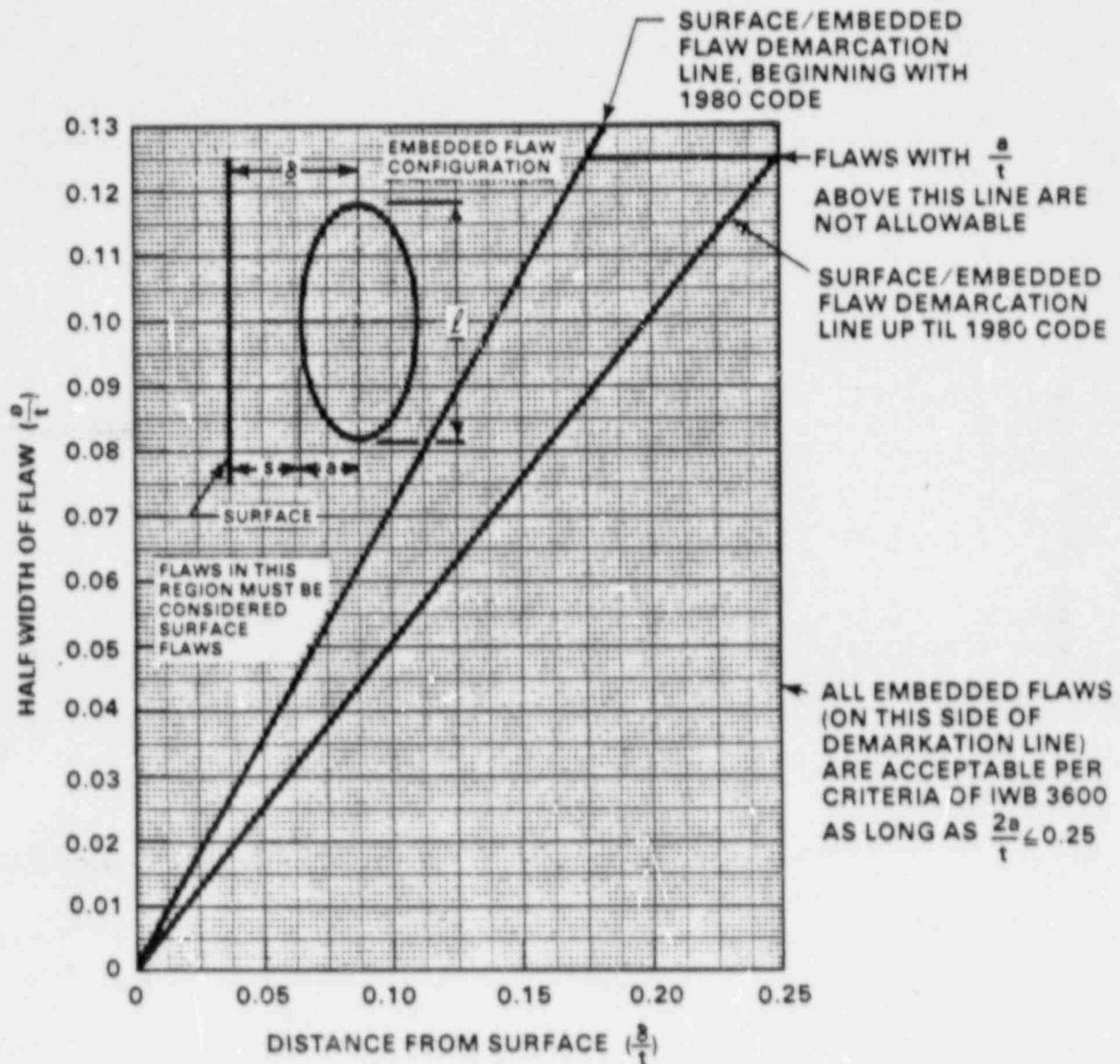


Figure A-5.5 Evaluation Chart for Lower Head Ring to Lower Head Weld

<u>X</u>	Inside Surface	—	Surface Flaw	<u>X</u>	Longitudinal Flaw
<u>X</u>	Outside Surface	<u>X</u>	Embedded Flaw	<u>X</u>	Circumferential Flaw

APPENDIX B  
CRITICAL FLAW SIZE RESULTS

TABLE B-1  
 CRITICAL FLAW SIZE SUMMARY FOR BELTLINE REGION  
 (INSIDE SURFACE)

Condition	Flaw Orient.	Continuous Flaw		Aspect Ratio = 6.0		Aspect Ratio = 2.0	
		inches	a/t	inches	a/t	inches	a/t
E/F (Steam Gen. Tube Rupture)	Long.	$a_i = 2.50$	(0.323)	$a_i = 5.51$	(0.711)	$a_i = 7.75$	(1.0)
	Circ.	$a_i = 7.75$	(1.0)	$a_i = 7.75$	(1.0)	$a_i = 7.75$	(1.0)
E/F (LSB)	Long.	$a_i = \text{N/A}$	N/A	$a_i = 3.39$	(0.44)	$a_i = \text{N/A}$	N/A
	Circ.	$a_i = 2.21$	(0.34)	$a_i = 7.75$	(1.00)	$a_i = 7.75$	(1.0)
E/F (Small LOCA)	Long.	$a_i = 2.25$	(0.33)	$a_i = 5.74$	(0.74)	$a_i = 7.75$	(1.0)
	Circ.	$a_i = 7.75$	(1.00)	$a_i = 7.75$	(1.00)	$a_i = 7.75$	(1.0)
E/F (Large LOCA)	Long.	$a_i = 7.75$	(1.00)	$a_i = 7.75$	(1.00)	$a_i = 7.75$	(1.0)
	Circ.	$a_i = 7.75$	(1.00)	$a_i = 7.75$	(1.00)	$a_i = 7.75$	(1.0)
N/U (Excessive Feedwater Flow)	Long.	$a_c = 3.83$	(0.494)	$a_c = 7.75$	(1.00)	$a_c = 7.75$	(1.0)
	Circ.	$a_c = 7.75$	(1.00)	$a_c = 7.75$	(1.00)	$a_c = 7.75$	(1.0)

TABLE B-2  
CRITICAL FLAW SIZE SUMMARY FOR BELTLINE REGION - OUTSIDE SURFACE

Condition	Flaw Orient.	Continuous Flaw		Aspect Ratio = 6:1		Aspect Ratio = 2:1	
		inches	a/t	inches	a/t	inches	a/t
N/U/T Cold Hydro	Long.	$a_c = 3.54$	7.75	$a_c = 7.75$	1.0	$a_c = 7.75$	1.0
	Circ.	$a_c = 7.75$	7.75	$a_c = 7.75$	1.0	$a_c = 7.75$	1.0
E/F	Long.	$a_i = N/A^*$	N/A*	$a_i = N/A^*$	N/A*	$a_i = N/A^*$	N/A*
	Circ.	$a_i = N/A^*$	N/A*	$a_i = N/A^*$	N/A*	$a_i = N/A^*$	N/A*

LEGEND:

$a_c$  Minimum critical flaw size under normal conditions  
 $a_i$  Minimum critical flaw size under faulted conditions

\*The emergency/faulted (E/F) case was found to be less critical at the outside surface than the normal/upset/test (N/U/T) conditions, because the stresses are compressive for the E/F conditions. Therefore, these cases were not subjected to fracture analyses.

TABLE B-3  
 CRITICAL FLAW SIZE SUMMARY FOR  
 INLET NOZZLE TO SHELL WELD - INSIDE SURFACE

Condition	Flaw Orient.	Continuous Flow		Aspect Ratio = 6:1		Aspect Ratio = 2:1	
		inches	a/t	inches	a/t	inches	a/t
N/U/T Excessive Feedwater Flow	Long.	$a_c = 5.41$	.514	$a_c = 10.53$	1.0	$a_c = 10.53$	1.0
	Circ.	$a_c = \text{N/A}$	N/A	$a_c = \text{N/A}$	N/A	$a_c = 9.16$	1.0
E/F LOCA	Long.	$a_i = 1.032$	.098	$a_i = 10.53$	1.0	$a_i = 10.53$	1.0
	Circ.	$a_i = 1.27$	.121	$a_i = 10.53$	1.0	$a_i = 10.53$	1.0

LEGEND:

$a_c$  Minimum critical flaw size under normal conditions

$a_i$  Minimum critical flaw size under faulted conditions

\*Governing transient for charts

TABLE B-4  
 CRITICAL FLAW SIZE SUMMARY FOR  
 INLET NOZZLE TO SHELL WELD - OUTSIDE SURFACE

Condition	Flaw Orient.	Continuous Flow		Aspect Ratio = 6:1		Aspect Ratio = 2:1	
		inches	a/t	inches	a/t	inches	a/t
N/U/T	Long.	$a_c = 4.10$	.389	$a_c = 7.16$	.68	$a_c = 10.53$	1.0
Loss of Flow*	Circ.	$a_c = 8.29$	.788	$a_c = 10.53$	1.0	$a_c = 10.53$	1.0
E/F	Long.	$a_i = N/A^*$	N/A*	$a_i = N/A^*$	N/A*	$a_i = N/A^*$	N/A*
	Circ.	$a_i = N/A^*$	N/A*	$a_i = N/A^*$	N/A*	$a_i = N/A^*$	N/A*

LEGEND:

- $a_c$  Minimum critical flaw size under normal conditions
- $a_i$  Minimum critical flaw size under faulted conditions

\*The emergency/faulted (E/F) case was found to be less critical at the outside surface than the normal/upset/test (N/U/T) conditions, because the stresses are compressive for the E/F conditions. Therefore, these cases were not subjected to fracture analyses.

TABLE B-5  
 CRITICAL FLAW SIZE SUMMARY FOR OUTLET NOZZLE TO SHELL WELD  
 (Inside Surface)

Condition	Flaw Orient.	Continuous Flow		Aspect Ratio = 6:1		Aspect Ratio = 2:1	
		inches	a/t	inches	a/t	inches	a/t
N/U/T	Long.	$a_c = 5.81$	0.523	$a_c = 11.11$	1.0	$a_c = 11.11$	1.0
Turbine Roll*	Circ.	$a_c = 11.11$	1.0	$a_c = 11.11$	1.0	$a_c = 11.11$	1.0
E/F	Long.	$a_i = 1.29$	0.116	$a_i = 2.72$	0.245	$a_i = 11.11$	1.0
LSB	Circ.	$a_i = \text{N/A}$	N/A	$a_i = \text{N/A}$	N/A	$a_i = \text{N/A}$	N/A

LEGEND:

$a_c$  Minimum critical flaw size under normal conditions, cold hydro

$a_i$  Minimum critical flaw size under faulted conditions

N/A Results not available

\*Governing transient for charts

TABLE B-6  
 CRITICAL FLAW SIZE SUMMARY FOR  
 OUTLET NOZZLE TO SHELL WELD  
 (Outside Surface)

Condition	Flaw Orient.	Continuous Flaw		Aspect Ratio = 6:1		Aspect Ratio = 2:1	
		inches	a/t	inches	a/t	inches	a/t
N/U/T Cold Hydro	Long.	$a_c = 3.22$	0.29	$a_c = 4.99$	0.45	$a_c = 11.11$	1.0
	Circ.	$a_c = \text{N/A}$	N/A	$a_c = \text{N/A}$	N/A	$a_c = \text{N/A}$	N/A
E/F	Long.	$a_i = \text{N/A}$	N/A	$a_i = \text{N/A}$	N/A	$a_i = \text{N/A}$	N/A
	Circ.	$a_i = \text{N/A}$	N/A	$a_i = \text{N/A}$	N/A	$a_i = \text{N/A}$	N/A

LEGEND:

$a_c$  Minimum critical flaw size under normal conditions, cold hydro

$a_i$  Minimum critical flaw size under faulted conditions

\*The emergency/faulted (E/F) case was found to be less critical at the outside surface than the normal/upset/test (N/U/T) conditions, because the stresses are compressive for the E/F conditions. Therefore, these cases were not subjected to fracture analyses.

N/A Results not available

TABLE B-7  
 CRITICAL FLAW SIZE SUMMARY FOR  
 LOWER HEAD RING TO LOWER SHELL WELD  
 (INSIDE SURFACE)

Condition	Flaw Orient.	Continuous Flaw		Aspect Ratio = 6:1		Aspect Ratio = 2:1	
		inches	a/t	inches	a/t	inches	a/t
N/U/T Excessive Feedwater Flow*	Long.	$a_c = 2.93$	0.60	$a_c = 4.875$	1.0	$a_c = 4.875$	1.0
	Circ.	$a_c = 4.875$	1.0	$a_c = 4.875$	1.0	$a_c = 4.875$	1.0
E/F	Long.	$a_i = 2.12$	0.436	$a_i = 4.875$	1.000	$a_i = 4.875$	1.0
LSB	Circ.	$a_i = 4.875$	1.000	$a_i = 4.875$	1.000	$a_i = 4.875$	1.0

LEGEND:

- $a_c$  Minimum critical flaw size under normal conditions
- $a_i$  Minimum critical flaw size under faulted conditions

\*Governing transient for charts

TABLE B-8  
 CRITICAL FLAW SIZE SUMMARY FOR  
 LOWER HEAD RING TO LOWER HEAD WELD  
 (OUTSIDE SURFACE)

Condition	Flaw Orient.	Continuous Flow		Aspect Ratio = 6:1		Aspect Ratio = 2:1	
		inches	a/t	inches	a/t	inches	a/t
N/U/T Turbine Roll*	Long.	$a_c = 2.398$	0.492	$a_c = 4.875$	1.0	$a_c = 4.875$	1.0
	Circ.	$a_c = 3.193$	0.655	$a_c = 4.875$	1.0	$a_c = 4.875$	1.0
E/F LSB	Long.	$a_i = 2.672$	4.875	$a_i = 4.875$	1.0	$a_i = 4.875$	1.0
	Circ.	$a_i = 4.051$	4.875	$a_i = 4.875^c$	1.0	$a_i = 4.875$	1.0

LEGEND:

$a_c$  Minimum critical flaw size under normal conditions

$a_i$  Minimum critical flaw size under faulted conditions

\*Governing transient for charts

APPENDIX C  
FATIGUE CRACK GROWTH RESULTS

BELTLINE REGION SURFACE FLAW FATIGUE CRACK GROWTH  
 - LONGITUDINAL FLAW

	INITIAL CRACK LENGTH	CRACK LENGTH AFTER YEAR			
		10	20	30	40
a/l = 0.0	0.100	0.10297	0.10560	0.10834	0.11141
	0.300	0.31799	0.33316	0.34905	0.36636
	0.500	0.53457	0.56587	0.59941	0.633666
	0.800	0.86544	0.92893	0.99871	1.07716
	1.000	1.08915	1.17854	1.27880	1.39385
	1.200	1.31613	1.43681	1.57620	1.74225
	1.300	1.43140	1.57062	1.73477	1.93512
	1.550	1.72659	1.92503	2.17617	2.48940
a/l = 0.167	0.100	0.10112	0.10194	0.10276	0.10362
	0.300	0.30905	0.31666	0.32432	0.33239
	0.500	0.51781	0.53233	0.54707	0.56250
	0.800	0.82772	0.85118	0.87491	0.89958
	1.000	1.03325	1.06173	1.09053	1.12031
	1.200	1.23805	1.27093	1.30415	1.33830
	1.300	1.34018	1.37499	1.41018	1.44626
	1.550	1.59475	1.63402	1.67375	1.71434

BELTLINE REGION SURFACE FLAW FATIGUE CRACK GROWTH  
 - CIRCUMFERENTIAL FLAW

	INITIAL CRACK LENGTH	CRACK LENGTH AFTER YEAR			
		10	20	30	40
$a/l = 0.0$	0.100	0.10029	0.10051	0.10071	0.10093
	0.300	0.30559	0.30980	0.31392	0.31842
	0.500	0.51655	0.53068	0.54518	0.56063
	0.800	0.83247	0.86220	0.89248	0.92424
	1.000	1.04105	1.07914	1.11826	1.15934
	1.200	1.25608	1.30162	1.34794	1.39615
	1.300	1.35949	1.40802	1.45890	1.51202
	1.550	1.61870	1.67575	1.73367	1.79345
$a/l = 0.167$	0.100	0.10010	0.10018	0.10024	0.10032
	0.300	0.30188	0.30329	0.30463	0.30608
	0.500	0.50722	0.51287	0.51841	0.52425
	0.800	0.81267	0.82270	0.83265	0.84294
	1.000	1.01548	1.02830	1.04104	1.05429
	1.200	1.22245	1.23762	1.25260	1.26808
	1.300	1.32275	1.33802	1.35302	1.36841
	1.550	1.57467	1.59177	1.60868	1.62596

BELTLINE REGION EMBEDDED FLAW FATIGUE CRACK GROWTH  
(ASPECT RATIO 1:10) - LONGITUDINAL FLAW

		INITIAL CRACK LENGTH	CRACK LENGTH AFTER YEAR			
			10	20	30	40
T = 7.75 in. δ = 0.48438 in.	0.200	0.20023	0.20041	0.20060	0.20078	
	0.250	0.25035	0.25064	0.25092	0.25120	
	0.300	0.30050	0.30091	0.30131	0.30171	
	0.320	0.32057	0.32103	0.32148	0.32194	
T = 7.75 in. δ = 0.72656 in.	0.350	0.35061	0.35108	0.35156	0.35205	
	0.400	0.40079	0.40141	0.40203	0.40266	
	0.450	0.45099	0.45178	0.45257	0.45336	
	0.500	0.50122	0.50219	0.50317	0.50415	
T = 7.75 in. δ = 0.96875 in.	0.560	0.56138	0.56247	0.56356	0.56465	
	0.640	0.64180	0.64322	0.64465	0.64609	
	0.650	0.65186	0.65333	0.65480	0.65628	
T = 7.75 in. δ = 1.45313 in.	0.700	0.70184	0.70324	0.70465	0.70607	
	0.800	0.80239	0.80423	0.80608	0.80794	
	0.900	0.90303	0.90537	0.90773	0.91009	
	1.000	1.00375	1.00667	1.00960	1.01255	
T = 7.75 in. δ = 1.9375 in.	0.900	0.90256	0.90445	0.90635	0.90826	
	1.050	1.05353	1.05616	1.05881	1.06147	
	1.200	1.20468	1.20822	1.21178	1.21536	
	1.350	1.35605	1.36067	1.36533	1.37003	

BELTLINE REGION EMBEDDED FLAW FATIGUE CRACK GROWTH  
(ASPECT RATIO 1:10) - CIRCUMFERENTIAL FLAW

		INITIAL CRACK LENGTH	CRACK LENGTH AFTER YEAR			
			10	20	30	40
T = 7.75 in. δ = 0.484 in.	0.200	0.20005	0.20009	0.20013	0.20017	
	0.250	0.25008	0.25014	0.25020	0.25026	
	0.300	0.30012	0.30021	0.30030	0.30039	
	0.320	0.32014	0.32024	0.32034	0.32045	
T = 7.75 in. δ = 0.726 in.	0.350	0.35011	0.35020	0.35028	0.35037	
	0.400	0.40015	0.40026	0.40038	0.40049	
	0.450	0.45020	0.45034	0.45049	0.45064	
	0.500	0.50025	0.50044	0.50062	0.50081	
T = 7.75 in. δ = 0.968 in.	0.560	0.56022	0.56039	0.56056	0.56073	
	0.640	0.64031	0.64054	0.64076	0.64100	
	0.650	0.65032	0.65056	0.65079	0.65103	
T = 7.75 in. δ = 1.453 in.	0.700	0.70020	0.70035	0.70051	0.70066	
	0.800	0.80027	0.80048	0.80069	0.80090	
	0.900	0.90036	0.90064	0.90092	0.90120	
	1.000	1.00047	1.00084	1.00120	1.00157	
T = 7.75 in. δ = 1.9375 in.	0.900	0.90022	0.90040	0.90058	0.90075	
	1.050	1.05032	1.05057	1.05082	1.05108	
	1.200	1.20044	1.20079	1.20114	1.20149	
	1.350	1.35060	1.35107	1.35155	1.35202	

BOTTOM HEAD TRANSITION REGION SURFACE FLAW FATIGUE CRACK GROWTH  
- LONGITUDINAL FLAW

	INITIAL CRACK LENGTH	CRACK LENGTH AFTER YEAR			
		10	20	30	40
$a/t = 0.0$	0.200	0.20611	0.21181	0.21765	0.22403
	0.400	0.41674	0.43204	0.44779	0.46462
	0.600	0.62901	0.65583	0.68379	0.71390
	0.800	0.84305	0.88375	0.92696	0.97401
	1.000	1.05994	1.11881	1.18331	1.25582
	1.200	1.28289	1.36900	1.46790	1.58561
$a/t = 0.167$	0.200	0.20284	0.20537	0.20787	0.21056
	0.400	0.40789	0.41500	0.42208	0.42946
	0.600	0.61219	0.62322	0.63425	0.64567
	0.800	0.81567	0.82979	0.84391	0.85839
	1.000	1.01836	1.03480	1.05132	1.06812
	1.200	1.22093	1.23958	1.25836	1.27741

BOTTOM HEAD TRANSITION REGION SURFACE FLAW FATIGUE CRACK GROWTH  
- CIRCUMFERENTIAL FLAW

	INITIAL CRACK LENGTH	CRACK LENGTH AFTER YEAR			
		10	20	30	40
$a/l = 0.0$	0.200	0.20867	0.21455	0.22044	0.22694
	0.400	0.42194	0.43971	0.45805	0.47791
	0.600	0.63691	0.66909	0.70256	0.73844
	0.800	0.84889	0.89244	0.93771	0.98568
	1.000	1.09942	1.11310	1.16874	1.22748
	1.200	1.26925	1.33273	1.39853	1.46793
$a/l = 0.167$	0.200	0.20395	0.20667	0.20930	0.21218
	0.400	0.41127	0.41934	0.42739	0.43597
	0.600	0.61745	0.63097	0.64448	0.65855
	0.800	0.82088	0.83734	0.85373	0.87057
	1.000	1.02307	1.04152	1.05989	1.07863
	1.200	1.22461	1.24463	1.26452	1.28475

BOTTOM HEAD TRANSITION REGION EMBEDDED FLAW FATIGUE CRACK GROWTH  
(ASPECT RATIO 1:10) - LONGITUDINAL FLAW

		INITIAL CRACK LENGTH	CRACK LENGTH AFTER YEAR			
			10	20	30	40
T = 4.875 in. δ = 0.304	0.200	0.20015	0.20027	0.20039	0.20051	
	0.250	0.25023	0.25042	0.25060	0.25079	
	0.300	0.30033	0.30060	0.30086	0.30113	
	0.320	0.32037	0.32068	0.32098	0.32128	
T = 4.875 in. δ = 0.457 in.	0.210	0.21015	0.21027	0.21039	0.21051	
	0.240	0.24019	0.24035	0.24050	0.24066	
	0.270	0.27024	0.27044	0.27063	0.27083	
	0.300	0.30030	0.30054	0.30078	0.30102	
T = 4.875 in. δ = 0.609 in.	0.250	0.25019	0.25035	0.25050	0.25065	
	0.300	0.30027	0.30049	0.30071	0.30093	
	0.350	0.35037	0.35067	0.35096	0.35126	
	0.400	0.40048	0.40087	0.40126	0.40164	
T = 4.875 in. δ = 0.914 in.	0.400	0.40042	0.40074	0.40107	0.40139	
	0.480	0.48060	0.48107	0.48154	0.48201	
	0.560	0.56081	0.56146	0.56210	0.56274	
	0.600	0.60094	0.60167	0.60241	0.60316	
T = 4.875 in. δ = 1.218	0.700	0.70110	0.70195	0.70280	0.70365	
	0.800	0.80145	0.80258	0.80371	0.80484	
	0.830	0.83157	0.83279	0.83401	0.83524	

BOTTOM HEAD TRANSITION REGION EMBEDDED FLAW FATIGUE CRACK GROWTH  
(ASPECT RATIO 1:10) - CIRCUMFERENTIAL FLAW

		INITIAL CRACK LENGTH	CRACK LENGTH AFTER YEAR			
			10	20	30	40
T = 4.875 in. δ = 0.304 in.		0.200	0.20016	0.20029	0.20042	0.20055
		0.250	0.25025	0.25045	0.25065	0.25086
		0.300	0.30036	0.30066	0.30095	0.30124
		0.320	0.32041	0.32075	0.32108	0.32142
T = 4.875 in. δ = 0.457 in.		0.210	0.21015	0.21026	0.21038	0.21050
		0.240	0.24019	0.24035	0.24050	0.24066
		0.270	0.27024	0.27044	0.27063	0.27083
		0.300	0.30030	0.30054	0.30079	0.30103
T = 4.875 in. δ = 0.609 in.		0.250	0.25017	0.25032	0.25046	0.25060
		0.300	0.30025	0.30046	0.30066	0.30087
		0.350	0.35035	0.35063	0.35091	0.35119
		0.400	0.40046	0.40083	0.40120	0.40158
T = 4.875 in. δ = 0.914 in.		0.400	0.40034	0.40061	0.40088	0.40115
		0.480	0.48049	0.48089	0.48129	0.48169
		0.560	0.56068	0.56124	0.56179	0.56235
		0.600	0.60079	0.60144	0.60209	0.60274

OUTLET NOZZLE FULL PENETRATION REGION SURFACE  
 FLAW FATIGUE CRACK GROWTH - LONGITUDINAL FLAW

	INITIAL CRACK LENGTH	CRACK LENGTH AFTER YEAR			
		10	20	30	40
$a/t = 0.0$	0.600	0.62372	0.64156	0.65967	0.67874
	0.800	0.83187	0.85678	0.88216	0.90881
	0.900	0.93587	0.96436	0.99342	1.02389
	1.000	1.03981	1.07187	1.10460	1.13888
$a/t = 0.167$	0.600	0.61408	0.62411	0.63412	0.64448
	0.800	0.81786	0.83094	0.84403	0.85750
	0.900	0.91955	0.93410	0.94862	0.96354
	1.000	1.02113	1.03707	1.05298	1.06935

OUTLET NOZZLE FULL PENETRATION REGION SURFACE FLAW  
 FATIGUE CRACK GROWTH - CIRCUMFERENTIAL FLAW

	INITIAL CRACK LENGTH	CRACK LENGTH AFTER YEAR			
		10	20	30	40
a/t = 0.0	0.600	0.61789	0.63146	0.64506	0.65951
	0.700	0.72180	0.73886	0.75607	0.77435
	0.900	0.93645	0.96804	1.00083	1.03600
	1.000	1.04240	1.07995	1.11910	1.16114
	1.300	1.57806	1.65196	1.72992	1.81322
	2.000	2.11111	2.21849	2.33122	2.63124
a/t = 0.167	0.600	0.61026	0.61740	0.62442	0.63182
	0.700	0.71254	0.72168	0.73071	0.74020
	0.900	0.91728	0.93052	0.94367	0.95737
	1.000	1.01931	1.03433	1.04926	1.06480
	1.300	1.52902	1.55282	1.57657	1.60099
	2.000	2.03642	2.06730	2.09793	2.12925

OUTLET NOZZLE TO VESSEL WELD REGION EMBEDDED FLAW FATIGUE CRACK GROWTH  
(ASPECT RATIO 1:10) - LONGITUDINAL FLAW

		INITIAL CRACK LENGTH	CRACK LENGTH AFTER YEAR			
			10	20	30	40
T = 11.11 in. δ = 0.694 in.		0.100	0.10002	0.10004	0.10006	0.10008
		0.300	0.30019	0.30034	0.30050	0.30065
		0.400	0.40034	0.40060	0.40087	0.40114
		0.500	0.50052	0.50094	0.50135	0.50177
T = 11.11 in. δ = 1.041 in.		0.200	0.20008	0.20014	0.20020	0.20026
		0.400	0.40029	0.40052	0.40075	0.40099
		0.600	0.60064	0.60116	0.60167	0.60219
		0.700	0.70088	0.70158	0.70228	0.70298
T = 11.11 in. δ = 1.388 in.		0.300	0.30015	0.30027	0.30039	0.30051
		0.600	0.60058	0.60103	0.60149	0.60194
		0.900	0.90129	0.90231	0.90334	0.90437
		0.950	0.95144	0.95258	0.95373	0.95488
T = 11.11 in. δ = 2.083 in.		0.500	0.50035	0.50062	0.50088	0.50115
		0.900	0.90103	0.90192	0.90276	0.90360
		1.300	1.30226	1.30402	1.30578	1.30755
		1.400	1.40263	1.40468	1.40674	1.40881
T = 11.11 in. δ = 2.777 in.		0.500	0.50030	0.50051	0.50073	0.50094
		0.900	0.90094	0.90162	0.90230	0.90298
		1.300	1.30195	1.30339	1.30483	1.30629
		1.400	1.40226	1.40395	1.40563	1.40733

OUTLET NOZZLE TO VESSEL WELD REGION FATIGUE CRACK GROWTH  
(ASPECT RATIO 1:10) - CIRCUMFERENTIAL FLAW

		INITIAL CRACK LENGTH	CRACK LENGTH AFTER YEAR			
			10	20	30	40
T = 11.11 in. δ = 0.694 in.	0.100	0.10002	0.10004	0.10006	0.10008	
	0.300	0.30021	0.30037	0.30063	0.30069	
	0.400	0.40038	0.40067	0.40096	0.40125	
	0.500	0.50061	0.50108	0.50154	0.50202	
T = 11.11 in. δ = 1.041 in.	0.200	0.20006	0.20011	0.20015	0.20020	
	0.400	0.40025	0.40044	0.40064	0.40083	
	0.600	0.60060	0.60107	0.60154	0.60202	
	0.700	0.70085	0.70153	0.70219	0.70287	
T = 11.11 in. δ = 1.388 in.	0.300	0.30009	0.30016	0.30023	0.30030	
	0.600	0.60039	0.60070	0.60101	0.60133	
	0.900	0.90101	0.90183	0.90263	0.90345	
	0.950	0.95116	0.95209	0.95301	0.95395	
T = 11.11 in. δ = 2.083	0.500	0.50010	0.50018	0.50023	0.50034	
	0.900	0.90040	0.90073	0.90106	0.90139	
	1.300	1.30109	1.30200	1.30290	1.30382	
	1.400	1.40135	1.40247	1.40358	1.40471	
T = 11.11 in. δ = 2.777 in.	0.500	0.50004	0.50006	0.50009	0.50012	
	0.900	0.90015	0.90026	0.90037	0.90049	
	1.300	1.30039	1.30071	1.30103	1.30135	
	1.400	1.40049	1.40089	1.40128	1.40169	

INLET NOZZLE TO SHELL WELD REGION SURFACE FLAW  
FATIGUE CRACK GROWTH - LONGITUDINAL FLAW

ASPECT RATIO	INITIAL CRACK LENGTH	CRACK LENGTH AFTER YEAR			
		10	20	30	40
a/t = 0.0	0.500	0.52595	0.54453	0.56368	0.58450
	0.700	0.74109	0.77358	0.80773	0.84500
	0.900	0.95764	1.00601	1.05734	1.11288
	1.100	1.17359	1.23695	1.30396	1.37652
	1.400	1.49720	1.58445	1.67839	1.78131
	1.600	1.71485	1.82101	1.93612	2.06368
a/t = 0.167	0.500	0.51307	0.52074	0.52827	0.53630
	0.700	0.71856	0.73045	0.74219	0.75451
	0.900	0.92308	0.93856	0.95389	0.96986
	1.100	1.12676	1.14524	1.16356	1.18252
	1.400	1.43070	1.45251	1.47414	1.49632
	1.600	1.63262	1.65624	1.67959	1.70352

Note: Crack growth analysis not performed for circumferential flaws because of low stress values. The longitudinal flaw results were used in developing the flaw charts.

INLET NOZZLE TO VESSEL WELD REGION EMBEDDED FLAW FATIGUE CRACK GROWTH  
(ASPECT RATIO 1:10) - LONGITUDINAL FLAW

	INITIAL CRACK LENGTH	CRACK LENGTH AFTER YEAR			
		10	20	30	40
T = 10.53 in. δ = 0.658 in.	0.200	0.20009	0.20013	0.20017	0.20021
	0.300	0.30020	0.30029	0.30037	0.30046
	0.400	0.40030	0.40052	0.40067	0.40083
	0.450	0.45046	0.45066	0.45086	0.45106
T = 10.53 in. δ = 0.987 in.	0.500	0.50042	0.50061	0.50081	0.50100
	0.600	0.60062	0.60090	0.60118	0.60146
	0.700	0.70087	0.70126	0.70165	0.70204
δ = T/8 T = 10.53 in. δ = 1.316 in.	0.700	0.70067	0.70099	0.70130	0.70162
	0.800	0.80090	0.80132	0.80173	0.80215
	0.900	0.90117	0.90171	0.90224	0.90279
T = 10.53 in. δ = 1.974 in.	1.100	1.10122	1.10186	1.10250	1.10314
	1.200	1.20148	1.20224	1.20301	1.20377
	1.300	1.30178	1.30267	1.30357	1.30448
	1.400	1.40211	1.40316	1.40421	1.40527
T = 10.53 in. δ = 2.632 in.	1.100	1.10099	1.10158	1.10218	1.10278
	1.200	1.20118	1.20188	1.20258	1.20329
	1.300	1.30139	1.30221	1.30303	1.30385
	1.400	1.40162	1.40257	1.40351	1.40446

Note: Crack growth analysis not performed for circumferential flaws because of low stress values. The longitudinal flaw results were used in